2012

Role of lymph node fibroblasts in T cell priming

Stefanie Siegert

UNIL | Université de Lausanne
Faculté de biologie et de médecine
Département de biochimie

Role of lymph node fibroblasts in T cell priming

Thèse de doctorat ès sciences de la vie (PhD)

présentée à la

Faculté de biologie et de médicine

de l'Université de Lausanne par

Stefanie Siegert

Biologiste diplômé de l'Université de Erlangen-Nürnberg, Allemagne

Jury

Prof. Dr. Monika Hegi, Présidente

Prof. Dr. Sanjiv Luther, Directeur de thèse

Prof. Dr. Fabienne Tacchini-Cottier, experte et représentative du PhD programme

Prof. Dr. Hans Acha-Orbea, expert

Prof. Dr. Graham Anderson, expert externe

Lausanne 2012

UNIL | Université de Lausanne
Faculté de biologie
et de médecine

Ecole Doctorale

Doctorat ès sciences de la vie

Imprimatur

Vu le rapport présenté par le jury d'examen, composé de

Président	Madame Prof. Monika **Hegi**
Directeur de thèse	Monsieur Prof. Sanjiv **Luther**
Experts	Madame Prof. Fabienne **Tacchini-Cottier**
	Monsieur Prof. Hans **Acha-Orbea**
	Monsieur Prof. Graham **Anderson**

le Conseil de Faculté autorise l'impression de la thèse de

Madame Stefanie Siegert

Biologiste diplômée de l'Université Erlangen-Nurnberg

intitulée

Role of lymph node fibroblasts in T cell priming

Lausanne, le 3 février 2012

pour Le Doyen
de la Faculté de Biologie et de Médecine

Prof. Monika Hegi

Table of Contents

Acknowledgments

First of all I would like to express my sincere gratitude to my supervisor Sanjiv Luther, for his constant enthusiasm and support. Sanjiv, you always encouraged me to have my own ideas and in many discussions you taught me how to approach and answer scientific questions, which will be of great value for my future. Although my project took quite some unexpected turns, you found the right portion of criticism, but you were always supportive. No boss is perfect, but you are definitely very close.

I would like to thank the members of my thesis committee - Graham Anderson, Fabienne Tacchini-Cottier and Hans Acha-Orbea- for accepting to be part of my jury and even more for very stimulating ideas and discussions.

Special thanks also to the various collaborators, who contributed to this thesis with reagents, great ideas and discussions: Dietmar Zehn, Chris Buckley, Ben Marsland, Greta Guarda, Anne Wilson and Melody Swartz.

In addition, I would like to thank Anne Wilson and Danny Labes (flow cytometry facility University Lausanne) for all their competent help with the FACS machines.

Many thanks to the Boehringer-Ingelheim Fond, not only for the financial but also for the personal support.

Many thanks to the current lab members for creating a very nice and stimulating working atmosphere. Leo, tu as toujours été motivé à m'aider avec mes innombrables expériences et je t'en serais infiniment reconnaissante pour ça. Cela a été un plaisir de travailler avec toi et de prendre le café avec toi. Stéphanie, merci pour ton introduction à l´histologie et à la microscopie, mais plus important merci pour ton amitié. Hsin Ying, it was a real pleasure to work with you and I'm grateful for your help. Furthermore, I really enjoyed learning a lot about Taiwanese culture from you. Chen-Ying, it was great to be in the lab with you, thanks for your help but even more for filling in the remaining gaps I had about Taiwanese culture. Karin, vielen Dank für deine Hilfe; jetzt ist es an dir, die Deutschen würdig im Labor zu vertreten.

Moreover, I would like to thank all the former lab members, Alex, Mirjam and Tobias: Danke für die Starthilfe im Labor und in Lausanne, aber noch viel mehr für eure Freundschaft.

Merci beaucoup, Françoise et Simine, pour votre aide, vous êtes vraiment super.

Thanks to Alex, Manfredo, Mara and Jachen, for creating a great atmosphere in the shared lab-space. Alex, merci beaucoup de m'avoir aidé avec l'administration suisse, mais plus important d'être une très bonne amie. Merci aussi à vous, Mélanie et Philippe, pour les agréables repas et cafés.

Many thanks to my friends, who helped me to forget and get over the frustrations that come along during a doctoral thesis: Monique, Matilde, Sharmal, Enno, Kilian, Anja, Hannes, Mathieu and Debora. Thank you for your friendship, which means a lot to me and which I hope will last many years more.

Papa, herzlichen Dank für deine immerwährende Unterstützung, ohne die mein Studium sehr viel schwieriger gewesen wäre.

Oma und Opa, danke, dass ihr immer für mich da seid und mich immer bekräftigt habt in meinen Entscheidungen.

Mama, du warst immer da für mich, hast mich gefördert und mich immer bestärkt, alles erreichen zu können, was ich möchte. Ohne dich wäre ich wahrscheinlich nicht, wo ich heute bin. Vielen Dank.

Emanuel, du hast mich während der Doktorarbeit unterstützt, wo es nur möglich war. Hast mit mir gelitten und dich mit mir gefreut, aber vor allem hast du mir immer neuen Mut gegeben nicht aufzugeben. Ich bin dir unendlich dankbar, dass du dein Leben mit mir teilst und freue mich auf unsere gemeinsame Zukunft.

Summary

Secondary lymphoid organs, such as lymph nodes or spleen, are the only places in our body where primary adaptive immune responses are efficiently elicited. These organs have distinct B and T cell rich zones and T lymphocytes constantly migrate from the bloodstream into T zones to scan dendritic cells (DCs) for antigens they present. Specialized fibroblasts, the T zone reticular cells (TRCs), span the T zone in the form a three-dimensional network. TRCs guide incoming T cells in their migration, both chemically, by the secretion of the chemokines CCL19 and CCL21, and physically, by construction of a road system to which also DCs adhere. In this way TRCs are thought to facilitate encounters of T cells with antigen-bearing DCs and thereby accelerate the selection of rare antigen-specific T cells. The resulting T cell activation, proliferation and differentiation all take place within the TRC network. However, the influence of TRCs on T cell activation has so far not been elucidated with the possible reasons being that TRCs represent a relative rare cell population and that mice devoid of TRCs have not been described.

To circumvent these technical limitations, we established TRC clones and lines to have an abundant source to functionally characterize TRCs. Both the clones and lines show a fibroblastic phenotype, express a surface marker profile comparable to *ex vivo* TRCs and produce extracellular matrix molecules. However, expression of *Ccl19*, *Ccl21* and *IL-7* is lost and could not be restored by cytokine stimulation. When these TRC clones or lines were cultured in a three-dimensional cell culture system, their morphology changed and resembled that of *in vivo* TRCs as they formed networks. By adding T cells and antigen-loaded DCs to these cultures we successfully reconstructed lymphoid T zones that allowed antigen-specific T cell activation.

To characterize the role of TRCs in T cell priming, TRCs were co-cultured with antigen-specific T cells in the presence antigen-loaded DCs. Surprisingly, the presence of TRC lines and *ex vivo* TRCs inhibited rather than enhanced $CD8^+$ T cell activation, proliferation and effector cell differentiation. TRCs shared this feature with fibroblasts from non-lymphoid tissues as well as mesenchymal stromal cells. TRCs were identified as a strong source of nitric oxide (NO) thereby directly dampening T cell expansion as well as reducing the T cell priming capacity of DCs. The expression of inducible NO synthase (iNOS) was up-regulated in a subset of TRCs by both DC-signals as well as interferon-γ produced by primed $CD8^+$ T cells. Importantly, iNOS expression was induced during viral infection *in vivo* in both lymph node TRCs and DCs. Consistent with a role for NO as a negative regulator, the primary T cell response was exaggerated in $iNOS^{-/-}$ mice. Our findings highlight that in addition to their established positive roles in T cell responses TRCs and DCs cooperate in a negative feedback loop to attenuate T cell expansion during acute inflammation.

Résumé

Les organes lymphoïdes secondaires, comme les ganglions lymphoïdes ou la rate, sont les seuls sites dans notre corps où la réponse primaire des lymphocytes B et T est initiée efficacement. Ces organes ont des zones différentes, riches en cellules B ou T. Des lymphocytes T circulent constamment du sang vers les zones T, où ils échantillonent la surface des cellules dendritiques (DCs) pour identifier les antigènes qu'ils présentent. Des fibroblastes spécialisés – nommés 'T zone reticular cells (TRCs)' forment un réseau tridimensionnel dans la zone T. Les TRCs guident la migration des cellules T par deux moyens: chimiquement, par la sécrétion des chimiokines CCL19 et CCL21 et physiquement, par la construction d'un réseau routier en trois dimensions, auquel adhèrent aussi des DCs. Dans ce cas, on pense que la présence des TRCs facilite les rencontres entre les cellules T et les DCs chargées de l'antigène et accélère la sélection des rares cellules T spécifiques. Ensuite, l'activation de cellules T, ainsi que la prolifération et la différenciation se produisent toutes à l'intérieur du réseau des TRCs. L'influence des TRCs sur l'activation des cellules T n'est que très peu caractérisée, en partie parce que les TRCs représentent une population rare et que les souris déficientes dans les TRCs n'ont pas encore été découvertes.

Pour contourner ces limitations techniques, nous avons établi des clones et des lignées cellulaires de TRC pour obtenir une source indéfinie de ces cellules permettant leur caractérisation fonctionnelle**.** Les clones et lignées établis ont un phénotype de fibroblaste, ils expriment des molécules de surface similaires aux TRCs *ex vivo* et produisent de la matrice extracellulaire. Mais l'expression de *Ccl19, Ccl21* et *Il-7* est perdue et ne peut pas être rétablie par stimulation avec différentes cytokines. Les clones TRC ou les lignées cultivées en un système tridimensionnel de culture cellulaire, montrent une morphologie changée, qui ressemble à celle de TRC *ex vivo* inclus la construction de réseaux tridimensionnels.

Pour caractériser le rôle des TRC dans l'activation des cellules T, nous avons cultivé des TRCs avec des cellules T spécifiques et des DCs chargées avec l'antigène. Etonnamment, la présence des TRC (lignées et *ex vivo*) inhibait plutôt qu'elle améliorait l'activation, la prolifération et la différenciation des lymphocytes T $CD8^+$. Les TRCs partageaient cette fonction avec des fibroblastes des organes non lymphoïdes et des cellules souches du type mésenchymateux. Dans ces conditions, les TRCs sont une source importante d'oxyde nitrique (NO) et par ce fait limitent directement l'expansion des cellules T et réduisent aussi la capacité des DCs à activer les cellules T. L'expression de l'enzyme NO synthase inductible (iNOS) est régulée à la hausse par des signaux dérivés des DCs et par l'interféron-γ produit par des cellules T de type $CD8^+$ activées. Plus important, l'expression d'iNOS est induite pendant une infection virale *in vivo*, dans les TRCs et dans les DCs. Par conséquent, la réponse primaire de cellules T est exagérée dans des souris $iNOS^{-/-}$. Nos résultats mettent en évidence qu'en plus de leur rôle positif bien établi dans la réponse immunitaire, les TRCs et les DCs coopèrent dans une boucle de rétroaction négative pour atténuer l'expansion des cellules T pendant l'inflammation aigüe pour protéger l'intégrité et la fonctionnalité des organes lymphoïdes secondaires.

Abbreviations

2D	Two dimensional
3D	Three dimensional
AICD	Activation induced cell death
Aire	Autoimmune regulator
BAFF	B-cell activating factor
BCR	B cell receptor
BEC	Blood endothelial cell
BM	Bone marrow
BMDC	Bone marrow derived dendritic cell
CCL	Chemokine (C-C motif) ligand
CCR	Chemokine (C-C-motif) receptor
CD	Cluster of differentiation
CTLA-4	Cytotoxic T lymphocytes associated antigen 4
CXCL	Chemokine (C-X-C-motif) ligand
DC	Dendritic cell
DEAF-1	Deformed epidermal autoregulatory factor 1
EAE	Experimental autoimmune (sometimes allergic) encephalomyelitis
EC	Endothelial cell
ECM	Extracellular matrix
FACS	Fluorescent activated cell sorting
FDC	Follicular dendritic cell
Foxp3	Forkhead box P3
FRC	Fibroblastic reticular cell
GC	Germinal center
GITR	Glucocorticoid-inducible tumor necrosis factor receptor
GM-CSF	Granulocyte-macrophage colony-stimulating factor
gp38	Glycoprotein 38 (= podoplanin)
HEV	High endothelial venule
i.v.	Intravenous
IC	Immune-complexes
ICAM	Intercellular adhesion molecule
IDO	Indoleamine 2,3.dioxygenase
IF	Immunofluorescence
iFABP	Intestinal fatty acid binding protein
IFNγ	Interferon gamma
IL	Interleukin
iNOS	Inducible nitric oxide synthase
IS	Immunological synapse
iT_{REG}	Induced regulatory T cell
JAM	Junctional adhesion molecule
LCMV	Lymphocytic choriomeningitis virus
LEC	Lymphatic endothelial cell
LFA-1	Leukocyte function-associated antigen-1
Lin	Lineage
LN	Lymph node
LPS	Lipo-polysaccharide
LT	Lymphotoxin
LTi	Lymphoid tissue inducer
LTβR	Lymphotoxin beta receptor
MAdCAM	Mucosal addressin-cell adhesion molecule
MHC	Major histocompatibility complex
mLN	Mesenteric lymph node
MRC	Marginal reticular cells
MSC	Mesenchymal stem/stromal cell
MW	Molecular weight
NO	Nitric oxide
nT_{REG}	Natural regulatory T cell
OT	Ovalbumin transgenic

OVA	Ovalbumin
PD1	Programmed cell death 1
PDGF	Platelet derived growth factor
PD-L1	Programmed cell death ligand 1
pLN	Peripheral lymph node
PNAd	Peripheral node addressin
PP	Peyer's patch
PTA	Peripheral-tissue restricted antigen
s.c.	Subcutaneous
S1P	Sphingosine 1-phosphate
SCS	Subcapsular sinus
SLO	Secondary lymphoid organs
TCR	T cell receptor
TEC	Thymic epithelial cells
T_{FH}	Follicular T helper cells
TGFβ	Transforming growth factor beta
T_H	Helper T cell
TLR	Toll like receptor
TNF	Tumor necrosis factor
TRC	T zone fibroblastic reticular cell
VCAM	Vascular cell adhesion molecule
VEGF	Vascular endothelial growth factor
VSV	Vesicular stomatitis virus
WT	Wildtype

1. Introduction

1. Introduction: the immune system

Our health is constantly threatened by a large variety of pathogens. To protect the body against these threats we possess a sophisticated weapon: the immune system. The first lines of defense are the epithelial surfaces of our body, the skin and the internal epithelial surfaces such as in the gastro-intestinal tract or the lung. Epithelial cells are tightly connected and provide an effective physical barrier for pathogens. Furthermore, they are reinforced by other mechanisms such as the mucus flow that prevents adherence of pathogens or the production of antimicrobial peptides (Hornef et al., 2002; Gallo et al., 2002). The second line of defense is the so-called innate immunity, which consists of different cells, such as neutrophils, macrophages and dendritic cells (DCs). Part of these cells are constantly monitoring peripheral tissues as well as blood for potential dangers. Conserved molecules expressed by pathogens, but not host cells, are recognized by 'pattern recognition receptors' on the surface of innate immune cells. If pathogens succeed to enter the body, patrolling innate immune cells arrive rapidly at the side of infection, where they engulf microbes and process them. In addition, chemokines and pro-inflammatory cytokines are secreted, which recruit more immune cells to the place of infection and alert the adaptive immune system, our third line of defense (Kawai and Akira, 2011; Takeda et al., 2003; Coombes and Robey, 2010; Junt et al., 2008). Macrophages and DCs are called antigen-presenting cells (APCs), as they present processed antigen in the context of MHC (major histocompatibility complex) class II molecules on their surface to T cells. This is crucial to activate them and therefore macrophages and DCs bridge innate and adaptive immunity. Besides T cells also B lymphocytes are activated during an adaptive immune response (Junt et al., 2008; Randolph et al., 2008; Coombes and Robey, 2010).

In contrast to the innate immune response, the activation the adaptive immune cells, with the main players being B and T lymphocytes, is slow. Each single T or B cell recognizes only one specific antigen, with the naïve T cell precursor frequency for a given antigen being in the range of 20-2000 T cells. In the case of infection, these rare antigen-specific T cells are spread over all secondary lymphoid organs; have to first find the APC in order to be activated. Secondary lymphoid organs, such as lymph nodes, function as a meeting point to bring these cells together (Junt et al., 2008). Once lymphocytes productively interact with APCs including proper co-stimulation, they expand enormously and differentiate into effector cells. The result of a protective immune response is the generation of plasma cells secreting high-affinity antibodies, $CD4^+$ T helper cells producing cytokines and $CD8^+$ T cells with cytotoxic activity, which together in most cases effectively eliminate the cause of infection. Importantly, during the adaptive immune response some lymphocytes differentiate into memory cells. This immunological memory makes the adaptive response to secondary infections with the same pathogen faster and more efficient. The achievement of good immunological memory and high antibody titres are the goal of most vaccines (Williams and Bevan, 2007; Junt et al., 2008; Zhu et al., 2010; Batista and Harwood, 2009; Phan et al., 2009; Laemmermann and Sixt, 2008).

1.1. Secondary lymphoid organs: structure and function

The organs of the immune system are divided into primary and secondary lymphoid organs. Leukocytes are constantly produced in the primary lymphoid organs: the bone marrow (BM) generates B cells and innate immune cells and the thymus T cells. Mature, naïve lymphocytes leave the BM or the thymus after the completion of their maturation and then migrate constantly between secondary lymphoid organs (SLO) by using the bloodstream and lymph (Junt et al., 2008; Cyster, 2005). These organs, such as lymph nodes (LNs) or the spleen, serve as meeting points for antigen, APCs and lymphocytes and are the only places, where adaptive immune responses are efficiently mounted. This was demonstrated in mice with the spontaneous alymphoplasia (*aly/aly*) mutation, which leads to the complete lack of LNs and Peyer's Patches as well as disturbed splenic architecture. These mice show a severely impaired capability to mount efficient adaptive immune responses. Furthermore, reduced SLO integrity in various other mouse models was shown to correlate with weaker immune reactivity against viral infection (Karrer et al., 1997; Junt et al., 2008; Cyster, 2005).

SLO are strategically placed in the body and constantly monitor the body fluids for pathogens, thus allowing them to sample and concentrate antigen. The spleen surveys blood, LNs filter lymph and mucosal-associated lymphoid tissues monitor intestinal and respiratory mucosal surfaces (Cyster, 2005; Bajenoff et al., 2007; Junt et al., 2008). All SLO show a similar micro-architecture: They are highly compartmentalized and several distinct zones can be distinguished, including the B cell rich B zone (B-follicle, cortex) and the T cell rich T zone (paracortex) (figure 1.1 right). As most of this thesis is focused on LNs, only these will be described in detail.

Lymphocytes enter the LN via specialized blood vessels, the high endothelial venules (HEV), located mostly in the outer T zone. From here B and T cells are attracted by constitutively expressed chemokines towards their respective zones: $CXCR5^+$ B cells are attracted to the CXCL13 rich B zone, while $CCR7^+$ T cells are retained within the CCL21 and CCL19 rich T zone (figure 1.1 right and 1.6 left) (Cyster, 2005; Junt et al., 2008). T and B cells are moving with an average speed of 8-11μm (T cells) or 6μm (B cells) per minute and constantly scan the LN for antigen (Mueller and Germain, 2009; Batista and Harwood, 2009). If their respective antigen is not presented, they will leave after 12-18h (T cells) or 24h (B cells) through efferent lymphatic vessels in the medulla. The exit from SLO is mediated via sphingosine 1-phosphate (S1P), which is present in the lymph and interacts with the S1P-receptor 1 that is highly expressed on naïve T and B cells (Cyster, 2005) Lymphocytes in the efferent lymphatic vessels will be transported back to the bloodstream via the thoracic duct and continue their search for antigen in other SLO (Laemmermann and Sixt, 2008; Mueller and Germain, 2009).

1.2. Stromal cells in secondary lymphoid organs

The structural backbone of lymphoid organs is made up of radio-resistant non-hematopoietic stromal cells (figure 1.1, left). For a long time, these cells were thought to be only of structural importance. By

contrast, various recent reports demonstrated them to create a specific and dynamic microenvironment, which is functionally influencing the immune response (Mueller and Germain, 2009; Laemmermann and Sixt, 2008; Junt et al., 2008). Besides the endothelial stromal cell populations, different subtypes of fibroblastic stromal cells were characterized in various SLO compartments: B zone stromal cells, T zone stromal cells as well as the recently identified marginal reticular cells (figure 1.1 right) (Roozendaal and Mebius, 2011; Mueller and Germain, 2009).

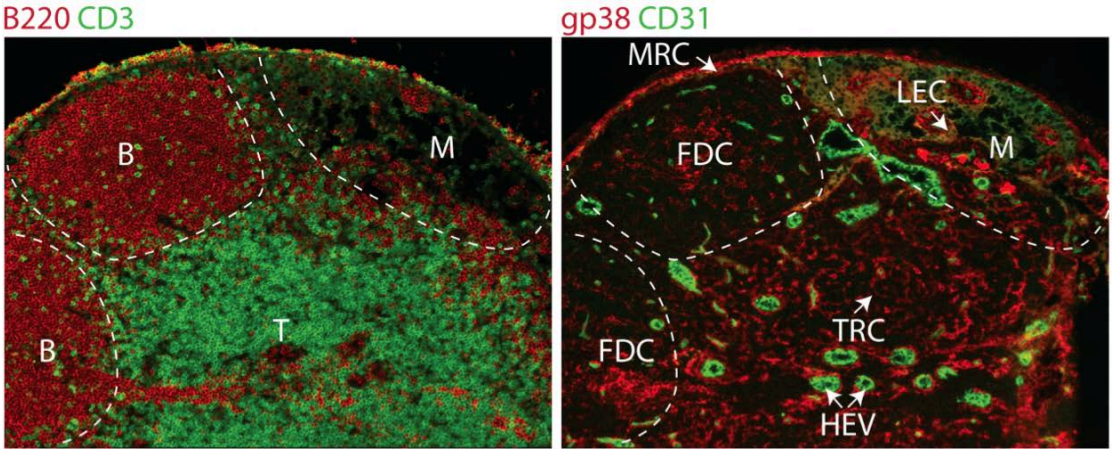

Figure 1.1: Different LN microenvironments are formed by distinct stromal cells
Consecutive pLN sections were stained for the hematopoietic compartment (B cells in red; T cells in green) (left) allowing to distinguish B cell follicles (B), the T zone (T) and the medulla (M). Labelling with stromal cell markers (gp38 in red and CD31 in green) (right) identifies 5 different stromal cell populations: gp38+ CD31+ LECs in the medulla and subcapsular sinus (SCS), gp38- CD31+ HEVs mainly in the T zone, gp38+ CD31- TRCs in the T zone, gp38+ CD31- MRCs below the SCS and gp38+ CD31- activated FDCs in the B zone. (Picture courtesy from S. Favre)

1.2.1. Endothelial cells

LNs are connected to both the blood and lymph circulation. Afferent lymphatic vessels draining peripheral tissues end in the subcapsular sinus (SCS) surrounding the LN (figure 1.3 left). The lymph contains a variety of molecules, such as cytokines or antigen, but also cells such as DCs (Laemmermann and Sixt, 2008; Randolph et al., 2008). Lymphatic endothelial cells (LECs) are identified by a combination of different surface molecules: CD31, gp38 (glycoprotein38 = podoplanin), Prox-1 (prospero homeobox protein 1) and LYVE-1 (lymphatic vessel endothelial hyaluronan receptor). In addition, they typically produce the chemokine CCL21 which attracts DCs and promotes their entry into lymphatic vessels (Randolph et al., 2008; Laemmermann and Sixt, 2008). Lymph cannot freely enter the LN and is mainly canalled around it before being collected in efferent lymphatic vessels localized in the medulla. However, part of the lymph enters small microchannels in the T zone, called conduits, which will be discussed below.

Blood vessels present in the LN are mostly the above-mentioned specialized HEVs. Compared to normal venules they display special features: they consist of a blood endothelial cell (BEC) layer with plump morphology, surrounded by a thick basal lamina and a prominent perivascular sheath or channel (Gretz et

al., 1997; Miyasaka and Tanaka, 2004). In addition, several chemokines are displayed by HEVs, some constitutively produced by BECs themselves, such as CCL21, while others, such as CCL19 or CXCL12, are produced by other cell types and transported to the HEV followed by transcytosis and luminal display (Miyasaka and Tanaka, 2004). HEVs in peripheral LN (pLN) express the L-selectin (CD62L) ligand PNAd (peripheral-node addressin), while HEVs of mucosal associated SLO, such as mesenteric LN (mLN), express the $\alpha_4\beta_7$ integrin ligand MAdCAM-1 (mucosal vascular addressin cell adhesion molecule 1). Both play a role in the entry of lymphocytes into the LN, which is mediated by a cascade of events (figure 1.2): engagement of CD62L induces slow rolling of lymphocytes on the vessel. In pLN this is mediated by CD62L - PNAd interactions, while in mLN by CD62L- and $\alpha_4\beta_7$ - MAdCAM interactions. In the next step, CCL21 on HEV triggers CCR7 on lymphocytes and induces firm adhesion on the vessel wall, mostly mediated by LFA-1 – ICAM-1 interactions, which is followed by transmigration of lymphocytes into the T zone (Mueller and Germain, 2009; Miyasaka and Tanaka, 2004)

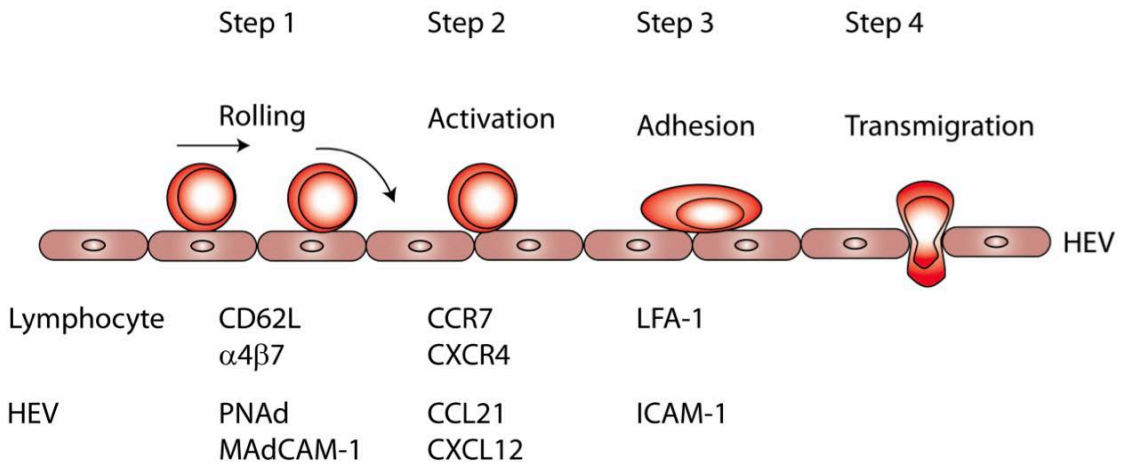

Figure 1.2: A cascade of events is necessary for lymphocyte entry in LN via HEV
Interactions of CD62L (pLN) and α4β7 integrin (mLN) with PNAd and MAdCAM, respectively, induce rolling of lymphocytes on the vessel wall. In the next step, triggering of CCR7 and/or CXCR4 by CCL21 and CXCL12 leads to activation of integrins followed by the firm adhesion mediated by LFA-1 – ICAM-1 interactions eventually leading to transmigration across the endothelial barrier. Based on (von Andrian and Mempel, 2003; Miyasaka and Tanaka, 2004).

1.2.2. B zone stromal cells

Follicular dendritic cells (FDCs) are the most studied and most prominent B zone stromal cells (Figure 1.3 right). They can be identified by the expression of the complement receptor CR-1 (CD35) and -2 (CD21), ICAM-1 (intracellular adhesion molecule), VCAM-1 (vascular cell adhesion molecule), MAdCAM-1, FDC-M1 and -M2 and LTβR (lymphotoxin beta receptor) (Allen and Cyster, 2008; Batista and Harwood, 2009). In the course of T-dependent B cell responses, some B cells generate germinal centres (GCs) in which affinity maturation and class switching takes place (figure 1.6 right). Activated FDCs in GCs were shown to up-regulate ICAM-1 and VCAM-1, which was demonstrated to be implicated in the survival of GC-B cells (Vinuesa et al., 2010). A unique feature of FDCs is their ability to

trap intact antigen in the form of immune-complexes (IC), which can be composed of antigen-antibody, antigen-complement or antigen-antibody-complement. ICs are trapped on FDCs by either CD21/35 or in a complement-independent way by the Fc receptor FcγRIIb (CD32) and are then presented to both, naïve and activated B cells (Allen and Cyster, 2008). Interestingly, non-cognate B cells were shown to capture IC from SCS macrophages and deliver them to FDCs (Phan et al., 2007). The presentation of IC to naïve cognate B cells leads to their activation, though the importance of IC-presentation on FDCs *in vivo* is still debated (Allen and Cyster, 2008; Cyster, 2010). ICs presented by FDCs in germinal centres are thought to provide a long-term source of antigen, which plays a role for positive selection and competition of B cells while they undergo affinity maturation in germinal centres (Vinuesa et al., 2010; Batista and Harwood, 2009; Allen and Cyster, 2008; Tew et al., 2001). Furthermore, FDCs were shown to be the main source of CXCL13 in the B zone, which attracts B cells via the chemokines receptor CXCR5 and possibly also enhances their motility (Allen and Cyster, 2008; Allen et al., 2007)(figure 1.3 right). In addition, B zone stromal cells (not only FDCs) are a source of BAFF (B-cell activating factor), a B cell trophic factor important for maintaining B cell homeostasis, but also B cell proliferation and differentiation (Batista and Harwood, 2009).

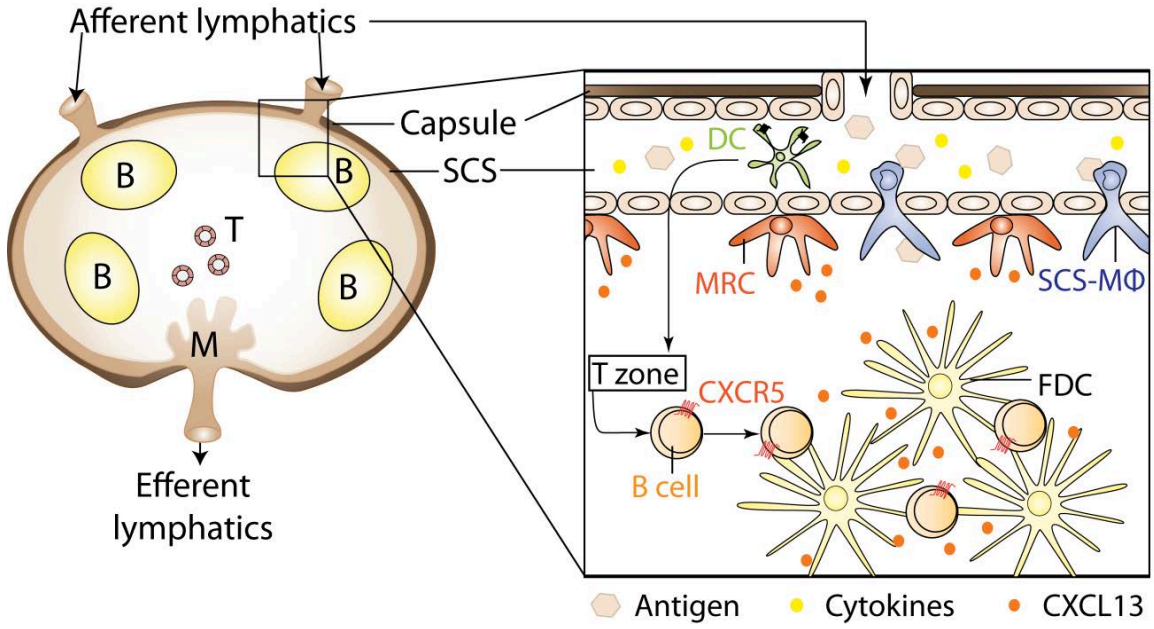

Figure 1.3: Schematic overview of the cellular composition of the lymph node B zone
CCR7+ DCs migrating to the LN via afferent lymphatic vessels arrive in the SCS, leave the lymph by migrating across the lymphatic cell boundary into the T zone, attracted by the chemokines CCL19 and CCL21. The SCS is lined by SCS macrophages, which capture antigen from the lymph and present it to B cells or transfer it into the B zone. Furthermore CXCL13 producing MRCs are found underneath the SCS. The B zone itself is spanned by a network of CXCL13 producing FDCs. CXCR5+ B cells enter the LN via HEV, travel on the TRC network (not shown) to the CXCL13+ B zone in which they migrate along the FDC network and search for antigen.(Cyster, 2010; Junt et al., 2008; Bajenoff et al., 2006)

1.2.3. T zone stromal cells

The T zone is spanned by a three-dimensional network formed by T zone reticular cells, also called T zone fibroblastic reticular cells (TRCs or T-FRCs) (Figure 1.4a). These cells express high levels of gp38 (podoplanin), ICAM-1, VCAM-1, LTβR, PDGFRα and β. TRCs have myofibroblastic features as shown by desmin and αSMA (alpha smooth muscle actin) expression as well as their ability to contract collagen-I (Link et al., 2007; Tomei et al., 2009b). TRCs are the main source of the homeostatic chemokines CCL21 and CCL19 in LN which trigger the chemokine receptor CCR7 and thereby attract and compartmentalize naïve T cells but also DCs within the T zone (Luther et al., 2000) (Figure 1.4 a,b and 1.5). Furthermore, both chemokines were demonstrated to enhance the T cell motility in the T zone and to provide a retention signal for migrating lymphocytes (figure 1.5) (Cyster, 2005; Worbs et al., 2008; Pham et al., 2008; Mueller and Germain, 2009). In addition, CCR7 triggering was shown to enhance dendrite formation by DCs and to positively influence DC maturation (figure 1.5) (Sanchez-Sanchez et al., 2006).

Link and colleagues demonstrated that TRCs are the main source of IL-7 in LN, with IL-7 being a critical survival factor for circulating naïve T cells (Figure 1.4 and 1.5) (Link et al., 2007). But TRCs not only influence the hematopoietic compartment in SLO, as in a study from Chyou and colleagues, TRCs were shown to produce VEGF (vascular endothelial growth factor), thereby regulating the LN vasculature in homeostasis but also inflammation (Chyou et al., 2008).

TRCs secrete several extracellular matrix (ECM) molecules and this is enhanced in *in vitro* co-cultures of TRC lines with activated lymphocytes or TNFα and LTα3 (Katakai et al., 2004). *In vivo* the TRCs produced ECM molecules form a unique channel system in LNs, the so-called conduits. These are small micro-channels consisting of a collagen I core surrounded by a microfibrillar zone and a basal membrane, which are enwrapped by TRCs (Sixt et al., 2005)(Figure 1.4a,b). Conduits connect the SCS with the HEVs in the T zone and are thought to act as an information highway for small molecules. First tracer studies from Gretz and colleagues demonstrated that high molecular weight (MW) molecules are excluded from the LN cortex and are only found in the SCS and the medullary sinuses. In contrast, small molecular weight molecules (MW < 40kDa), enter the paracortex and highlight the reticular network (Gretz et al., 2000). Several chemokines were shown to be rapidly transported to the HEV via the conduits after subcutaneous injection. This was confirmed for endogenously produced chemokines, such as MCP-1 (Gretz et al., 2000; Palframan et al., 2001; Roozendaal et al., 2008; Laemmermann and Sixt, 2008). Most of the conduit system is enwrapped by TRCs, but gaps exist, which are mostly occupied with LN-resident DCs. It was shown that these DCs can extend protrusions through the basal membrane into the conduit and sample antigen from it (Figure 1.4b) (Sixt et al., 2005). Taken together, the conduit system is thought to serve as an information highway, which alerts the LN in the case of an infection. Thus, allowing the LN to rapidly prepare for the initiation of an immune response (also see 1.3) (Roozendaal et al., 2008).

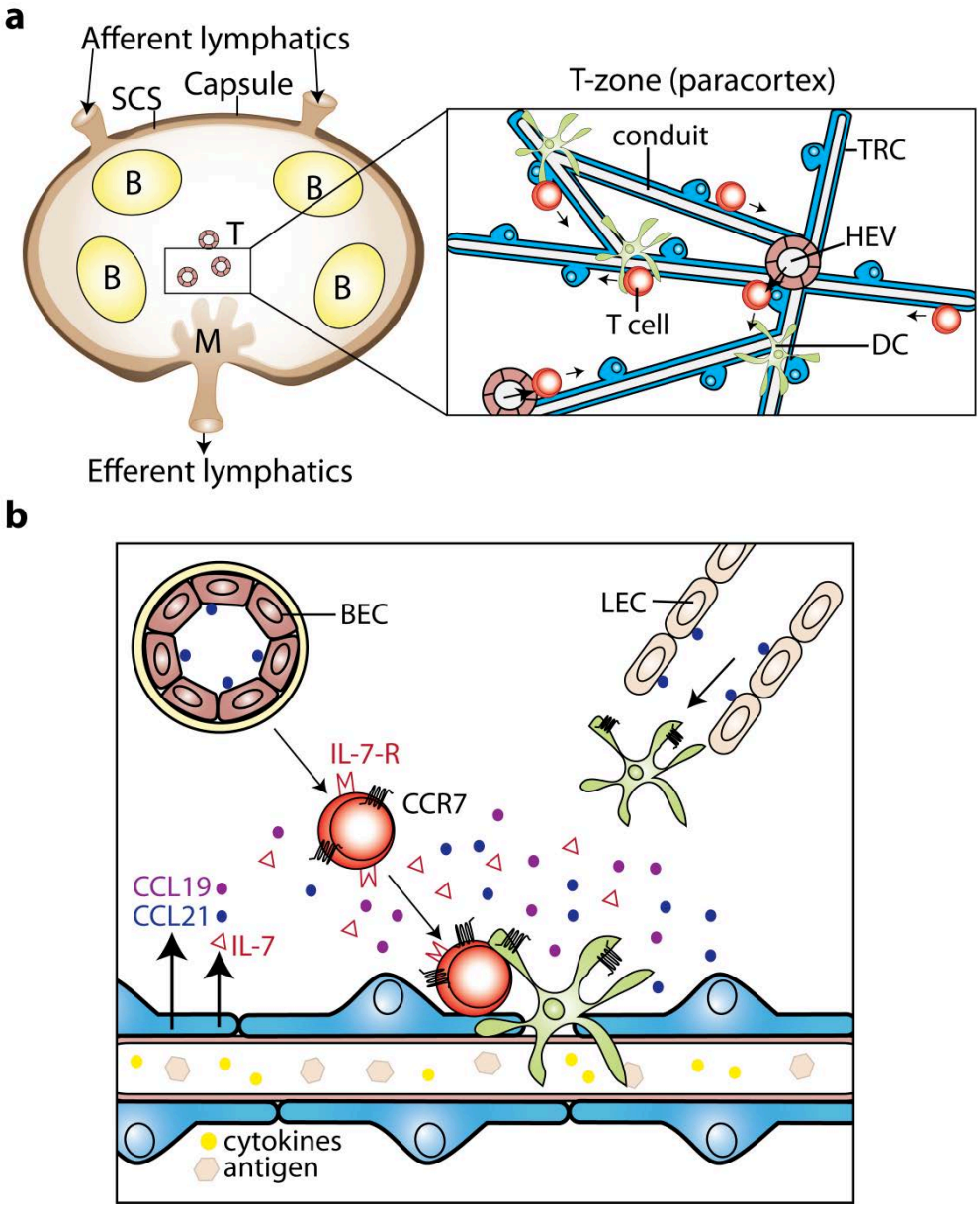

Figure 1.4: Schematic overview of the cellular composition of the lymph node T zone including the conduit network

(**a**) TRCs in the T zone form an extensive three-dimensional network including the conduit system. The latter are micro-channels containing small molecules (MW < 40kDa), such as cytokines or antigen derived from the lymph. This allows the rapid transport of these small molecules from the SCS to the HEVs in the T zone. DCs are associated with the TRC network and T cells entering the LN via HEVs migrate along the TRC network, thereby passing the DCs. (**b**) TRCs produce the chemokines CCL19 and CCL21, which attract both T cells and DCs. Furthermore, CCR7 triggering enhances T cell motility but also increases dendrite formation of DCs and positively influences DC maturation. LN resident DCs cover TRC-free spaces on the conduits and extend protrusions into these micro-channels, allowing them to sample antigen. In addition, TRCs produce IL-7, which is an important survival signals for naïve T cells expressing IL-7 receptor. All three cytokines may be bound to extracellular proteoglycans and therefore be spatially restricted close to the source (not shown)(Link et al., 2007; Mueller and Germain, 2009; Turley et al., 2010; Lindquist et al., 2004; Sanchez-Sanchez et al., 2006; Sixt et al., 2005; Laemmermann and Sixt, 2008).

Based on the histological analysis of LN, Gretz and colleagues proposed already in 1996 that the unique three-dimensional sponge-like network built by TRCs in the LN might serve as a scaffold to guide lymphocyte migration (Gretz et al., 1996, 1997). In 2006 this was experimentally confirmed by Bajenoff and colleagues. Using intravital microscopy, migrating lymphocytes were demonstrated to crawl along TRC fibres in a random migration. While T cells remain associated with the TRC network and stay in the T zone, B cells cross the T-B zone border and 'jump' onto the FDC network, which guides their migration in the B zone (Bajenoff et al., 2006)

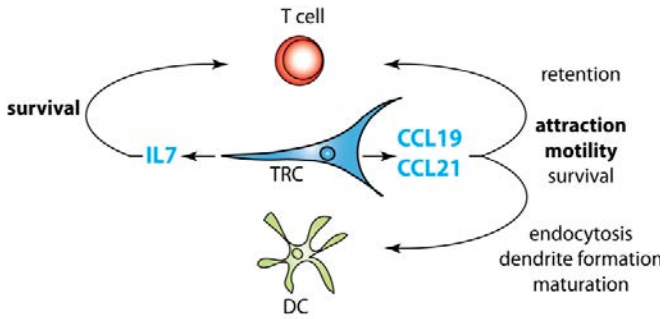

Figure 1.5: Summary of TRC influence on T cells and DCs
TRCs are a main source of IL-7 in the LN, which is an important survival signal for circulating T cells. In addition, TRCs produce the chemokines CCL19 and CCL21, which attract and enhance the motility of both, T cells and DCs. In addition, both chemokines have been implicated in survival of T cells and DCs. CCR7 triggering in T cells was shown to retain them in the T zone, enhancing the time they spend to search for antigen. Also maturation, endocytosis and dendrite formation of DCs is positively influenced by CCL19 and CCL21. (Link et al., 2007; Pham et al., 2008; Sanchez-Sanchez et al., 2006; Worbs et al., 2008; Mueller and Germain, 2009)

1.2.4. Marginal reticular cells

Katakai and colleagues recently identified marginal reticular cells (MRCs) as a unique mesenchymal reticular cell type located underneath the SCS of LNs. As TRCs MRCs express gp38, ICAM-1, VCAM-1, LTβR and PDGFRβ, but in addition constitutively express MAdCAM-1, TRANCE and CXCL13. Unlike FDCs MRCs are negative for CR1 and FcγRII/III. MRCs share some features with stromal organizer cells, which are crucial to drive the SLO organogenesis during embryonic development but their precise function remains to be elucidated (Katakai et al., 2008; Roozendaal and Mebius, 2011).

1.3. The initiation of an adaptive immune response in the LN

The LN structure was shown to change dramatically following infection. Pro-inflammatory mediators, such as MCP-1, produced at the place of infection are rapidly transported via the lymph to the draining LN. Using the conduit system in the T zone they quickly reach the HEVs, which is important for monocyte recruitment from the blood (Palframan et al., 2001). DCs, that encountered antigen in the periphery and are activated by 'danger' signals (e.g. TLR stimulation), travel to the draining LN using the lymphatics (figure 1.6a) (Randolph et al., 2008). Furthermore, the vessel diameter widens leading to increased blood flow. Together with the up-regulated CCL21 expression this increases lymphocyte influx into the LN. At the same time, egress of lymphocytes from the LN is shut down. Therefore, a huge number of naïve lymphocytes accumulate in the LN, which enhances the probability that antigen-specific lymphocyte finds the corresponding APC (Junt et al., 2008).

1.3.1. Antigen sampling in the LN

LNs are very effective in sampling and concentrating antigen, with antigen being delivered by different routes: either as soluble antigen passively transported in the lymph or actively carried by cells, such as DCs (Randolph et al., 2008; Junt et al., 2008). Soluble antigen in the lymph is transported to the SCS, which inner surface is lined by SCS CD169+ macrophages and CD11b+ DCs that both efficiently take up antigen. The filtration of the lymph by SCS macrophages was shown to be a crucial event to prevent spreading of pathogens into the blood or in the case of vesicular stomatitis virus (VSV) infection into the brain (Iannacone et al., 2010; Junt et al., 2007). SCS macrophages can process antigen and directly present it to lymphocytes, but were also shown to efficiently shuttle intact antigen from the SCS into the B zone by surface mediated molecular transport (Junt et al., 2007; Cyster, 2010). MRCs were proposed to play a role in this route of antigen delivery as well, based on their prominent localization below the SCS (Katakai et al., 2008). Furthermore, SCS macrophages were shown to capture immune-complexes, which are transferred into the B zone and finally displayed by FDCs (Junt et al., 2008). Small molecular weight molecules contained in the lymph can enter the LN cortex via the conduit system, as described above. LN-resident DCs associated with the conduit system sample this antigen and present it to lymphocytes (Sixt et al., 2005).

The second way of antigen delivery to the LN is the transport by cells, such as DCs. DCs, which are known to be the most effective APCs are present in peripheral tissues and 'stand guard' to immediately catch intruders in the body. In case of an infection DCs will engulf the pathogen, process it and present antigen in the context of MHC molecules at its surface. This in combination with pro-inflammatory signals leads to the maturation of DCs: the surface expression of MHCI, MHCII and co-stimulatory molecules such as CD80 or CD86 are induced, while the capacity for phagocytosis decreases. In addition, the chemokine receptor CCR7 is up-regulated allowing maturing antigen-bearing DCs to travel through afferent lymphatic vessels to the LN (Randolph et al., 2008). Once in the LNs they first accumulate in proximity to HEVs in the outer T zone, but later disperse throughout the whole T zone, where they settle

down on the TRC network (figure 1.6) (Lindquist et al., 2004). While DCs are rather sessile cells, their dendrites are constantly moving and probing their environment. Due to that DCs were calculated to contact approximately 5000 T cells per hour (Miller et al., 2004a).

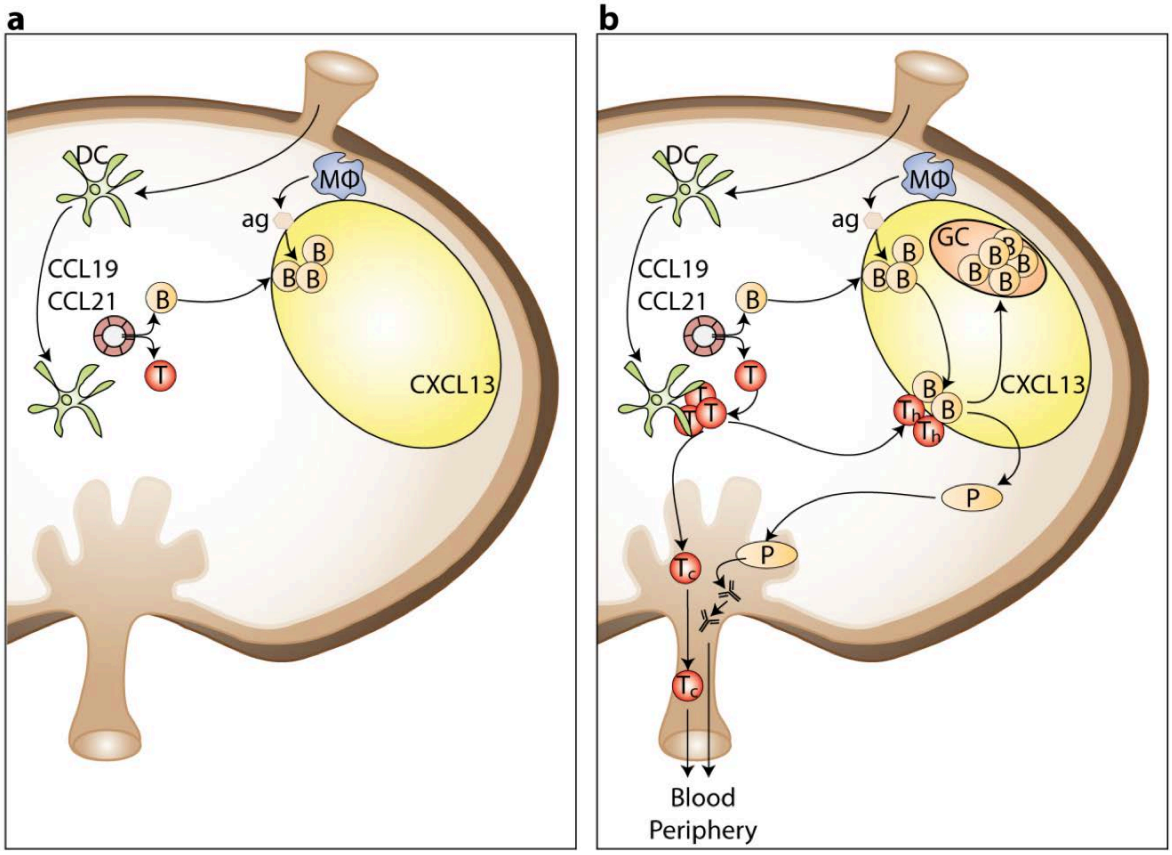

Figure 1.6 Cellular interactions in the LN that lead to the initiation of an adaptive immune response
(**a**) Naive recirculating lymphocytes enter the LN via HEVs, then CCR7$^+$ T cells (T) scan the CC21 and CCL19 rich T zone for antigen, while CXCR5$^+$ B cells (B) migrate to the CXCL13 rich B zone. Antigen-bearing CCR7$^+$ DCs enter through afferent lymphatic vessels and migrate into the T zone via interfollicular regions. SCS lining macrophages (MΦ) capture antigen (ag) from the lymph and transport it to the follicles. In addition, conduits transport soluble antigen into the T zone and the follicle. (**b**) After antigen encounter and the appropriate co-stimulatory signals, T cells start to proliferate and differentiate into effectors cells. Cytotoxic T cells (T_c) migrate to medulla, leave the LN through the efferent lymphatics and travel to the place of infection using the bloodstream. While some T helper cells (T_h) also migrate to the site of infection, others up-regulate CXCR5 and migrate to the T-B zone border. B cells encounter antigen in the follicles, subsequently up-regulate CCR7 and localize to the T-B zone border, where they interact with primed ag-specific T helper cells. Productive interaction with T helper cells induces the differentiation of activated B cells into short-lived plasmacells (P) that localize in the medulla. Only few primed B cells seed and establish the GCs, where they proliferate and undergo affinity maturation as well as class switching to become long lived high affinity antibody producing plasma cells. (Cyster, 2005; Shapiro-Shelef and Calame, 2005; Junt et al., 2008; Cyster, 2010).

1.3.2. T cell priming

As described above, naïve T cells are constantly entering the LN via the HEV and scan the LN for antigen-bearing DCs (figure 1.4a and 1.6). Multiple signals are needed for T cell priming: the first is the triggering of their T cell receptor (TCR) by MHC-peptide complexes and the second is co-stimulation by surface receptors and cytokines. The best characterized co-stimulatory pathway is the interaction of CD28, expressed on the T cell with CD80 (B7.1) and CD86 (B7.2), which are both up-regulated on activated DCs. In addition, cytokines such as type I IFN influences the outcome of T cell priming and this will be discussed in detail below (Williams and Bevan, 2007). The use of high resolution imaging of T cell APC interactions *in vitro* revealed the concept of the so-called immunological synapse (IS) formation. The IS is a supra-molecular complex consisting of a central TCR-peptide-MHC cluster (cSMAC = central supramolecular activation complex), surrounded by a peripheral SMAC (pSMAC) characterized amongst others by LFA-1 - ICAM-1 clusters (Fooksman et al., 2010). However, the formation of IS *in vivo* is still under debate (Sumen et al., 2004; Henrickson and von Andrian, 2007). In a first attempt to study T cell priming in a more physiological context Gunzer and colleagues used a three-dimensional collagen matrix to study T cell priming. Surprisingly, though T cells were efficiently activated, only short-lived and transient T - DC interactions could be observed, but rarely stable interactions or IS formation (Gunzer et al., 2000). The authors proposed the 'serial encounter model': T cells accumulate and integrate activating signals during short-lived interactions with APC and are only fully activated after having passed a certain threshold (Gunzer et al., 2000; Friedl and Gunzer, 2001). However, the physiological relevance of this model was heavily debated, as within SLO collagen fibres are almost completely sheathed from T cells (Dustin and de Fougerolles, 2001). As another interpretation of these results Dustin and colleagues proposed collagen to be a negative regulator of IS formation. This interpretation could explain why collagen and other ECM in LNs are typically not exposed to lymphocytes, but enwrapped by TRCs, in contrast to most other tissues (Dustin and de Fougerolles, 2001; Dustin et al., 2001).

The recent technical development of intra-vital microscopy finally allowed to directly observe T cell priming in real time *in vivo* (Bousso, 2008; Germain et al., 2008). Mempel and colleagues showed that T cell activation after subcutaneous injection of peptide-pulsed DCs can be divided into three distinct phases: First, T cells and DCs form short-lived interactions, which lead to the up-regulation of the activation markers CD69 and CD44 on the T cells. This is followed by the second phase in which T cells and DCs from long-lived conjugates leading to interleukin-2 (IL-2) and interferon-γ (IFNγ) production by primed T cells as well as the up-regulation of CD25. In the third phase T cells dissociate from DCs and rapidly proliferate until they leave the LN (Mempel et al., 2004; Henrickson and von Andrian, 2007). Depending on the experimental way of antigen-delivery different results could be observed: while antigen presented by migratory DCs from the skin induced short-lived and transient interactions, direct targeting of LN resident DCs resulted in immediate long-lived interactions (Mempel et al., 2004; Sumen et al., 2004; Miller et al., 2004b; Shakhar et al., 2005). Overall, a positive correlation seems to exist between the

stimulation strength (antigen availability, antigen affinity, co-stimulatory molecules etc.) and the induction of long-lasting T-DC interactions (Henrickson and von Andrian, 2007; Bousso, 2008; Germain et al., 2008). The first phase of short-lived transient interaction could be interpreted as time in which T cells gather information about the context of the infection: antigen-density, antigen-affinity, number of APCs and other features. This would give T cells the possibility to integrate all these information and might be essential for the induction of an immune response versus tolerance. One report using explanted LN showed that long-lasting T-DC interactions occurred in immunizing but not tolerizing conditions (Hugues et al., 2004). This could not be confirmed in a second study (Shakhar et al., 2005) in which the authors used the same system of antigen-delivery as the first report but the imaging was performed in the intact LN of the live mouse.

1.3.2.1 Role of T zone stroma in T cell priming

Several evidences suggest an influence of TRCs on T cell priming. As described, TRCs physically guide T cells in their migration, while DCs are associated with the TRC network (Lindquist et al., 2004; Bajenoff et al., 2008). In this way the TRC network 'forces' incoming naïve T cells to scan TRC-associated DCs for antigen (Luther et al., 2011). In addition, they produce the homeostatic chemokines CCL19 and CCL21, which not only influence T cell migration (as described earlier), but also act as co-stimulatory signals in T cell activation (Flanagan et al., 2004; Friedman et al., 2006). As described, CCR7 stimulation of DCs enhances their maturation, promotes dendrite formation, thereby increasing their surface for antigen presentation, and protects the cells from apoptosis (Sanchez-Sanchez et al., 2006; Mueller and Germain, 2009). During the course of an immune-response the expression of CCL19 and CCL21 appears to be down-regulated. This goes along with the down-regulation of the CCR7 receptor on activated T cells. The regulation of homeostatic chemokines in the immune response by TRCs might influence the balance between retention and egress of activated T cell from the LN (Mueller and Germain, 2009). In addition, lymphoid stroma was shown to influence the quality of the immune response. TRCs in mLN but not pLN express the vitamin A metabolite retinoic acid which induces on T cells primed in mLN the expression of the gut-homing receptors CCR9 and $\alpha 4\beta 7$ (Hammerschmidt et al., 2008).

1.3.2.2 T zone stroma as target of viral infection

Several intracellular pathogens were shown to infect TRCs, a prominent example being lymphocytic choriomeningitis virus (LCMV) (Mueller et al., 2007). In this context two different strains of LCMV have been examined: LCMV WE leads to acute infection which is effectively cleared, and LCMV clone 13 that establishes a chronic infection and generalized immunosuppression (Mueller et al., 2007). Both strains infect TRCs but only LCMV WE infection leads to cytotoxic T cell mediated destruction of the TRC network, which is inhibited by PD-L1 up-regulation on TRCs in the case of LCMV clone 13 infection (Mueller et al., 2007; Scandella et al., 2008). The loss of the splenic TRC network following LCMV WE infection was shown to lead to infection-associated immunodeficiency against secondary infections (Scandella et al., 2008). This illustrates the likely importance of an intact TRC network for the induction

of efficient immune responses. Other pathogens shown to infect TRCs include Leishmania donovani, Leishmania major, Simian immunodeficiency virus, Ebola virus, Marburg virus, Lassa virus and murine cytomegalovirus (Mueller and Germain, 2009; Junt et al., 2008). One could speculate that destruction of the TRC network might be one mechanism exploited by some pathogens to prevent the rapid induction of an adaptive immune response.

1.3.3 T cell differentiation

Although both CD8 and CD4 T cells need TCR triggering and co-stimulation to be primed, their requirement for full activation are distinct. Only short exposure to antigen is sufficient for CD8 T cells to initiate their proliferation and differentiation, while CD4 T cells need longer antigen-mediated stimulation for sustained proliferation (Williams and Bevan, 2007; Haring et al., 2006; Kaech et al., 2002).

1.3.3.1. Cytotoxic T cell differentiation

Naïve antigen-specific CD8 T cells expand dramatically after activation - up to 10.000 fold - (Haring et al., 2006) before differentiating into cytotoxic T cells. Interestingly, already within the first 1-3 days following acute infection, the expansion of cytotoxic T cells, their acquisition of effector function as well as memory development are programmed (Williams and Bevan, 2007; Haring et al., 2006). Optimal development of cytotoxic T cell responses need the presence of a third signal, besides TCR triggering and co-stimulation. This signal can be IL-12, IFNα/β or IFNγ (Williams and Bevan, 2007; Haring et al., 2006). There is an on-going debate about the need of CD4 T cell help for CD8 T cell responses. There exists a negative correlation between high levels of inflammation and the need of T cell help. So far most evidence suggests that CD4 help is dispensable for acute CD8 responses in an inflammatory setting, but is critical for robust memory formation (Williams and Bevan, 2007; Castellino and Germain, 2006).

Differentiated cytotoxic T cells leave the inflamed LN and travel to the side of infection. When cytotoxic T cells recognize peptide-MHCI complexes on pathogen-infected cells, their cytoskeleton is rearranged and a cytotoxic IS with the target cell is formed. As lytic granules are only released in the cleft of the cytotoxic IS, killing by cytotoxic T cells is highly specific to infected cells and leaves healthy neighbouring cells unaffected (Russell and Ley, 2002; Dustin and Long, 2010). Besides the secretion of effector cytokines, such as IFNγ or TNFα, cytotoxic T cells, use two different modes of eliminating target cells: Ca^{2+}- dependent perforin/granzyme release or Ca^{2+}-independent FasL (CD95-ligand) mediated killing. Both pathways induce apoptosis of the target cells (Russell and Ley, 2002; Barry and Bleackley, 2002; Dustin and Long, 2010). After completion of their task – ideally with the pathogen being cleared from the body – most cytotoxic effector cells undergo apoptosis, while a small pool of memory cells persists and mounts rapid responses following re-exposure to the pathogen (Williams and Bevan, 2007)

1.3.3.2. T helper cell differentiation

The differentiation of naïve CD4 T cells into effectors cells is much more complicated than that of CD8 T cells, as they can differentiate into several distinct T helper (T_H) subsets - T_{H1}, T_{H2}, T_{H17}, follicular T

helper cells (T_{FH}) - or into induced regulatory T cells (iT_{reg}). Different subsets produce distinct 'signature' cytokines and in this way control adaptive immune responses to different pathogens (figure 1.7): T_{H1} are important to control intracellular pathogens, while T_{H2} are critical for extracellular pathogens, for example helminthes. T_{H17}, which were originally identified due to their role in autoimmune diseases, such as experimental autoimmune encephalomyelitis (EAE), are also important in the protection against microbial challenges, such as extracellular bacteria and fungi. (Zhu and Paul, 2008; Zhu et al., 2010). In contrast to the other subsets, CXCR5+ T_{FH} are resident in the B follicle where they provide B cell help. They are essential for the generation of plasma cells producing high affinity antibodies and memory B cells (Crotty, 2011). iT_{reg} are important for maintenance of self-tolerance as well as for the regulation of immune responses and will be discussed in detail below.

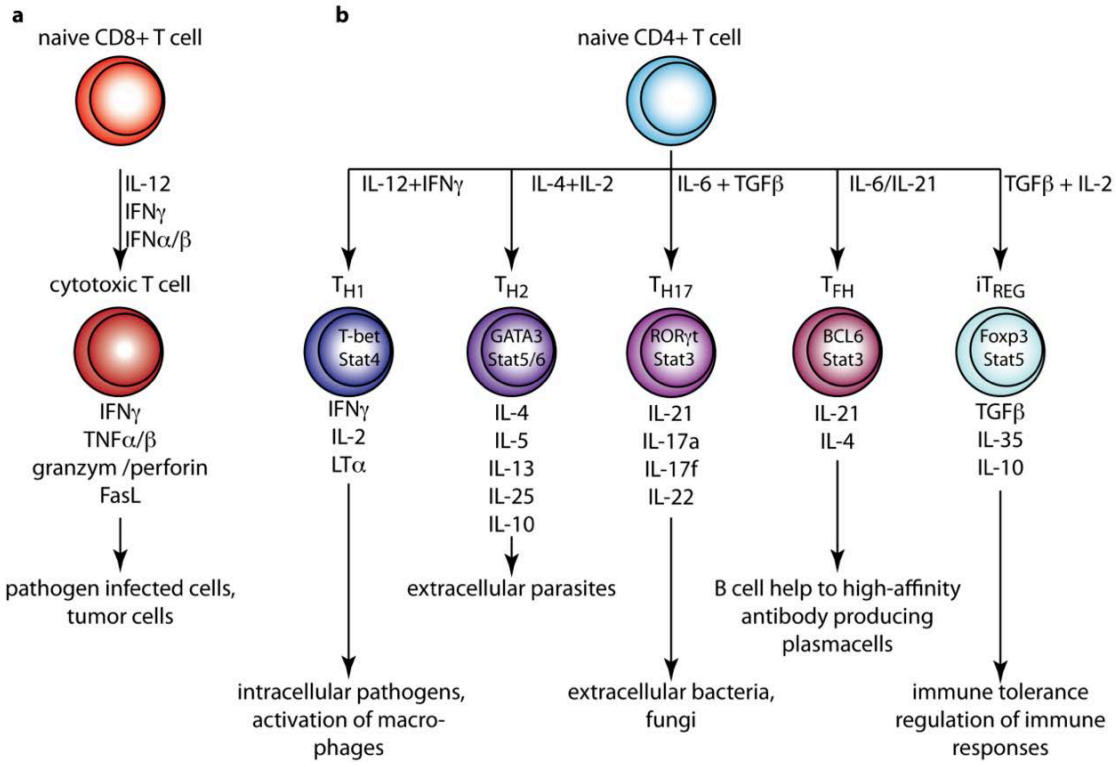

Figure 1.7: Naïve T cells differentiate into distinct subsets
TCR triggering and co-stimulatory signals lead to the expansion and differentiation of naïve T cells. (**a**) For optimal CD8 T cell responses (expansion, differentiation and memory formation) an additional third signal is needed, which can be delivered by IL-12, IFNγ or IFNα/β. Fully differentiated $CD8^+$ cytotoxic T cell travel to the place of infection, where they induce apoptosis in target cells either by the release of lytic granules (containing granzymes and perforin) or mediated via the Fas-Ligand pathway. In addition, they secrete cytokines such as IFNγ or TNFα/β. (Williams and Bevan, 2007; Haring et al., 2006; Russell and Ley, 2002; Barry and Bleackley, 2002) (**b**) Naïve $CD4^+$ T cells have the potential to differentiate into at least 5 different subsets: T_{H1}, T_{H2}, T_{H17}, T_{FH} or iT_{REG} dependent on the cytokines present during priming, for example IL-12 and IFNγ induce T_{H1} differentiation. For each of the subsets master transcription factors have been described, for example T-bet and Stat4 are essential for T_{H1}. Recent evidences suggest Blimp-1 to have similar function in CD8 differentiation, however also the transcription factors T-bet, Eomes and BCL-6 are important (Belz and Kallies, 2010; Kallies et al., 2009). Each T_H subset expresses 'signature' cytokines, for example IFNγ production by T_{H1}, and is important in the clearance of distinct pathogens (Zhu and Paul, 2008; Zhu et al., 2010; Crotty, 2011).

The differentiation into a distinct CD4 subset depends among other factors on the cytokine environment during priming, which induces a specific 'master' lineage transcription factor determining the fate of a primed CD4 T cell (Figure 1.7). However, the differentiation into the CD4 effector lineages is not irreversible, as considerable plasticity between the different subsets was described (Murphy and Stockinger, 2010).

1.3.4. B cell activation and differentiation

The B cell receptor (BCR), in contrast to the TCR, binds intact antigens in their native form. Different cell types were shown to present antigen to B cells: SCS macrophages, DCs and FDCs (Cyster, 2010). Two types of B cell antigens exist: T-cell dependent and T cell independent antigens. The latter are antigens which cross-link the BCR leading to B cell activation and differentiation into IgM-producing plasma cells (Shapiro-Shelef and Calame, 2005). When the BCR recognizes T-dependent antigens in the follicle, the B cell up-regulates CCR7, while CXCR5 expression levels remain high (Figure 1.6b). This leads to the re-localization of B cells to the T-B border where they encounter primed antigen-specific T helper cells that have up-regulated CXCR5 after TCR triggering (Cyster, 2005). The majority of B cells directly differentiates into short lived plasma cells, which localize to the medulla while a fraction of activated B cells establishes GCs. During the GC reaction B cells strongly proliferate, accompanied by affinity maturation and immunoglobulin class switching, for which the help from T_{FH} is essential (Crotty, 2011). During the GC reaction long-lived plasma cells producing high-affinity-antibodies are generated that leave the LN via efferent lymphatic vessels and home via the bloodstream to the BM and mucosal surfaces, where they can reside for years. A second result of the GC reaction are memory B cells (Cyster, 2005; Shapiro-Shelef and Calame, 2005).

1.4. Control of immune responses and tolerance induction

Antigen receptors of lymphocytes (B and T cell receptor) are generated in a random fashion by V (D) J recombination. This process generates specific receptors against millions of potential antigens but at the cost of producing self-reactive lymphocytes as well. To prevent autoimmune disease, self-reactive T and B cells must be eliminated or silenced. The immune system has developed several ways to ensure this. Typically two types of tolerance induction are distinguished: central and peripheral tolerance. Central tolerance is established in the BM (B cell tolerance) and the thymus (T cell tolerance). As the work of this thesis is mostly focused on T cells, only establishment of T cell tolerance will be discussed in more detail. In the thymus T cell precursors that have rearranged their TCR undergo a positive and negative selection process. First, they have to recognize self-peptide-MHC complexes with low avidity to be positively selected. Second, autoreactive T cells that recognize self-peptide-MHC complexes with high avidity are negatively selected (Anderson et al., 2006; Starr et al., 2003; Palmer, 2003). Medullary thymic epithelial cells (mTEC) and medullary DCs express a wide range of peripheral tissues-restricted antigens (PTA), a process called promiscuous gene expression. The expression of many but not all PTA is regulated by the transcription factor autoimmune regulator (Aire). As a consequence absence or mutations in Aire lead to the development of autoimmune disease (Anderson et al., 2007; Kyewski and Klein, 2006; Metzger and Anderson, 2011). Self-reactive thymocytes whose TCR recognizes these PTA presented by mTEC or DCs in the context of MHC molecules, are eliminated (= 'negative selection'). Though central tolerance is quite effective, it is not complete and T cells expressing low-affinity TCR against self-antigen are found in the peripheral T cell pool (Kyewski and Klein, 2006). To avoid autoimmunity by these self-reactive T cells various peripheral tolerance mechanisms prevent their activation.

1.4.1. Tolerance induction by T cell intrinsic mechanisms or mediated by DCs

Early experiments *in vitro* showed that TCR triggering without co-stimulation leads to a state of unresponsiveness to antigen restimulation, termed anergy. More recent studies indicated that it is not only the absence of co-stimulation but rather signalling through different receptors, such as the CD28 homologue CTLA-4 (cytotoxic T-lymphocyte-associated antigen 4) or PD-1 (programmed cell death 1) (Walker and Abbas, 2002; Allen et al., 2011; Bour-Jordan et al., 2011; Fife and Bluestone, 2008). In addition to anergy, also the induction of apoptosis serves to eliminate self-reactive T cells in a process called activation induced cell death (AICD). Experiments with knock out mice showed that among other molecules CD95 and IL-2 are crucial for AICD (Walker and Abbas, 2002).

Dendritic cells play a major role in peripheral self-tolerance induction. DCs constantly capture antigen, for example from dying cells, and process it. The presentation of self-peptides as well as harmless environmental peptides on MHC molecules in steady-state was suggested to play a major role in peripheral tolerance induction. When apoptotic cells containing OVA were injected into mice, DCs took up OVA and presented it in the LN to T cells. Transferred OVA-specific T cells proliferated first but were then deleted from the mice showing that presentation of self-peptides acquired from dying cells and

presented by DCs in steady-state conditions induces tolerance (Liu et al., 2002; Steinman et al., 2003). Studies in which antigen was directly targeted to DCs with or without maturation stimuli indicated that the same DC can induce tolerance or immunity depending on its maturation status. These studies made use of the endocytosis receptor DEC-205 expressed by LN resident DCs. Antigen coupled to an anti-DEC-205 antibody is efficiently taken up by DCs and presented by them. Injection of antigen coupled to anti-DEC-205 leads to induction of tolerance by clonal deletion: antigen-specific T cells divide several times before they are eliminated. In contrast, co-injection of anti-CD40 antibody that induces DC maturation leads to a robust immune response (Turley et al., 2010; Steinman et al., 2003). Recently, evidence was provided for the existence of suppressive or regulatory DC subsets. These DCs can directly inhibit T cell activation by producing suppressive molecules, such as indoleamine 2,3-dioxygenase (IDO) or nitric oxide (NO), or indirectly by promoting the development of regulatory T cells (T_{REG}). The regulation and development of the regulatory DC subsets is still not fully understood and remains to be elucidated (Steinman et al., 2003; Turley et al., 2010; Svensson and Kaye, 2006).

1.4.2. Regulatory T cells

T_{REG} are important players ensuring peripheral tolerance: depletion or disruption of T_{REG} function leads to development of autoimmune disease in mice and men (Sakaguchi et al., 2008). Natural nT_{REG} arise during T cell development in the thymus and are thought to represent a separated lineage to cytotoxic T cells and T helper cells. They constitutively express CD4, CD25, CTLA-4 and GITR (glucocorticoid-inducible tumor necrosis factor receptor). The transcription factor FoxP3 (forkhead box P3) and IL-2 were shown to be essential for their development and function (Sakaguchi et al., 2008; Bluestone and Abbas, 2003; Belkaid and Rouse, 2005; Shevach, 2006).

However, as described above, naïve peripheral T cells can be converted to so called inducible iT_{REG} in a TGFβ (transforming growth factor beta)-dependent manner, which is greatly enhanced by retinoic acid (Allen et al., 2011; Sakaguchi et al., 2008). Though FoxP3 expression in mice correlates with suppressive T cell features, this is not uniformly the case in humans (Shevach, 2006). In addition $FoxP3^-$ $CD4^+$ IL-10-producing T cells have been identified (termed T_{R1}), which exert suppressive activity. *In vitro* T_{R1} can be generated by antigen stimulation in the presence of IL-10, while *in vivo* they are produced during certain infections (Shevach, 2006).

T_{REG} show different mechanisms to suppress immune responses: secretion of immune-suppressive cytokines, such as IL-10; cell-contact-dependent suppression, for example via CTLA-4; functional modification or killing of APC, for example stimulation of DCs to induce their expression of IDO (Sakaguchi et al., 2008; Vignali et al., 2008). Besides their role in peripheral tolerance, T_{REG} are important to regulate excessive immune responses, thereby preventing tissue-destruction (Belkaid and Rouse, 2005).

1.4.3. Stromal cells in SLO as new member of peripheral tolerance promoting cell types

Only in recent years, different LN stromal cell types were demonstrated to express and present PTAs. One of the first observations was made in a study from Lee and colleagues using the iFABP-OVA model, in which a truncated OVA form is expressed under the control of the small intestine specific iFABP (intestinal fatty-acid binding protein) promoter. Surprisingly, TRCs in non-draining LN showed OVA expression and transfer of OVA specific CD8+ T cells (OT-I T cells) led to their clonal deletion (Lee et al., 2007; Turley et al., 2010). Several studies showed that multiple PTA are expressed by TRCs under steady-state conditions (Turley et al., 2010). Interestingly, not only TRCs but also other LN stroma cells, such as LECs, BECs and epithelial cells within the gp38-CD31- population were described to express PTA (Fletcher et al., 2010, 2011b; Turley et al., 2010). Promiscuous gene expression by mTEC is in part controlled by the transcription factor Aire (Metzger and Anderson, 2011; Anderson et al., 2007; Kyewski and Klein, 2006). Though a rare subset of Aire expressing epithelial cells were found in the T zone of LNs (Metzger and Anderson, 2011), TRCs, LECs and BECs are negative for Aire but express Deaf1 (deformed epidermal autoregulatory factor 1) which was shown to upregulate PTA expression. Similar to DCs LN stroma cells express TLR 3 but in contrast to DCs stimulation with its ligand led to reduced capacity in stimulating T cell proliferation (Fletcher et al., 2010).

In addition, stromal cells from the spleen have been shown to promote the development of suppressive DCs. Svensson and colleagues showed that *ex vivo* isolated splenic stromal cells support the development of CD117+ Lin- precursor cells into IL-10 producing suppressive DCs (Svensson et al., 2004). In another report, Zhang and colleagues showed that LPS-activated bone-marrow derived DCs (BMDCs) co-cultured with cell lines form neonatal splenic stroma induces suppressive DCs in a cell-cell contact dependent manner, which produce NO and suppress T cell responses (Zhang et al., 2004). In both studies, the splenic stromal cells were only poorly characterized and it is unclear whether these were FRCs-like cells or not. The *in vivo* counterpart of suppressive DCs was identified, though their dependency on SLO stromal cells *in vivo* remains to be elucidated (Zhang et al., 2004; Svensson et al., 2004; Svensson and Kaye, 2006).

1.4.4. Regulation of immune responses by mesenchymal stem or stromal cells

Mesenchymal stem cells (MSCs) were originally described as plastic-adherent stromal cells isolated from the BM with the capacity to differentiate into multiple mesodermal lineages, including bone, fat and cartilage. Though MSCs show features such as self-renewal and multi-lineage differentiation, it is debated whether they truly are stem cells. Therefore it was suggested that the term multipotent mesenchymal stromal cells (abbreviation as well MSC) is more accurate (Nauta and Fibbe, 2007; Uccelli et al., 2008; Haniffa et al., 2009; Sato et al., 2010).

In addition to BM, many other tissues contain MSCs, including adult adipose tissue, umbilical cord blood and several fetal tissues (Nauta and Fibbe, 2007). So far no unique surface markers for MSCs have been

identified, however, they are negative for classical hematopoietic (CD45) and endothelial markers (CD31), while they show expression of unspecific markers, such as CD105 or CD44 (Keating, 2006; Nauta and Fibbe, 2007; Uccelli et al., 2008). Experimentally, their identity is usually defined by plastic-adherence and the capacity to differentiate into osteocytes, adipocytes and chondrocytes (Nauta and Fibbe, 2007). In the last 20 years the immune-suppressive features of MSCs were established in many clinical studies, for example to suppress graft-versus-host disease (Haniffa et al., 2009; Sato et al., 2010). Different ways of MSC-mediated suppression have been described (figure 1.8).

1.4.4.1. MSC-mediated modulation of DC function

MSCs were shown to interfere with DC differentiation, maturation and function (figure 1.8b). Co-culture of DCs with MSCs decreased their expression of co-stimulatory molecules and pro-inflammatory cytokines and skewed their phenotype towards regulatory DCs producing IL-10. These effects are mediated by soluble factors, e.g. IL-6, M-CSF, PGE_2 (Uccelli et al., 2008; Nauta and Fibbe, 2007). A recent report also showed that MSCs decrease the ability of DCs to form productive immunological synapses with T cells (Aldinucci et al., 2010).

1.4.4.2. MSC-mediated suppression of T cell activation

Numerous reports described the direct suppressive effect of MSCs on T cell activation (figure 1.8a). MSCs inhibit T cell proliferation induced by mitogens, anti - CD3/28 antibodies, allogeneic cells or antigen presented by APC. Interestingly, inhibition can be mediated by autologous and allogeneic MSCs (Uccelli et al., 2008; Nauta and Fibbe, 2007; Sato et al., 2010). Though the mechanism of suppression has been studied extensively, it is controversial and incompletely understood. The discrepancies in the mechanism of suppression may be due to the isolation of different MSCs types from various tissues as well as different culture and stimulation conditions. The lack of unique MSCs markers make it difficult to have a clear standard of MSC type, including its differentiation or activation state (Nauta and Fibbe, 2007; Uccelli et al., 2008; Sato et al., 2010; Keating, 2006). MSCs show high similarity to 'ordinary' fibroblasts and several reports showed that fibroblasts isolated from adult tissues indeed showed the same suppressive effect on T cell proliferation as MSCs (Haniffa et al., 2007, 2009; Jones et al., 2007).

Transwell experiments indicate the involvement of cell-cell contact as well as soluble factors. Various molecules were shown to be produced by MSCs and to mediate suppression of T cell proliferation, such as TGFβ, IL-10, PGE_2, hepatocyte growth-factor (HGF), NO, IDO and others (figure 1.8). Some of these factors are constitutively produced by MSCs, while the expression of others such as NO and IDO is triggered by soluble factors, such as IFNγ derived from activated T cells (Uccelli et al., 2008; Sato et al., 2007; Keating, 2008; Sato et al., 2010). In a recent report MSCs were shown to express TLRs. Furthermore, MSC triggering via TLR3 and 4 was shown to reduce the suppression of T cell activation, thus suggesting a mechanism of dampening the suppressive capacity of MSCs during infections (Liotta et al., 2008).

However, blocking studies suggest that not a single factor produced by MSCs is responsible for suppression but rather the summary of several factors, though the exact contribution remains to be determined. (Uccelli et al., 2008; Nauta and Fibbe, 2007; Sato et al., 2010). Most studies used *ex vivo* expanded MSC, therefore, the physiological role of MSC mediated suppression is not really known. One hypothesis is that MSCs create an immune-privileged site in the BM to protect stem cells from potential harmful immune responses. In addition, as MSCs are found in the amniotic fluid, fetal blood, umbilical blood and other fetal tissues a role in fetal tolerance was suggested (Nauta and Fibbe, 2007).

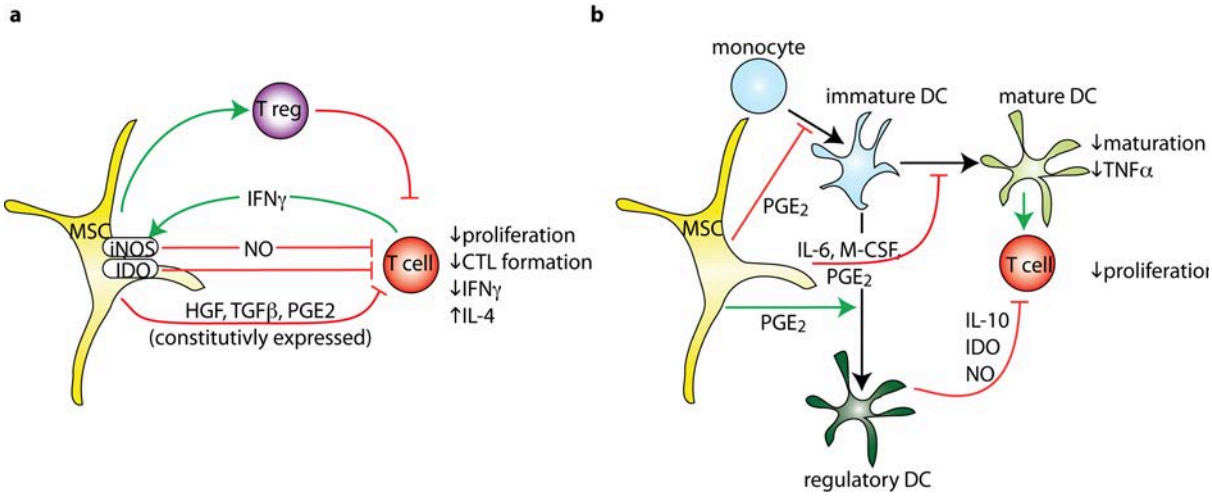

Figure 1.8: Mechanism of T cell suppression by MSCs
Different mechanisms have been described that contribute to suppression of T cell activation by MSCs. (**a**) Suppressive factors by MSCs can directly act on the T cells. These factors are either constitutively expressed or induced, typically by IFNγ stimulation. The latter creates a negative-feedback loop, as IFNγ is produced by activated but not naïve T cells. In addition MSCs were implicated in inducing T_{REG} development. (**b**) Suppressive factors by MSCs can indirectly act on T cells such as by altering DC maturation or activity. PGE_2 produced by MSCs inhibits the differentiation of monocytes into DCs and together with other MSC-produced factors interferes with DC maturation. In addition it favours differentiation of immature DCs into regulatory IL-10 producing DCs (Uccelli et al., 2008; Nauta and Fibbe, 2007; Haniffa et al., 2009; Sato et al., 2010).

1.5. Three dimensional cell cultures as basis for the establishment of an artificial LN

Most laboratories culture cells in conventional two-dimensional (2D) cell culture dishes. However*, in vivo* cells are embedded in a three-dimensional (3D) environment made by ECM molecules and resident stromal cells. To combine the advantages of *in vitro* culture, such as the ease of manipulation, with a more *in vivo* like environment, various 3D cell culture systems have been established (Pampaloni et al., 2007; Pedersen and Swartz, 2005; Haycock, 2011). Comparison of cells cultured in 2D or 3D revealed differences in morphology, matrix adhesion, cellular migration strategies, gene and protein expression (Pedersen and Swartz, 2005; Grinnell, 2003; Griffith and Swartz, 2006; Rhee, 2009). One simple approach to culture cells in 3D is to embed them in collagen gels, often mixed with other ECM molecules, such as the commercially available matrigel, that is a mix of basement membrane proteins produced by the tumor line EHS, such as laminin and collagen IV (Kleinman and Martin, 2005). However, matrix composition as well the physical properties such as the stiffness influence the cell behaviour. For example, depending on the matrix stiffness fibroblasts cultured in collagen gels show different cell morphology ranging from dendritic to bipolar appearance (Griffith and Swartz, 2006; Grinnell, 2003; Rhee, 2009; Kobayashi and Watanabe, 2010).

The culture of cells in 3D systems is the basis for the development of artificial organs *in vitro* and *in vivo*. Reconstruction of lymphoid tissues *in vitro* is of great interest, as it would allow the study of haematopoiesis or immune responses in a tightly controlled environment. Furthermore, due to the simplicity of *in vitro* cultures they would allow the rapid screening of drugs and their influence on immune cells. Giese and colleagues reported in 2006 the establishment of a human artificial LN: They established a bioreactor allowing long-term culture of DCs with T and B cells embedded within an agarose matrix (Giese et al., 2006). In a second study, Giese and colleagues reported that immunization of this human artificial LN with a commercially available Hepatitis A vaccine leads to a rapid proinflammatory response, as measured by increased levels of TNFα. Furthermore, after re-challenge with antigen T_{H2} cytokines are detected and plasma cells secreting antigen-specific antibodies are produced. In addition, the response to the vaccine could be abrogated by administration of an immune-suppressive drug. Therefore this human artificial LN is a valuable tool for testing immune function after vaccination *in vitro* (Giese et al., 2010). Currently, this system lacks the presence of stromal cells residing within a normal LN, which might influence the immune response.

The establishment of artificial LN and their transplantation is of great interest for the application in medicine. For example such LNs could be used to boost immune responses in immune-deficient patients or to induce an anti-tumor response. In a study from Watanabe and colleagues, a collagen-sponge in which a thymus derived LTα producing stromal cell line was embedded was transplanted under the kidney capsule. A few weeks after transplantation lymphocyte infiltrates in the transplants organized in distinct B and T cell areas and this was enhanced by the addition of activated DCs prior to

transplantation. Furthermore, the development of FDCs as well as the vascularisation of the transplants was observed (Suematsu and Watanabe, 2004). In a follow-up study, Okamoto and colleagues showed that these artificial LN supported adaptive immune responses which were maintained after transplantation into immune-deficient hosts, making the adaptation of this system for use in humans very attractive (Okamoto et al., 2007).

1.6. Aims of this thesis

Establishment and characterization of TRC clones and cell lines in 2D and 3D culture

Due to the lack of specific markers and efficient isolation protocols, TRCs were for a long time ignored by immunologists. These technical issues have been partially solved in the last years (Link et al., 2007), but TRCs represent rare cells (approximately 0.1% of the total LN population), making it difficult to isolate sufficient numbers to further characterize TRC function *in vitro*. Therefore, TRC clones and lines were established to obtain an abundant source of these cells. The surface marker profile of TRC clones and lines resembles closely that of *ex vivo* isolated TRCs and in addition they produce ECM molecules. However, the mRNA levels for *Ccl19, Ccl21* and *Il-7* are very low and could not be restored by stimulating the cells with different cytokines. To study TRC biology in a more physiological situation, a 3D culture system with TRC clones/lines was established and a more *in vivo* like cell morphology was observed, however CCL19, CCL21 and IL-7 levels remained low. When flow was applied to TRCs cultured in 3D, CCL21 levels were increased though not to physiological levels. In an attempt to reconstruct the lymphoid T zone *in vitro*, antigen-specific T cells and antigen-loaded dendritic cells were added to the 3D culture system and T cell activation could be observed, although it was reduced in presence of TRC. (Project described in results 2.1).

Characterization of the precise role of TRCs in T cell priming

Adaptive immune responses are initiated when T cells encounter antigen on dendritic cells (DCs) in T zones of secondary lymphoid organs. T zones contain a 3-dimensional scaffold of TRCs but currently it is unclear how TRCs influence T cell activation. Several evidences suggest TRCs as positive regulators of the immune response, but recently they were also implicated in peripheral tolerance induction. To define their precise role, we established a T cell activation assay in 2D culture, in which we studied T cell priming in presence or absence of TRCs. Surprisingly, TRCs attenuated $CD8^+$ T cell proliferation and differentiation. This was confirmed with several distinct TRC lines and *ex vivo* isolated TRCs. Studies with pharmacological inhibitors and blocking antibodies identified iNOS (inducible nitric oxide synthase) -responsible for NO production- and COX2 -responsible for prostaglandin production, including PGE_2- as mediators of this suppression. *In vitro* IFNγ produced by activated T cells was shown to induce iNOS in TRCs, which was further enhanced in the presence of DCs. This observation was supported by the transient induction of iNOS expression in TRCs and DCs upon VSV (vesicular stomatitis virus) infection of WT mice. VSV infected iNOS knock out mice showed an exaggerated primary T cell response, consistent with the notion of iNOS being an attenuator of strong immune responses. (Project described in results 2.2).

2. Results

2.1 Establishment and characterization of TRC clones and lines in 2D and 3D culture*

Summary

TRC represent are rare stromal cell population in the LN. To obtain an abundant source of these cells for their further functional characterization, TRC clones and lines were established. Both clones and lines show a fibroblastic phenotype, express a surface marker profile comparable to *ex vivo* TRC and produce extracellular matrix molecules. However, expression of *Ccl19*, *Ccl21* and *IL-7* was lost upon *in vitro* culture and could not be restored by cytokine stimulation. When TRC clones or lines were cultured in a three-dimensional (3D) cell culture system, their morphology changed and successfully reproduced the networks seen for TRC *in situ*. 3D culture *per se* did not restore the cytokine production but adding fluid flow restored some of it.

* Partially based on: Tomei AA, Siegert A, Britschgi MR, Luther SA, Swartz MA (2009): Fluid flow regulates stromal cell organization and CCL21expression in a tissue-engineered lymph node microenvironment, Journal of Immunology 183, 4273-4283

2.1.1. TRC clones

For a long time, stromal cells in the LN T zone have been neglected by immunologist, partially due to technical difficulties in working with these cells, notably the lack of isolation protocols and specific surface markers. After histological analysis of LN sections to identify reliable TRC marker combinations, A. Link established an isolation protocol and found a combination of markers (CD45$^-$ CD35$^-$ CD31$^-$ gp38$^+$) allowing the identification of TRC in cell suspension. This allowed for the first time the detailed analysis of TRC on a single cells level (Link et al., 2007). However, with less than 0.5% of the total LN population, TRC represent a rare cell population, making it technically tedious to perform experiments with *ex vivo* isolated TRC. To this end, we have set out to generate cell clones and later lines (see 2.1.2) to have an abundant source of TRC.

Before the start of my thesis work M. Britschgi and A. Link in our laboratory successfully established TRC clones from pLN of p53$^{-/-}$ and p19arf$^{-/-}$ mice (Tomei et al., 2009b) (partially unpublished). Both, p53 and p19, are tumour suppressor genes typically expressed in fibroblasts and we thought the lack of them will give the cells a first 'hit' with additional genetic modifications allowing their immortalization. To establish TRC lines, pLN were collagenase digested and the adherent cells cultured over several weeks. Surprisingly, in each case cells with a TRC-like phenotype outgrew the cultures. From some of these lines, TRC clones were established by limiting dilution.

2.1.1.1. Several features are preserved in TRC clones, but *Ccl19, Ccl21* and *Il-7* expression are lost

M. Britschgi performed a first surface phenotype characterization of different TRC clones by flow cytometry (table 2.1.1). Here we will focus on two selected clones from pLN, the p53$^{-/-}$ clone H7. 2A10 and the single p19arf$^{-/-}$ clone that express gp38 (podoplanin) but lack expression of the hematopoietic marker CD45.

Surface marker	*ex vivo* TRC	p53$^{-/-}$ clone	p19arf$^{-/-}$ clone	Surface marker	*ex vivo* TRC	p53$^{-/-}$ clone	p19arf$^{-/-}$ clone
CD45	-	-	-	BP-3	++	-	+/-
CD19	-	-	-	ICAM-1 (CD54)	++	+	++
CD11b	-	-	-	VCAM-1 (CD106)	++	+++	+++
PECAM (CD31)	-	-	-	PDGF-Rα (CD140a)	+++	++	++
CD35	-	-	-	PDGF-Rβ (CD140b)	++	+	+
CD105 (Endoglin)	++	+	++	LTβ–R	++	+++	+++
gp38	+++	+++	+++	TNF-R1	++	++	++

Table 2.1.1: Surface phenotype of TRC clones from naive pLN
Flow cytometric analysis of *ex vivo* TRC, the p53$^{-/-}$ TRC clone H7. 2A10 and the p19$^{-/-}$ TRC clone. '-' = no expression; '+' peak shift below 0.5 log; '++' peak shift between 0.5 and 1 log; '+++' peak shift above 1 log, all in relation to the no primary antibody control. (Analysis done by M. Britschgi and S. Siegert)(Tomei et al., 2009b)

The two clones express ICAM-1 and VCAM-1, though expression levels are slightly higher for VCAM-1 as compared to *ex vivo* TRCs and in the case of the p53$^{-/-}$ clone lower for ICAM-1. Furthermore, the expression of the mesenchymal cell markers PDGF-Rα and PDGF-Rβ is preserved (figure 2.1.1a).

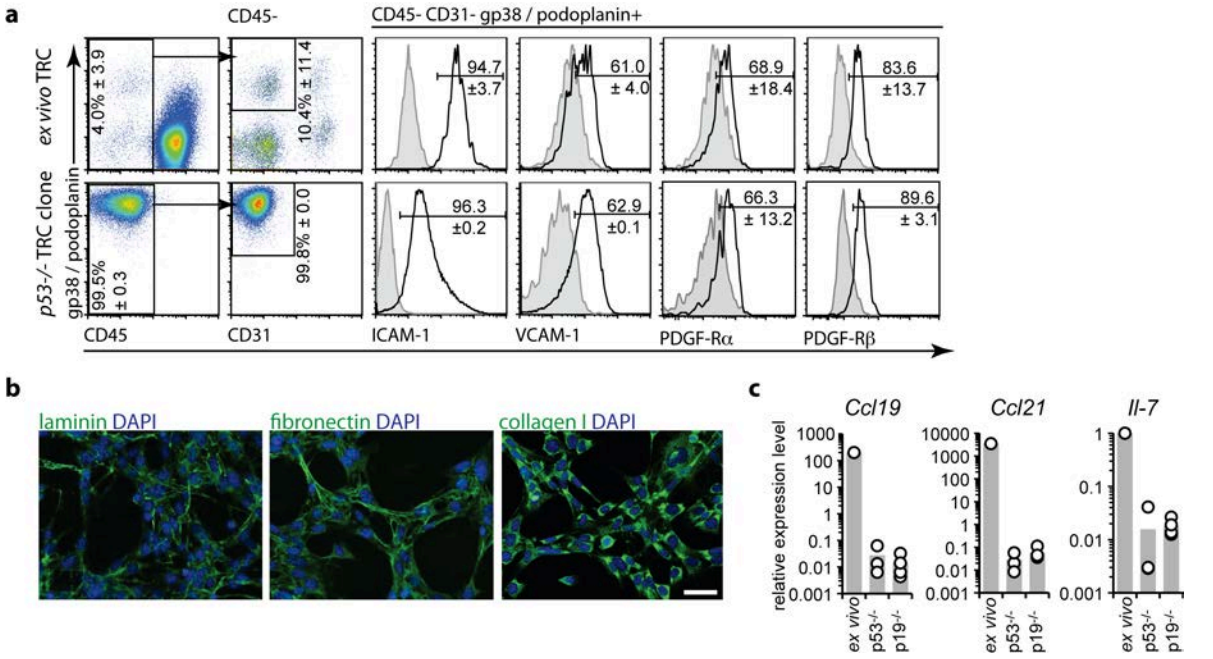

Figure 2.1.1: TRC clone phenotype
(**a**) Flow cytometric analysis of *ex vivo* isolated TRCs (upper panels) compared with the p53$^{-/-}$ TRC clone H7.2A10 (lower panels). Comparable results were obtained with the p19arf$^{-/-}$ clone. After dead cell exclusion, cells were analyzed for CD45 versus gp38 expression (1st column), CD45- cells were then further analyzed for gp38 (podoplanin) versus CD31 expression (2nd column). Histograms show the percentage of positive cells (± standard deviation) for the indicated markers on live CD45^{-} CD31^{-} gp38^{+} TRCs (Tomei et al., 2009a). (**b**) Immunohistochemical analysis of ECM production: The p53$^{-/-}$ clone was cultured for 3 days in chamber slides. After fixation of cells, laminin, fibronectin and collagen were labelled with antibodies (all shown in green). DAPI^{+} nuclei are shown in blue. Comparable results were obtained with the p19arf$^{-/-}$ clone. Scale bar 50µm. (**c**) Quantitative RT-PCR analysis of the two TRC clones (p53$^{-/-}$ and p19arf$^{-/-}$) for *Ccl21, Ccl19* and *Il-7* transcripts. Bar graphs show the relative expression level relative to the average of two housekeeping genes (*Hprt* and *Tbp). Ex vivo* TRCs are as shown previously in (Link et al., 2007).

In vivo TRCs are thought to be the major producers of ECM molecules and responsible for conduit formation. When TRC clones were cultured in chamber slides, laminin, fibronectin and collagen type-I proteins were detected by immunofluorescence (figure 2.1.1b). While laminin and fibronectin were part of intracellular as well as extracellular fibres, collagen-I was only found in intracellular compartments. This indicates that although collagen-I is produced it is not secreted. A main feature of TRCs *in vivo* is their expression of CCL19, CCL21 and IL-7; however this feature was lost in TRC clones (figure 2.1.1c). Together, these studies established that it is fairly easy to establish a TRC clone (or line) with a TRC-like surface phenotype and matrix production, but that additional factors are required to maintain other functions like cytokine expression.

2.1.1.2. Stimulation of TRC clone with recombinant cytokines does not restore *Ccl19, Ccl21* and *Il-7* expression

Cytokines such as TNFα and LTαβ are thought to regulate TRC development and activity *in vivo* including the induction of CCL19 and CCL21 expression (Cyster, 2005; Katakai et al., 2004; Schneider et al., 2004). Katakai and colleagues showed that stimulation of LN-derived TRC clones with TNFα up-regulates expression of CCL4, CCL5, CCL20 and CXCL10, but not CCL19 and CCL21. In addition, combined signalling via TNF-R and LTβ–R was shown to enhance ER-TR7+ ECM network formation (Katakai et al., 2004). Our hypothesis was that the low expression of CCL19, CCL21 and IL-7 in our TRC clones might be due to the lack of positive regulators *in vitro*. To test this hypothesis, TRC clones were stimulated with different recombinant cytokines to see whether the CCL19, CCL21 and IL-7 expression can be restored. When transcripts of TRC clones were analysed after stimulation with cytokines or agonistic antibody (TNFα, LTα3, anti–LTβ–R, IL-1α, IL-13, IL-6, TGFβ, IFNγ and PDGF-BB) for 16h, no changes in CCL19, CCL21 and IL-7 could be detected (not shown). In addition to analysis of cytokine transcripts, flow cytometric analysis was performed to detect potential phenotypic changes. Only stimulation with TNFα for 16 or 40h increased VCAM-1 expression (figure 2.1.2), while other tested markers (ICAM-1, CD31, CD35 and BP-3, as well as cell cycle analysis) remained unaffected (data not shown). Clones remained negative for MAdCAM-1, PNAd, CD35 and CD31 expression, even after cytokine stimulation. This suggests that TRC clones did not differentiate into other cell types, such as $CD35^+$ FDCs or $MAdCAM\text{-}1^+$ MRCs. Overall, the results indicate that simple re-stimulation of TRC clones with one cytokine at a time, including TNFα or LTαβ, was not sufficient to restore production of CCL19, CCL21 or IL-7.

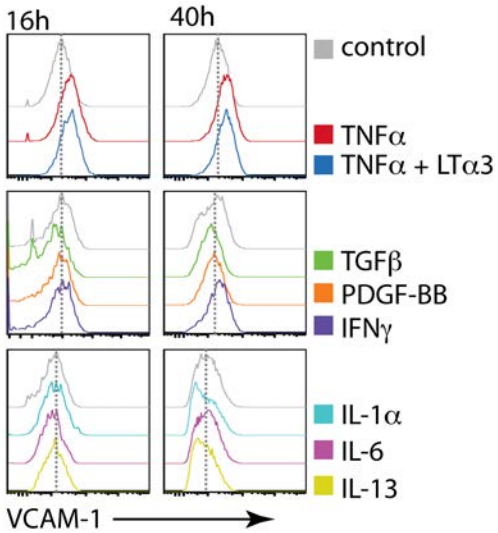

Figure 2.1.2: TNFα stimulation of TRC clone increases VCAM-1 expression
The p53-/- clone H7.2A10 was stimulated with indicated cytokines for 16 or 40h, and then cells were analysed by flow cytometry. Histograms show VCAM-1 expression on living CD45-gp38+ cells. Used concentrations: 10ng/ml TNFα, 10ng/ml LTα3, 10ng/ml TGFβ, 20ng/ml PDGF-BB, 10ng/ml IFNγ, 10ng/ml IL-1α, 25ng/ml IL-6, and 50ng/ml IL-13.

2.1.1.3. TRC clones cultured in a 3D culture system show *in vivo* like morphology and reticular network formation

Various cell types adopt a more *in vivo* like phenotype and function when grown in a 3D rather than 2D culture system (Pedersen and Swartz, 2005; Grinnell, 2003; Rhee, 2009). There are several different ways to culture cells in 3D. Most approaches use a gelatinous matrix to embed the cells, e.g. collagen, Matrigel (mixture of different ECM components) (Kleinman and Martin, 2005) or fibrin (Pedersen and Swartz, 2005; Haycock, 2011). To test whether TRC clones behave more *in vivo* like in 3D culture, TRCs were cultured in a collagen-I gel (in collaboration with A. Tomei and M. Swartz, EPF Lausanne, Switzerland). TRCs contracted the collagen fibres leading to rapid size reduction of collagen gels strengthening the notion that these are myo-fibroblasts. This property makes long-term culture almost impossible (Link et al., 2007; Tomei et al., 2009b). To avoid gel contraction a macro-porous polyurethane sponge (pore size 200-600μm) established by the group of M. Swartz was used as a stiff backbone comparable to the rigid LN capsule *in vivo* (figure 2.1.3a). This approach successfully prevented collagen contraction by the TRC clone (Tomei et al., 2009a, 2009b). The sponge culture also allows microscopical imaging although the sponge itself is slightly autofluorescent. TRC clones cultured in this 3D system were analysed by confocal microscopy. In contrast to their rather flattened morphology in 2D culture, they rapidly showed elongated and spindle-like morphology in 3D-culture, resembling their counterparts *in vivo*. Furthermore, within 3 days after start of culture TRC networks had formed within the collagen matrix (Figure 2.1.3b). Cells could be re-isolated from the 3D cultures using a collagenase digest and analysed by different techniques, such as flow cytometry or RT-PCR. After 3D culture TRCs maintained their typical surface marker expression. However, 3D culture was not sufficient to restore CCL19, CCL21 and IL-7 production to physiological levels (not shown) (Tomei et al., 2009b).

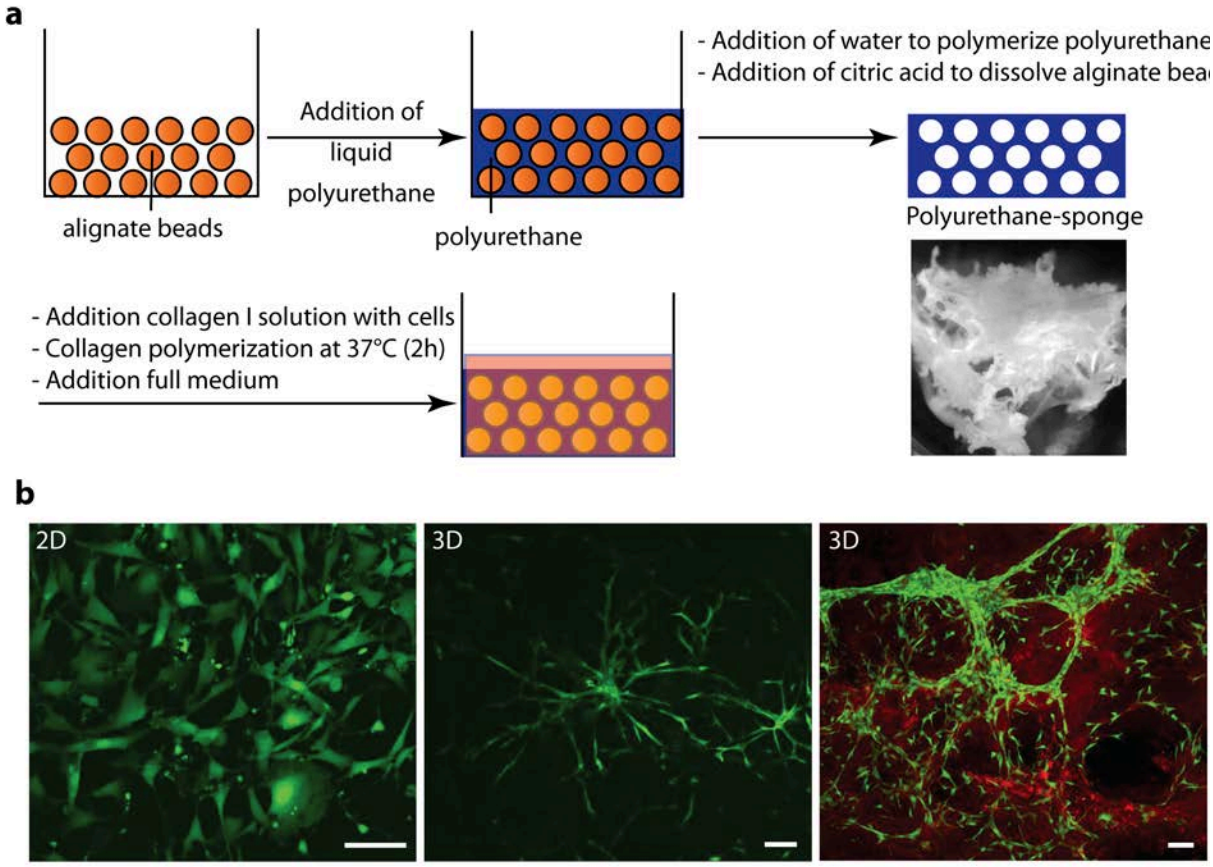

Figure 2.1.3: TRC clone cultured in 3D shows *in vivo* like morphology and network formation
(**a**) Schematic depiction of polyurethane-sponge production (as published in (Tomei et al., 2009a)): alginate beads are filled into a cast-device (e.g. 96-well plate). Liquid polyurethane is pipetted on the beads and after addition of water polyurethane polymerizes. Alginate beads are removed by dissolving them using citric acid. Sponges are washed and autoclaved prior to use. For 3D culture cells are mixed with collagen-I solution and filled into the sponge. After polymerization of collagen complete medium is added on top of the sponge. (**b**) Confocal microscopy of the $p53^{-/-}$ TRC clone (GFP+, green) cultured in 2D (left) or 3D (middle and right). Cells were cultured for 3 days in chamber slides and then analyzed by confocal microscopy (inverted Leica SP2 microscope). Red shows secondary harmonics of collagen. Shown are z-projections of image stacks (done using ImageJ software). Scale-bar 100µm.

2.1.1.4. Flow induces *Ccl21* expression in TRCs grown in a non-contractable 3D culture system

In vivo slow interstitial flow of lymph is constantly present in LNs, moving from the afferent lymphatics into the SCS and within the conduits through the paracortex before reaching the medulla and exiting via the efferent lymphatics (Laemmermann and Sixt, 2008). Lymph flow is increased early during tissue injury or infection (He et al., 2002; Modi et al., 2007) and correlates with increased levels of CCL19 and CCL21 levels in the LN during the first hours of the immune response (Scandella et al., 2008). As conduit-lining TRCs are constantly exposed to the incoming lymph, we hypothesized that the mechanical force of flowing lymph could contribute to the regulation of homeostatic chemokine expression.

The experiments described in the following - to test the effects of interstitial flow on chemokine production by TRCs - were performed by A. Tomei (M. Swartz group, EPFL) and have been published (Tomei et al., 2009b). When TRCs were cultured in a mixture of collagen and Matrigel (ratio 9:1) in the above described polyurethane sponges and flow was applied, CCL21 protein expression was increased as assessed by immuno-histochemical analysis. These results were confirmed and extended in another culture model that allowed more precise control of the applied flow: TRC clones were cultured in a collagen-matrigel matrix surrounded by a polyethylene cylinder (figure 2.1.4a). After 7 days of culture, enhanced TRC proliferation could be observed, but only in presence of the highest tested flow rate (figure 2.1.4.b). Interestingly, although the highest flow rate induced the highest *Ccl21* mRNA levels in TRCs, the lowest flow rate led to the highest secretion of CCL19 and CCL21 protein into the matrix as measured by ELISA on the digested matrix (figure 2.1.4c). But the detected chemokine transcript levels were still much lower than observed in *ex vivo* isolated TRCs (unpublished observation). To confirm the connection between lymph flow and CCL19/21 expression *in vivo*, afferent lymphatics of the inguinal LN were cut and 2 hours later CCL21 expression in the whole LN was measured. As predicted, blocking the flow to the LN decreased the CCL21 levels significantly, indicating a role of flow in CCL21 regulation. There was a trend, though not statistically significant, towards decreased CCL19 levels (figure 2.1.4e,f).

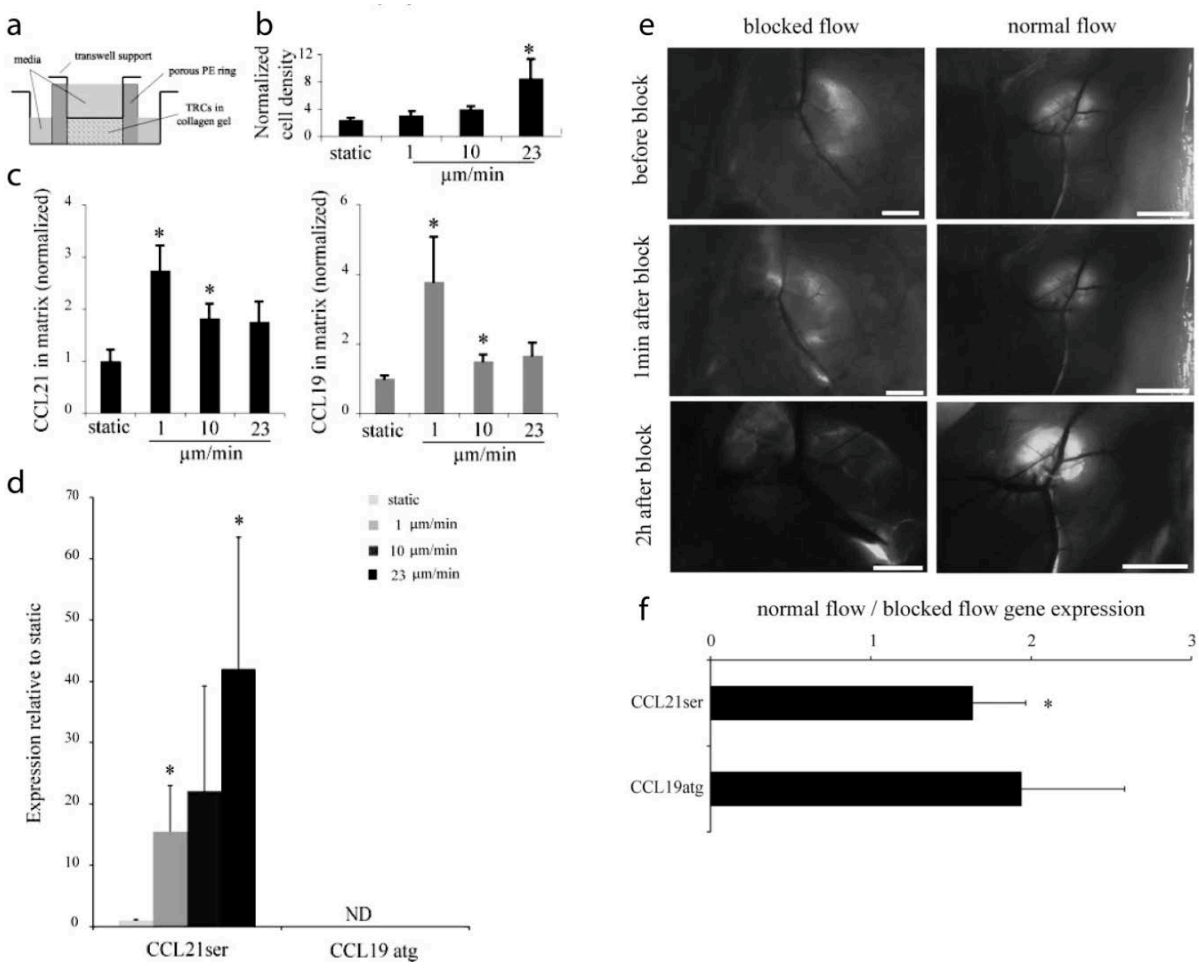

Figure 2.1.4: Fluid flow regulates CCL21 production by TRC clone
(**a-d**). TRCs were cultured in a collagen matrix within a porous polyethylene ring to prevent cell contraction over time, and fluid flow rates through the TRC matrix were controlled by the pressure head applied. (**a**) Scheme of the simplified 3D flow chamber (**b**) Cell density increased with the highest flow velocity tested (23µmm/min) after 7 days of culture. Data (n=3) were normalized to original cell densities (10^6 cells/ml). (**c**) Flow increased the secretion of CCL21 and CCL19 protein into the surrounding matrix, as compared with static controls and measured by ELISA on digested 3D cultures (n=12). (**d**) Flow in 3D induces an increase in the gene expression of *Ccl2-ser* as represented by quantitative real-time PCR (n=12). In mice two gene copies of *Ccl21* exist: *Ccl21-leu* is expressed in lymphatics of non-lymphoid organs, while *Ccl21-ser* is expressed in lymphoid organs e.g. by TRCs in LNs (Förster et al., 2008). *Ccl19-atg* transcripts were not detectable (ND). Several *Ccl19* transcribed gene copies exist, but only one the *Ccl19-atg* transcript encodes CCL19 protein (Luther et al., 2000). (**e**) Lymph flow through the inguinal LN was prevented by cutting the afferent and efferent lymphatic vessels. To visualize successful ablation of afferent lymph flow, FITC dextran uptake by the LN was measured in the case of 'blocked flow' and compared with the 'normal flow'. Scale bars represent 1mm (left) or 2.5 mm (right). (**f**) After 2h of blocked lymph flow, expression of *Ccl21-ser* and *Ccl19-atg* transcripts was assessed in the LN and *Ccl21-ser* expression was found to be significantly decreased in the blocked LN ($p < 0.05$) compared with their corresponding control LN (n=7). Quantitative real-time PCR results are displayed as the ratio between normal flow and blocked flow. Data derived from (Tomei et al., 2009b).

2.1.2. TRC lines from lymph nodes of C57BL/6 mice

The long-term goal of establishing a 3D system with TRCs was to re-construct the lymphoid T zone *in vitro* by the addition of T cells and DCs. However, as the established TRC clones were from LN of either p53-/- or p19arf-/- mice which are on a mixed C57BL/6 x 129 background (both H-2^b, but differences in minor histocompatibility loci) (Fischer-Lindahl, 1997) the clones were not suitable for co-culture with polyclonal C57BL/6 T cells. To get around this limitation, TRC lines were established from pLN and mLN of naive C57BL/6 mice. In addition, lines from pLN of ubiquitin-GFP transgenic mice on a C57BL/6 background were generated to obtain fluorescent TRC lines, which are easily detectable in histology and provide a tool for time-lapse analysis.

2.1.2.1. TRC lines resemble *in vivo* TRCs, but lack CCL19, CCL21 and IL-7 expression

Two entirely independent cell lines were established for each condition (C57BL/6 pLN, C57BL/6 mLN, Ubiquitin-GFP pLN). As for the generation of TRC clones, LN were collagenase-digested and TRCs enriched by panning. Initially, adherent cells grew very slowly and the morphology revealed heterogeneity among the cells. 2-3 months after start of culture the cells started to proliferate faster, and often became more homogeneous in their fibroblastic morphology. Flow cytometric analysis of cells at this time point showed that over 99% of cells were $CD45^-$ indicating that only non-hematopoietic cells had survived (figure 2.1.5a and 2.1.6a). Interestingly, after 3 months of culture the majority of mLN-derived cells were $CD31^{int}$ $gp38^+$ resembling the phenotype of LECs, but not TRCs. However, when mLN cells were re-analysed 2 months later, the majority of cells had a TRC-like surface phenotype (CD31- gp38+), although the gp38 expression level was lower than in pLN-derived TRC lines (figure 2.1.5a).

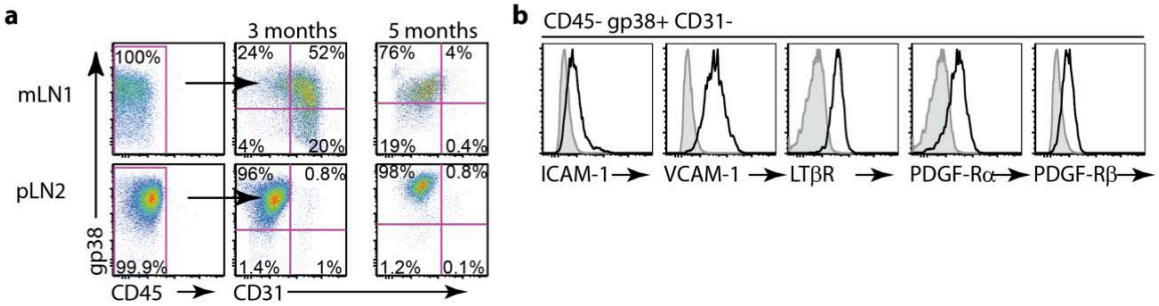

Figure 2.1.5 Fibroblasts with TRC-like phenotype grow out of LN stromal cell cultures
pLN or mLN from naive adult C57BL/6 mice were collagenase digested and adherent cells cultured *in vitro*. (**a**) Flow cytometric analysis of the lines mLN1 and pLN2. Dot plots show CD45 versus gp38 expression (1^{st} column), or CD31 versus gp38 expression on $CD45^-$ cells after 3 (2^{nd} column) or 5 months (3^{rd} column) of culture. (**b**) Histograms show indicated markers on $CD45^-$ $gp38^+$ $CD31^-$ mLN cells. Grey =no primary antibody control.

This indicates that over time TRC-like fibroblasts grew out of the original mix of TRCs and LECs. As for this thesis the main interest was in pLN-derived TRCs, the mLN lines were not further characterized after the initial surface phenotype analysis (figure 2.1.5b). Much to our surprise, the obtained cell lines could be cultured for more than 50 passages; however, for experiments cells below passage 28 were used. In

conclusion, there was no need for using mice with a 'first hit' to generate long-lived primary fibroblast lines.

The vast majority of pLN-derived cell lines were $CD31^-$ $gp38^+$ and were negative for CD35, EpCAM, and MAdCAM-1, suggesting that these cells are probably not FDCs, epithelial cells nor MRCs (table 2.1.2 and figure 2.1.6a). Similar to the *ex vivo* TRCs, the pLN2-TRC lines expressed the adhesion molecules ICAM-1 and VCAM-1 as well as PDGF-Rα and PDGF-Rβ (table 2.1.2 and figure 2.1.6a,b). Only very little MHC-II and no CD80 or CD86 expression was detected in the TRC line or *ex vivo* isolated TRCs (table 2.1.2 and figure 2.1.6b).

Surface marker	*ex vivo* TRC	pLN2 TRC line	Surface marker	*ex vivo* TRC	pLN2 TRC line
CD45	-	-	CD105	++	++
CD11b	-	-	gp38	+++	+++
CD11c	-	-	ICAM-1	++	++
CD31	-	-	VCAM-1	++	+++
CD35	-	-	PDGF-Rα	+++	+++
CD80	-	-	PDGF-Rβ	++	+
CD86	-	-	LTβ–R	++	++
CCR7	-	-	TNF-RI	++	+
CTLA-4	n.d.	-	PD1	n.d.	++
MAdCAM-1	+/-	-	PD-L1	+	+++
MHCII	-/+	-/(+)			
BP-3	++	-			

Table 2.1.2: Surface phenotype of pLN2-TRC line
Flow cytometric analysis of *ex vivo* TRCs and the pLN2-TRC line analyzed between passage 18 and 25 (> 4 months in culture) '-' = no expression; '+' peak shift below 0.5 log; '++' peak shift between 0.5 and 1 log; '+++' peak shift above 1 log, all in relation to the no primary antibody control. n.d. = not done (analysis of *ex vivo* TRC phenotype, mostly done by A. Link and H.-Y. Huang)

After the initial flow cytometric characterization of the different lines, the C57BL/6 pLN2 line was mostly used for further experiments. Labelling the cells with an antibody against gp38 and analysis by immunofluorescence microscopy revealed typical fibroblastic morphology. The majority of pLN2-TRCs express $desmin^+$ intermediate filaments and alpha smooth-muscle actin $(\alpha SMA)^+$ stress fibres confirming their myo-fibroblastic properties (figure 2.1.6c) (Link et al., 2007). Microscopic analysis of ECM secretion by pLN2-TRCs cultured in chamber slides revealed production of fibronectin, laminin and collagen I (figure 2.1.6d) assembled into fibres and remodelled by the cells. When GFP-pLN-TRC line cells were cultured in the 3D culture system (as described for the clones), their morphology was elongated and stellate resembling that of *in vivo* TRCs. As with the TRC clone, network formation in 3D culture could be observed (figure 2.1.6e and not shown). However, TRC lines expressed only very low levels of CCL19, CCL21 and IL-7, as explained below (figure 2.1.7a).

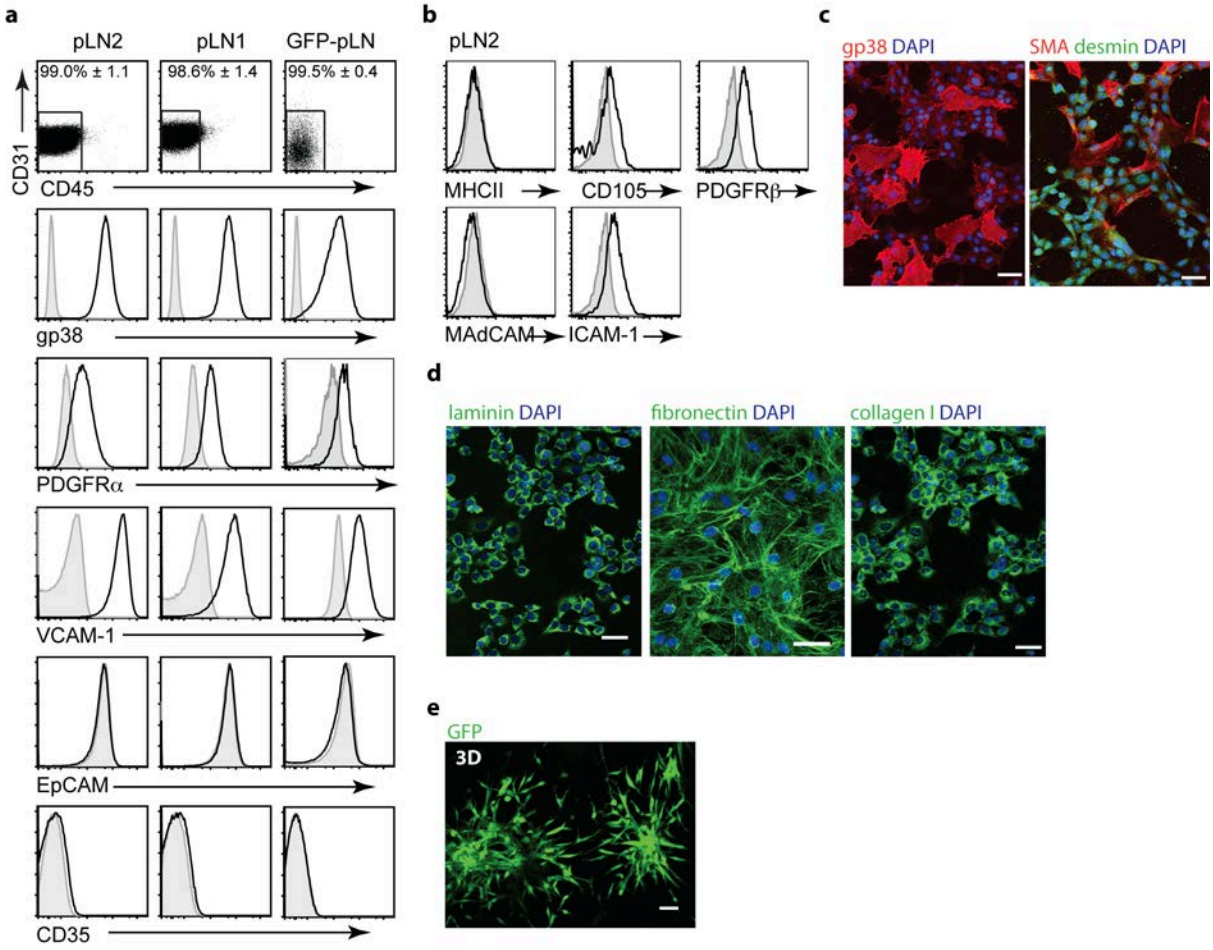

Figure 2.1.6: Phenotype of C57BL/6 pLN TRC lines
(**a,b**) Flow cytometric analysis of TRC lines established from naïve WT C57BL/6 ('pLN1' and 'pLN2') or Ubiquitin-GFP mice ('GFP-pLN') analyzed between passage 18-25 (>4 months of culture). (**a**) The first row shows CD45 versus CD31 expression, while the following rows show histograms for the indicated markers on CD45- CD31- cells. (**b**) Shows additional markers on the pLN2 TRC line (CD45- CD31-). (**c-e**) Immunohistochemical analysis of the TRC line pLN2 and its secreted products. Nuclei (DAPI) are shown in blue. (**c,d**) Cells were cultured in chamber slides for 3 days: shown are (**c**) cell morphology (TRCs labelled with gp38 in red), αSMA and desmin expression or (**d**) ECM molecules production. (**e**) GFP-pLN cells were cultured in the 3D culture system (as described in figure 2.1.3) for 2 days and analyzed by confocal microscopy. (**c-e**) Scale bar 50μm.

2.1.2.2. Cytokine stimulation of TRC line modulates some surface markers, but does not restore cytokine expression

During an immune response cytokines and other pro-inflammatory molecules such as TLR ligands are rapidly transported via lymph to the draining LN. As TRCs surround the conduits they will be exposed to these signals. To determine whether this induces changes in the TRC properties, pLN2-TRCs were cultured in the presence of different cytokines (TNFα, LTα3, IL-1β, IFNα or IFNγ), a cytokine receptor agonist (anti-LTβ–R) or TLR-ligands (LPS or Poly I:C) for 24 hours. Various surface markers were analysed for potential changes. In addition, cells were counted but no difference in cell numbers was observed with or without stimulation. Stimulation with several cytokines (TNFα, LTα3, IL-1β, IFNα or IFNγ) increased the size of the TRCs, while their granularity was unchanged in comparison to un-

stimulated cells (figure 2.1.7b). Interestingly, when cells were stimulated with TLR-ligands or a mix of TNFα, IL-1β and IL-6 no size increase was observed, but rather a trend to decreased size. This might be due to overstimulation, when all three cytokines are present. None of the cytokines induced expression of CD35, CD31 or MAdCAM-1, indicating that the TRC line probably did not differentiate into another stromal cell type (data not shown). Furthermore, in contrast to a recent report using *ex vivo* isolated FRCs (Fletcher et al., 2010) the pLN2-TRCs did not increase MHCII, CD40, CD80 and CD86 expression upon stimulation of cytokines or TLR-ligands (not shown). Several tested stimuli increased gp38 expression with the highest increase being induced by IL-1β and TNFα (figure 2.1.7b). Some modulation of VCAM-1 expression levels could be observed: the combination of TNFα with IL-1β and IL-6 led to a 4-fold increase, while LPS stimulation to a 2-fold increase (Figure 2.1.7b). Interestingly, the stimulation with IFNα and IFNγ dramatically increased PD-L1 expression on the pLN2-TRC, while only very little modulation of the LTβ–R could be observed (Figure 2.1.7b). For other tested markers, such as CD71, PDGF-Rα, PDGF-Rβ or CD44 no marked changes in expression level were observed (data not shown). These results indicate, that pLN2-TRCs are capable of responding to many different stimuli present during inflammatory responses, however, none of the tested cytokines nor LPS (TLR4-ligand) stimulation could induce CCL19, CCL21 or IL-7 expression (Figure 2.1.7a).

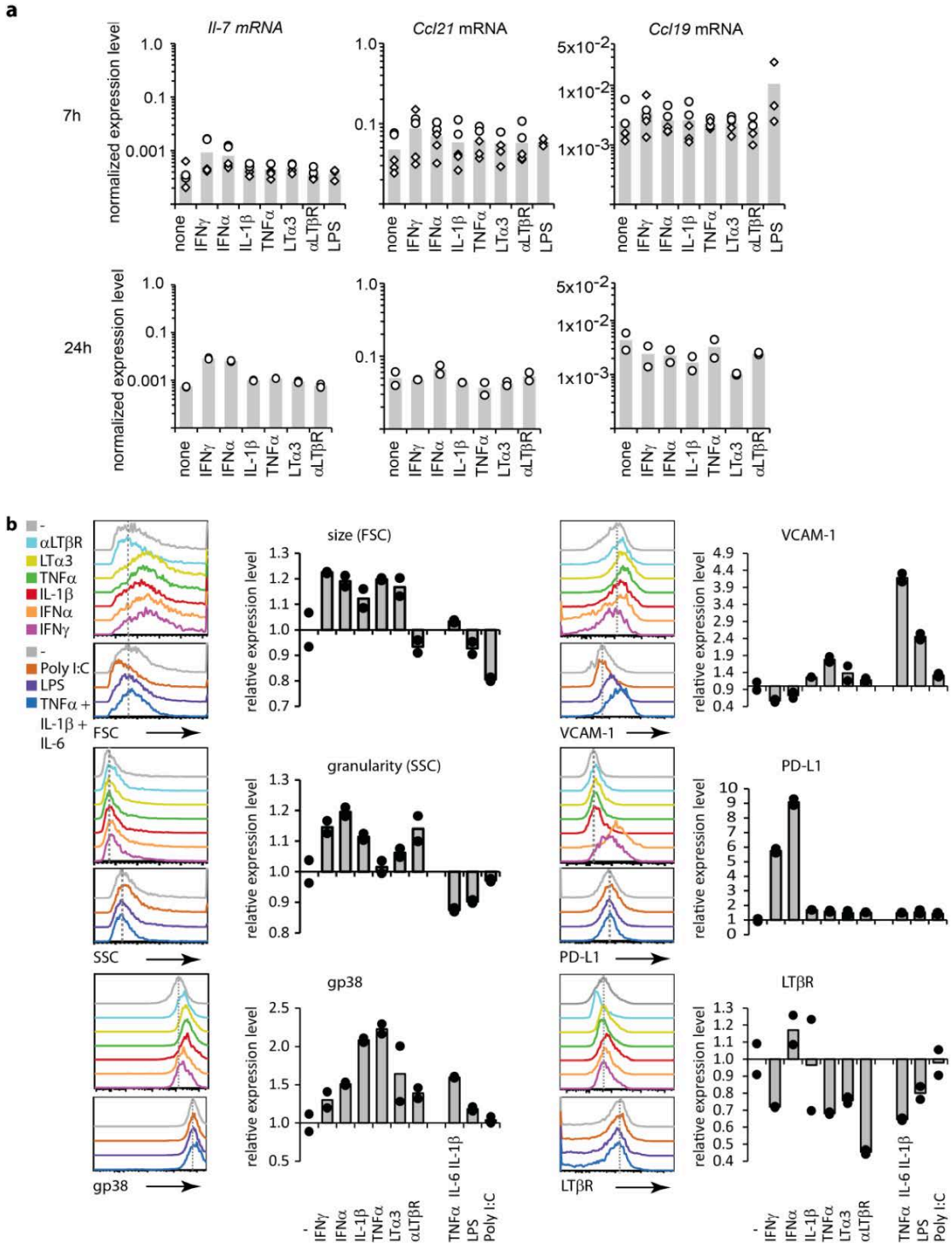

Figure 2.1.7: Cytokine stimulation of TRC-pLN2 line modulates some surface markers, but not cytokine expression

pLN2-TRCs were stimulated with various cytokines or receptor agonists. TNFα, LTα3, TGFβ, IFNγ, IL-1α, IL-1β (all 10ng/ml), IL-6 (25ng/ml), IFNα (500U/ml), anti-LTβR (1μg/ml), LPS (0.5μg/ml), Poly I:C (20μγ/ml) (**a**) Quantitative RT-PCR analysis of pLN2 line after 7h or 24h of stimulation. Shown is the expression level normalized to the average of the two housekeeping genes *Hprt* and *Tbp*. As published (Link et al., 2007) *ex vivo* TRCs show the following transcript levels *Il-7* ≈ 1, *Ccl21* ≈ 3500, *Ccl19* ≈ 200. (**b**) .Flow cytometric analysis of pLN2-TRC stimulated for 24h. Histograms show indicated markers, grey shows un-stimulated TRCs ('-'). Separated panels show different experiments. Bar graphs show the expression level as ratio relative to un-stimulated TRCs, as based on the median of fluorescence intensity. A relative expression level of 1 indicates no change in the fluorescence intensity. Relative expression level > 1 indicates increased, while < 1 indicates decreased expression levels or size/granularity.

2.1.2.3. Reconstruction of the lymphoid T zone *in vitro*

As mentioned before, the initial goal of establishing a 3D culture system with TRCs was to re-construct the lymphoid T zone, including T cells and DCs. This system should facilitate to analyse the role of TRCs in T cell priming. To this end, we first mixed ovalbumin (OVA)-specific CD8 T cells (OT-I) with polyclonal WT CD8 T cells in a ratio of 1:50 to mimic the *in vivo* situation, in which few antigen-specific T cells are intermingled with many polyclonal T cells. This T cell mix together with OVA-peptide-pulsed LPS-activated BMDCs (in a DC: T cell ratio of 1:10) was added on top of the 3D sponge culture system containing embedded TRCs or not. After 3-4 days of culture the cells were reisolated and the antigen-specific T cell response analysed. In the absence of TRCs, a strong activation of OVA-specific CD8+ T cells was observed, as assessed by size increase, proliferation (CFSE dilution) and modulation of activation markers (CD44, CD62L) (figure 2.1.8). Surprisingly, when TRCs were present, the proliferation of antigen-specific T cells was strongly reduced (figure 2.1.8). However, in a pilot time-lapse analysis of the 3D co-culture containing TRCs, T cells and DCs, DCs and T cells were only found in proximity of the collagen-gel surface but not deep within the gel. Inclusion of recombinant CCL21 in the gel did not improve the penetration depth (data not shown). This might be due to lack of oxygen in deeper regions of this 3D system and may indicate the need of a more sophisticated culture and microscope set-up improving oxygen diffusion into the sponge. As we observed a similar inhibition of T cell proliferation when TRCs were cocultured with T cells and DCs in normal 2D systems, we continued to characterize this observation in detail only in 2D cultures (described and discussed in the second results part 2.2). This system is technically easier and allows testing more conditions within one experiment.

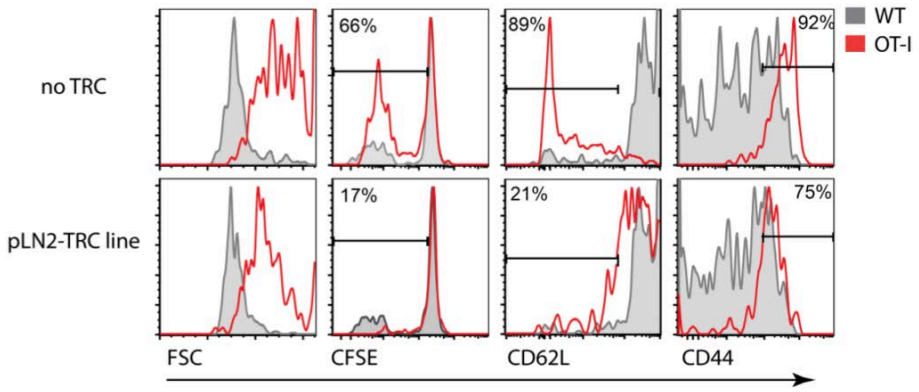

Figure 2.1.8: Antigen-specific T cells get efficiently activated in the 3D culture system
0.3 x 10^6 pLN2-TRC line cells were seeded in the 3D sponge culture system (as described in figure 2.1.2) and cultured for 2 days until TRC networks had formed. Then 0.2 x 10^6 LPS-activated and antigen-loaded BMDCs were added on top together with a total of 2 x 10^6 T cells, with T cells consisting of CFSE labelled OVA-specific CD8 T cells (= OT-I, red) mixed with polyclonal WT T cells (grey; 50% labelled with CFSE) in a ratio of 1:50. Cells were re-isolated after 3.5 days of co-culture and analyzed by flow-cytometry. Shown is the size of cells (FSC), their proliferation as assessed by CFSE dilution and the loss of CD62L as well as gain of CD44 as a measure of T cell activation.

2.1.2.4. Contributions by others

M. Britschgi and **A. Link,** two former lab members, established the TRC clones, and **M. Britschgi** performed the initial characterization. **A. Tomei** – under supervision of **M. Swartz** (EPFL)- established the polyurethane sponge used for the 3D culture system, helped with the set-up of 3D cultures with the TRC clone, performed all experiments with the application of flow and the related *in vivo* experiment with blocked flow. **H. Acha-Orbea** (UNIL) contributed transgenic mice.

2.1.3. Discussion of results with newly established TRC clones and lines

One difficulty in studying TRC function is their low percentage in LNs. Here I report the establishment of TRC clones and lines to obtain an abundant source of these cells as a basis for further characterization. Cell lines are widely used in research and their main advantage is that cells can be grown indefinitely and therefore large quantities can be easily obtained. However, to become immortalized cells undergo changes at the genomic and transcriptional level, which likely alter their behaviour compared to their *in vivo* counterparts. Cells can also de-differentiate *in vitro* during the several weeks of culture. Another advantage using cell lines or clones is that culture conditions can be precisely controlled and the identical cells are used in each experiment, which should improve reproducibility. However, results obtained with cell lines should, if possible, always be verified using *ex vivo* cells or ideally in an *in vivo* model.

Both, the cell clones and lines express a very similar surface marker profile as that of *ex vivo* isolated TRCs. While TRC clones and lines still produce ECM molecules, the expression of *Ccl19, Ccl21* and *Il-7* is lost. So overall the phenotype of TRC clones and lines is very similar. To establish TRC clones mice lacking a tumorsuppressor gene (p53 or p19arf) were used, as initially we assumed that a first 'hit' toward tumorigenesis is needed to obtain immortalized clones. However, TRC lines could be easily established from WT mice by long-term culture and maintained *in vitro* for over 50 passages. This indicates that the first 'hit' towards tumorigenesis is not necessary to obtain TRC lines. During long-term culture of adherent LN cells we observed that cells first grew slowly and showed a heterogeneous phenotype, but after 2-3 months started to grow rapidly and became a homogenous population. It might be possible that the cells growing out after 2-3 months of culture are derived from one progenitor cell, which acquired genetic mutations that allowed rapid growth *in vitro*. Therefore we cannot exclude that our cell lines might represent a clonal population.

FRC-like cell lines from murine LN or spleen, but also from human SLOs have been described by others and their basic phenotype characterization is summarized in table 2.1.3.(Katakai et al., 2004; Castro et al., 1997; Vega et al., 2006; Amé-Thomas et al., 2007). T zone FRCs were shown the be present in the spleen (Nolte et al., 2003; Ngo et al., 2001) therefore the lines generated from spleen represent most likely a similar cell type as LN derived TRC clones/lines, which were characterized in this thesis. However, the lack of reliable stromal cell markers which are maintained in culture make it difficult to establish whether a cell is truly a TRC, a dedifferentiated form of a TRC or another type of FRC.

		Our lines	Katakai et al.	Castro et al.	Hou et al.	Amé-Thomas et al.	Vega et al.
Organism		Mouse (C57BL/6)	Mouse (Balb/c)	Mouse (Balb/c)	Mouse (C57BL/6)	Human	Human
Organ		pLN	pLN	Spleen	Spleen	Tonsil	LN
Phenotype of unstimulated cells	CD45	-	-	-	-	-	-
	CD31	-	-	ND	-	ND	-
	FDC marker	-	-	-	-	ND	-
	gp38	+	+	ND	+	ND	ND
	MHCII	-/+	-	ND	-	ND	ND
	VCAM-1	+	+	+	+	-	ND
	ICAM-1	+	-/+	-	ND	-	ND
	MAdCAM-1	-	-/+	ND	-	ND	ND
	Mesenchymal markers	PDGFRα$^+$ PDGFRβ$^+$ CD105$^+$	ND	ND	ND	CD90$^+$ CD73$^+$ CD105$^+$	CD105$^+$
	LTβ-R	+	ND	ND	+	+	ND
	CCL19	-	-	ND	+	-	-
	CCL21	-	-	ND	-	-	-
	IL-7	-	-/+	ND	+	ND	-
	Detected by	RT-PCR of RNA	RT-PCR of RNA		RT-PCR of RNA	RT-PCR of RNA	Microarray of RNA
	ECM	+	+	ND	+	+	ND
Most likely represent		TRC	TRC and MAdCAM-1$^+$ MRC	Splenic TRC or red pulp stroma	Splenic TRC	Human TRC	Human TRC

Table 2.1.3 Phenotypic comparison of different FRC lines
The table compares the basic characterization done on FRC lines established by others and us. The surface phenotype of cell lines from Hou and colleagues are also shown in supplementary figure 2.2.1. The phenotypic comparison here is for unstimulated cells and phenotypic changes after stimulation are described in the text. Surface marker expression was analyzed by flow cytometry, cytokine expression by RT-PCR or microarray as indicated in the table and ECM production by immunohistochemistry. In case of the Katakai lines ICAM-1, MAdCAM-1 and IL-7 were detected in MRC lines, but not TRC lines. FDC marker: CD35 or FDC-M1. ND = no data; '+' detected; '-' not detected. (Katakai et al., 2004; Castro et al., 1997; Hou et al., 2010; Amé-Thomas et al., 2007; Vega et al., 2006; Katakai et al., 2008).

Surface marker profile and ECM production by TRC clones and lines

TRC clones /lines are negative for the FDC marker CD35, as shown by others and us (table 2.1.3) (Katakai et al., 2004; Hou et al., 2010; Castro et al., 1997; Vega et al., 2006). However, in early attempts to generate FDC lines it was observed that upon *in vitro* culture FDCs rapidly lost the expression of FDC markers, such as CD35 (Kim et al., 1994; Clark et al., 1992; Tsunoda et al., 1990). Therefore, it cannot formerly be excluded that FDCs that were present after *ex vivo* isolation of adherent cells lost CD21/35 expression and are still present in our TRC-like lines. However, two points argue against these cells being FDCs: 1) we have rarely observed CD35+ FDCs in our *ex vivo* isolates, 2) we see strong expression of ECM proteins what is typically not observed with FDCs.

Interestingly, ICAM-1 expression seems to vary on different lines (Katakai et al., 2004; Castro et al., 1997; Amé-Thomas et al., 2007). Only some of the lines reported by Katakai and colleagues showed constitutive ICAM-1 expression, while others only induced this marker after TNFα stimulation (Katakai et al., 2004). Also lines reported by Castro and colleagues were found to be negative for ICAM-1,which could not be induced by treatment with IFNγ (Castro et al., 1997). In contrast, our TRC cell clones/lines all showed constitutive ICAM-1 expression, which was not increased upon stimulation with TNFα or other tested cytokines such as IFNγ. It remains to be clarified whether ICAM-1 represents a marker that characterizes different TRC-subsets or activation states. Scandella and colleagues showed that short term-cultures of splenic T zone stromal cells show high surface expression of VCAM-1 and gp38, but only little ICAM-1 expression. However, when these cells were infected with LCMV ICAM-1 expression was increased arguing for ICAM-1 as an activation marker (Scandella et al., 2008).

TRCs constitutively express PD-L1, which was strongly increased on our TRC-lines in response to IFNγ and IFNα stimulation, but not after stimulation with other cytokines or TLR-ligands. This is in accordance with results obtained by Khan and colleagues (Khan et al., 2011). In addition, consistent with these results, Fletcher and colleagues observed PD-L1 up-regulation on *ex vivo* TRCs isolated from mice that were challenged with the TLR3 ligand Poly I:C (Fletcher et al., 2010). Nevertheless, in their report the observed PD-L1 up-regulation might not be due to direct stimulation of TRCs by Poly I:C, but possibly due to pro-inflammatory mediators such as type I IFN which may be produced by Poly I:C stimulated DCs (Gauzzi et al., 2010). Interestingly, Mueller and colleagues reported that TRCs infected by LCMV (clone 13) up-regulate PD-L1 expression, which protects them from being killed by $CD8^+$ T cells (Mueller et al., 2007). Together this suggests that PD-L1 might be an activation marker of TRCs, however its function on TRCs remains to be better defined.

The Katakai-FRC lines were shown to produce ECM fibres as detected by the ER-TR7 antibody. The ER-TR7-antigen is not characterized, but was shown be an ECM component specific for murine fibroblasts (Van Vliet et al., 1986; Katakai et al., 2004). The ECM formation by the FRC-lines was strongly enhanced after co-culture with lymphocytes or the combined stimulation of the TNF-R (by TNFα or LTα3) and the LTβ–R. ER-TR7 staining overlapped with laminin and fibronectin, but in contrast to ER-TR7, fibronectin secretion by FRCs seemed to be influenced very little or not at all by the presence of lymphocytes (Katakai et al., 2004). Here, we show collagen I, fibronectin and laminin production by our cell clones/lines. In preliminary experiments no enhanced ECM formation was observed after treatment with TNFα + LTα3 + anti-LTβ–R (alone or combined). However, only secretion of fibronectin and collagen I was analysed and at this point we cannot exclude that ER-TR7 is regulated differently.

Cytokine expression by TRC clones and lines

Katakai and colleagues reported the expression of several different chemokines by the FRC lines that were constitutively expressed: *Ccl2, Cxcl12, Cx3cl1, Ccl4* and *Ccl5*. TNFα stimulation increased *Ccl4* and *Ccl5* and furthermore induced *Ccl20* and *Cxcl10* expression. In a follow-up report, Katakai and colleagues showed that CXCL16 is induced in the TRC-line by different cytokines (IL-1β, IFNγ and TNFα) and LPS. CXCL16 expression by TRCs was confirmed *in vivo* and seems to be involved in adhesion of activated (CXCR6+) CD8 T cells to the TRC network (Hara et al., 2006). In a pilot experiment I analysed supernatant of the pLN2-TRC line by luminex technology, and CXCL10 (IP-10), CCL2 (MCP-1) and KC (CXCL1) could be detected as well as the cytokines IL-2, IL-5 and IL-6. However, similar to our cell clones/lines no *Ccl19* or *Ccl21* expression was detected in the Katakai-line with or without cytokine stimulation in the TRC line (Katakai et al., 2004). This is also consistent with the observation that TRCs cultured *in vitro* rapidly loose *Ccl19* and *Ccl21* expression (personal communication by T. Vogt). Nevertheless, in a follow-up report by Katakai and colleagues in which they describe the MRC subset, *Ccl19* could be induced in a MRC line after TNF-R and LTβ-R stimulation (Katakai et al., 2008). So far we could not reproduce this with our cell lines.

Together this shows, that TRCs cultured *in vitro* loose the *Ccl19* and *Ccl21* expression, which was not re-stored by stimulation with the tested cytokines, while other cytokines are still expressed or can be induced by cytokine stimulation. During SLO organogenesis LTαβ signals are crucial for CCL19 and CCL21 induction (van de Pavert and Mebius, 2010). Furthermore, intra-peritoneal injection of the agonistic LTβ-R antibody increases *Ccl19* and *Ccl21* expression in the spleen, suggesting that LTαβ signals in adult mice directly or indirectly augments homeostatic chemokine expression (Dejardin et al., 2002). However, our results indicate that in adult TRCs LTαβ signals are not sufficient to induce *Ccl19* and *Ccl21* expression. Still, other signals might be able to re-store the homeostatic chemokine expression in TRC lines and remain to be tested. It is likely that the regulation of CCL19 and CCL21 is complex and several signals need to be present, therefore complex mixtures such as lymph or cytokines cocktails should be tested. Furthermore, it might be interesting to co-culture TRC lines with other cells that are able to provide the appropriate signals. Scandella and colleagues showed that lymphoid tissues inducer (LTi) cells are important to restore the TRC network and the accompanying *Ccl19* and *Ccl21* expression, which are disturbed after LCMV infection. Furthermore, *Ccl19* but not *Ccl21* transcripts were maintained in *ex vivo* isolated splenic stromal cells ($gp38^+$) when co-cultured with LTi for 4 days *in vitro* (Scandella et al., 2008). Therefore, LTi cells represent a potential candidate to restore chemokines expression in TRC clones/lines. A recent report showed that JAM-C (junctional adhesion molecule C) expressed on TRCs is implicated in the regulation of *Ccl21* expression *in vivo* (Frontera et al., 2011). JAM-C was shown to be expressed on different cells types, such as endothelial cells or MSCs and to interact with itself, JAM-B, Mac-1 and CD11c (Zimmerli et al., 2009). It remains to be tested, whether TRC clones/lines express JAM-C and whether co-culture with cells expressing JAM-C ligands, for example endothelial cells, could restore CCL21 expression.

In a study in 2006 Vega and colleagues reported microarray analysis of humans FRC lines that they compared with human dermal fibroblasts (DF). Interestingly, *Ccl2* as well as *Il-1β* and *Il-6* expression were significantly higher in FRCs than DF. TNFα up-regulated several chemokines (*Ccl1, Ccl2, Ccl7, Ccl8, Ccl11, Ccl23, Cxcl1, Cxcl2, Cxcl3, Cxcl5, Cxcl8, Mip-1δ,* and *lymphotactin*) in FRCs; however, a very similar response to TNFα stimulation was seen in DF suggesting a common fibroblastic response to TNFα. In contrast to our findings, IL-6 or IL-13 stimulation induced *Ccl19* but not *Ccl21* in human FRCs. However, Vega and colleagues studied FRCs derived from LNs that showed benign hyperplasia, were reactive or had lymphoma and therefore these FRCs may be altered (Vega et al., 2006). In a study from Amé-Thomas and colleagues, the establishment of human FRC lines derived from tonsils is reported. In contrast to previous results with murine FRCs but similar to the reported murine MRC line, *Ccl19* was induced after combined TNFα/LTα1β2 stimulation for 3 days (Amé-Thomas et al., 2007; Katakai et al., 2004; Vega et al., 2006). So FRCs from activated human tonsils might represent MRCs or behave differently than TRCs from naive murine LN or spleen. Nevertheless, it is possible that during the establishment of lines, cells grow out that do not produce or never produced CCL19 and CCL21. Therefore, the culture conditions during establishment of cell lines might be crucial to preserve chemokines expression. It remains to be tested whether continuous presence of stimuli, such as TNFα and/or LTαβ, in cultures of *ex vivo* isolated TRCs might preserve CCL19 and CCL21 expression.

A characteristic feature of TRCs *in vivo* is the expression of *Il-7* (Link et al., 2007), which was lost in our TRC lines. *Il-7* was shown to be induced by LTβ signalling in MEFs (Vondenhoff et al., 2009). This was confirmed in TRC and MRC lines established by Katakai and colleagues, as LTα3 or LTβR stimulation increased *Il-7* expression in an additive manner. Interestingly, while unstimulated TRC lines show no or very few *Il-7* transcripts, MRC lines show some constitutive expression (Katakai et al., 2008). Besides LT signalling, IFNγ was shown to positively regulate *Il-7* expression in human and murine intestinal epithelial cells (Shalapour et al., 2010; Oshima et al., 2004). However, in our hands none of the tested stimuli (LTα3, TNFα, agonistic anti-LTβR, IL-1β, IFNγ, IFNα or LPS) restored *Il-7* levels in TRC lines to physiological levels. The discrepancy of these results to the previous reports cannot be explained so far. I have only checked *Il-7* transcripts after short-term stimulation (maximal 40h); maybe a longer stimulation is needed to see *Il-7* upregulation.

Culture of TRC clones and lines in a non-contractible 3D culture and the reconstruction of a lymphoid T zone *in vitro*

In recent years, the use of 3D cell culture systems has been more and more used to mimic *in vivo* like environments that nevertheless keep the advantages of *in vitro* culture. The reconstruction of lymphoid tissues is of great interest, for example for *in vitro* drug testing. Giese and colleagues reported the establishment of a human artificial LN, consisting of lymphocytes and DCs embedded in an agarose matrix. In this system an immune response to a Hepatitis A vaccine could be successfully reconstructed (Giese et al., 2010). However, the stromal cell compartment of SLO, FDCs as well as TRCs, is missing in

this human artificial LN. As both FDCs and TRCs strongly influence the immune response, it would be important to include them in such a system. In another approach, Kaminer-Israeli and colleagues report the co-culture of (murine) BMDCs together with a stromal cell line derived from murine bone marrow embedded in an alginate scaffold. Exogenously added T cells penetrated into the centre of the 3D culture system and T cell activation could be observed. Interestingly, similar to our results, presence of stromal cells inhibited T cell proliferation *in vitro*, but also *in vivo*, when this 3D system was transplanted under the kidney capsule (Kaminer-Israeli et al., 2010).

In this thesis we report our approach to reconstruct a lymphoid T zone: we could successfully culture TRC clones/lines in a special 3D system, consisting of a collagen gel polymerized within a rigid polyurethane scaffold. TRCs in this system show *in vivo* like morphology and cell-networks are formed. The lacking cytokine expression in TRC clone/lines might be due to cell de-differentiation in long-term culture. It is known, that extracellular mechanical signals feed back to the cells by transducing it into intracellular signals (Tomasek et al., 2002; Kleinman et al., 2003) and that mechanical properties of the matrix in 3D culture systems greatly influence cell biology (Griffith and Swartz, 2006). *In vivo* almost all tissues are tethered in a way that cell contraction will lead to increased mechanical stress of the surrounding matrix, with this again influencing the cells within these tissues. Mechanical signals are important for cell function. For example, fibroblasts can only differentiate into myo-fibroblasts when they are cultured in mechanically loaded or restrained collagen gels (Tomasek et al., 2002). Therefore, free floating unrestrained collagen lattices are not an ideal model for mechano-regulated processes (Tomasek et al., 2002; Pedersen and Swartz, 2005). Here we embedded the mechanically weak collagen gel within a rigid polyurethane sponge. This allows the cells to remodel the collagen matrix, but the whole device is stiff enough to withstand the contraction forces by the cells (Tomei et al., 2009a, 2009b). We think this device resembles closely LNs as in these organs the ECM is anchored to the rigid capsule that is comparable to the polyurethane sponge in our 3D system (Tomei et al., 2009b). Considering this, we hypothesized initially that culturing TRC clones/lines in a 3D environment under mechanical stress might lead to differentiation and restoration of CCL19, CCL21 and IL-7 production. However, that was not the case, indicating that mechanical signals alone are not sufficient. Nevertheless, the application of fluid flow on the 3D system induced some CCL21 and CCL19 secretion by the $p53^{-/-}$ TRC clone, but did not reach physiological levels (Tomei et al., 2009b) indicating that there are still signals missing.

In a recent report, Fletcher and colleagues reported the culture of *ex vivo* isolated TRCs in a collagen-matrigel matrix (Fletcher et al., 2011a). Consistent with our results, TRCs contracted this gels leading to size reduction. Interestingly, when Fletcher and colleagues added BMDCs or splenocytes to this system, these cells used the TRC network in these 3D cultures for their migration (Fletcher et al., 2011a). In our approach to reconstruct the lymphoid T zone *in vitro*, we added antigen-specific T cells together with activated and antigen-pulsed DCs to the 3D culture system and could observe T cell activation. However, both cell types seemed to stay at the edges of the collagen gel, presumably due to the relative lack of

oxygen deep within the 3D system. Problems with limited exchange of nutrients and waste metabolites arise in 3D cultures with a thickness greater than 1-2mm, which is exceeded in our sponge system (Haycock, 2011; Pedersen and Swartz, 2005). Therefore, technical adjustments are needed to improve our 3D culture system. Bioreactor systems have been established to overcome problems with oxygen and nutrient supply. Distinct systems exist to solve this issue, for example rotating vessel cultures or direct perfusion systems (Haycock, 2011; Pedersen and Swartz, 2005). However, in both systems cells would be cultured under flow conditions and so far it is not known how much flow or shear force T cells and DCs experience within the T zone parenchyma. As lymph is mostly canalled around the LN or in the conduit system, one might speculate that although TRCs experience flow through the conduits, T cells and DCs might be in an environment mostly free of flow and extracellular fluid (Kaldjian et al., 2001). This must be considered, if perfusion systems are used. An oxygen bubbling system, as reported (Kurata et al., 2007), or the integration of hollow fibres in the 3D scaffold might be a solution (Haycock, 2011). In the human artificial lymph node from Giese and colleagues this problem was solved by the integration of membranes in the bioreactor that are continuously perfused with CO_2 and O_2 (Giese et al., 2010).

There are several approaches that aim to reconstruct organs *in vitro* (Pampaloni et al., 2007; Kobayashi and Watanabe, 2010; Griffith and Swartz, 2006). Besides the *in vitro* application for research purposes, there is a lot of interest in the use of artificial organs for medical purposes. In 2007 Okamoto and colleagues reported that transplantation of a collagen sponge containing a LTα–producing thymus derived stromal line under the kidney capsule of mice led to vascularisation and infiltration by lymphocytes as well as generation of FDC networks. Distinct T and B cell zones were also observed. Importantly, adaptive immune response could be elicited in this transplanted LN and even transferred into immune-deficient mice (Kobayashi and Watanabe, 2010; Okamoto et al., 2007). Polyurethane is a biocompatible material and is used in the clinics, for example in form of vascular grafts for heart patients (Santerre et al., 2005). Therefore, it should be possible to transplant our 3D TRC culture system into mice, for example under the kidney capsule. It would be interesting to test whether lymphocytes would infiltrate such transplants and whether adaptive immune responses could be induced. Furthermore, it would be worthwhile to investigate whether in this *in vivo* environment the TRC cell lines would restore their CCL21, CCL19 and IL-7 expression, and whether they can differentiate into other fibroblast types. Interestingly, in their report Amé-Thomas and colleagues showed that treatment of BM-derived-MSCs with TNFα and LTα1β2 for 7 days induced their differentiation into FRC-like cells as based on the expression of ICAM-1, VCAM-1, *Ccl19* and ECM molecules (Amé-Thomas et al., 2007). This indicates that BM and possibly SLO contain MSCs and that these cells might be a precursor for FRCs. The transplantation of MSCs within the described 3D culture system might be a good way to test whether MSCs can also differentiate into FRCs *in vivo*. The use of GFP-tagged TRCs or MSCs would allow to fate-map the transferred cells.

Though TRC clones and lines reported here lost the expression of *Ccl19, Ccl21* and *Il-7*, many features of TRCs are preserved. Furthermore, 3D culture of these cells allows reconstructing an *in vivo* like lymphoid T zone in which recombinant cytokines such as CCL21 and IL-7 can be included. Therefore, the established clones/lines cultured in 2D but especially in 3D represent a valuable tool to study TRC biology.

2.2. Fibroblastic reticular cells attenuate T cell expansion by producing nitric oxide*

Summary

To define the precise role of TRCs in T cell priming an *in vitro* T cell activation assay was established. Activation of OVA-specific OT-I T cells by OVA-peptide presenting bone-marrow derived DCs (BMDCs) was studied in presence or absence of TRCs. Surprisingly, TRC lines and *ex vivo* TRCs inhibit T cell proliferation but not differentiation. TRCs share this feature with fibroblasts from non-lymphoid tissues as well as mesenchymal stromal cells. We identified FRC as strong source of nitric oxide (NO) thereby directly dampening T cell expansion as well as reducing the T cell priming capacity of DCs. The expression of inducible nitric oxide synthase (iNOS) was up-regulated in a subset of TRCs by both DC-signals as well as interferon-γ produced by primed CD8+ T cells. Importantly, iNOS expression was induced during viral infection *in vivo* in both LN TRCs and DCs. As a consequence, the primary T cell response was found to be exaggerated in iNOS$^{-/-}$ mice. Our findings highlight that in addition to their established positive roles in T cell responses TRCs and DCs cooperate in a negative feedback loop to attenuate T cell expansion during acute inflammation.

* Based on: Siegert S, Huang HY, Yang CY, Scarpellino L, Carrie L, Essex S, Nelson PJ, Heikenwalder M, Acha-Orbea H, Buckley CD, Marsland, BJ, Zehn D, Luther SA (2011): Fibroblastic reticular cells from lymph nodes attenuate T cell expansion by producing nitric oxide; PLoS One 6 (11) e27618

2.2.1. Lymph node TRCs dampen T cell expansion

To dissect the role of TRCs in T cell activation and differentiation, we initially adopted a reductionist approach: T cells were co-cultured with antigen-pulsed bone-marrow derived DCs (BMDCs), either in the presence or absence of TRCs. Given the difficulties in isolating pure TRC populations, several independent TRC cell lines were established from peripheral lymph nodes (pLN = pool of inguinal, axillary and brachial LN) of C57BL/6 wild-type (WT) mice (referred to as 'pLN1' and 'pLN2') or GFP-expressing mice ('GFP-pLN'). All these lines showed typical fibroblastic morphology and a uniform surface marker expression pattern comparable to *ex vivo* isolated TRCs (figure. 2.1.6 and table 2.1.2). In contrast to *ex vivo* TRCs (Link et al., 2007) cell lines expressed only low levels of *Ccl19*, *Ccl21* and *Il7* transcripts (figure 2.1.7a). To circumvent this caveat, initial experiments included exogenously added CCL19, CCL21 and IL-7 protein with no difference in the outcome (data not shown).

To study T cell priming CD45.1$^+$ congenic ovalbumin (OVA)-specific OT-I T cell receptor (TCR) transgenic CD8$^+$ T cells were labelled with the proliferation dye carboxyfluorescein succinimidyl ester (CFSE), mixed with unspecific WT T cells (CD45.2$^+$) in a ratio of 1:50, and cultured together with antigen-pulsed BMDCs on top of an adherent layer of the TRC line. TRCs were previously irradiated to limit their proliferation and nutrient consumption. Surprisingly, the total OT-I cell number was strongly decreased in presence of the TRC line pLN2 (figure. 2.2.1a). Using CFSE dilution to measure T cell proliferation, both the percentage and number of dividing OT-I T cells were strongly reduced in the presence of pLN2 (figure. 2.2.1b). The increase in cell size (FSC) and CD44 expression (figure. 2.2.1c) as well as the loss of CD62L expression (figure.2.2.1d) occurred in presence of TRCs but to a reduced extent. The co-cultures were supplemented with IL-7 and IL-2, so a lack of known pro-survival factors for naïve and activated T cells is unlikely to be the cause. In line with that, the number of naïve, undivided OT-I T cells was not affected by the TRC presence, nor was the up-regulation of the high-affinity receptor chain for IL-2, CD25, on dividing T cells (figure 2.2.1e).

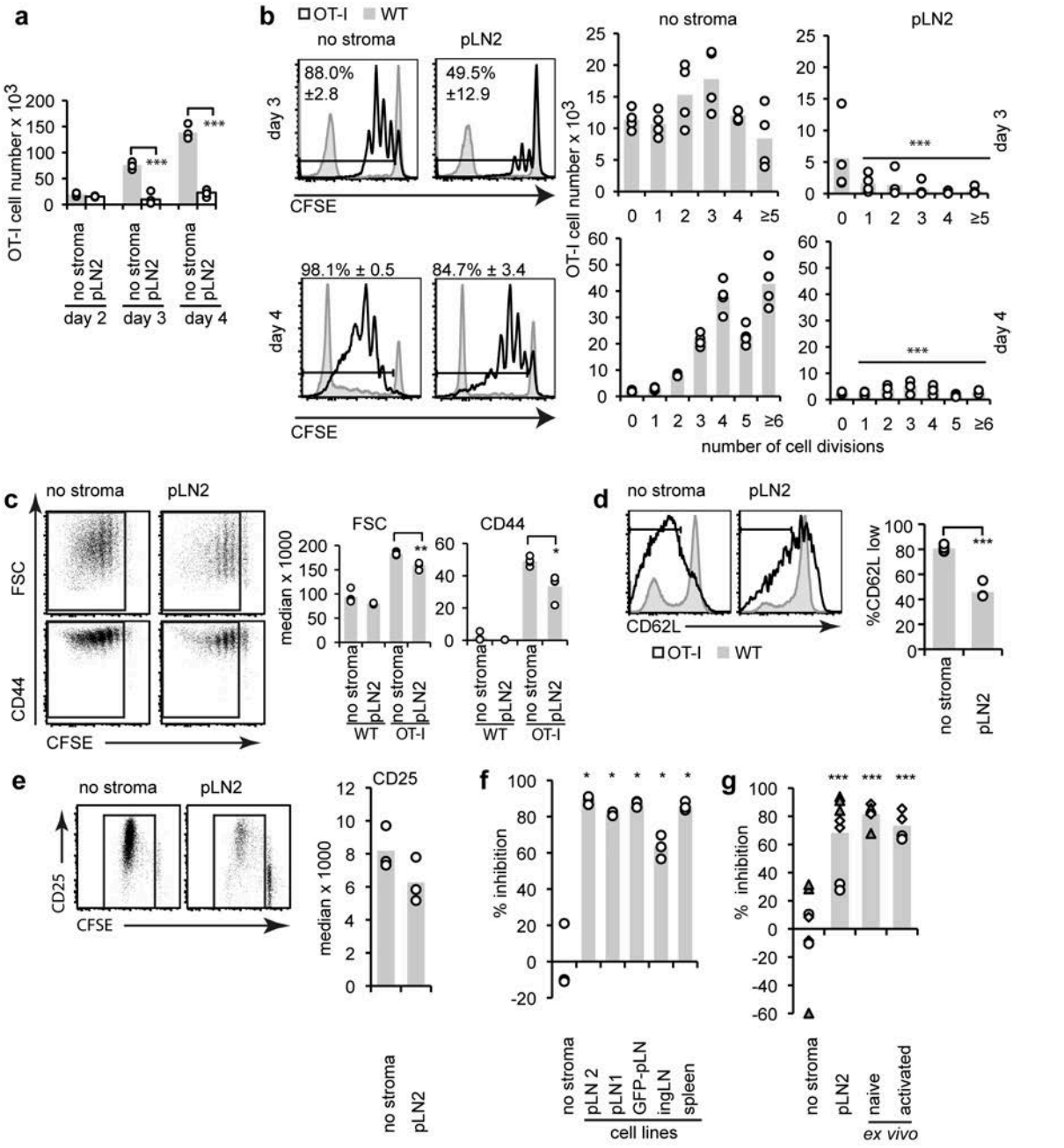

Figure 2.2.1: TRCs dampen the expansion of antigen-specific CD8+ T cells
Flow cytometric analysis of T cell activation: CFSE-labelled OT-I T cells were mixed in a ratio of 1:50 with WT T cells (50% CFSE-labelled) and cultured with LPS-activated and OVA-peptide pulsed BMDCs. The assay was performed without stromal cells ('no stroma') or in the presence of TRCs from distinct sources (1:1:200 ratio of TRC to BMDCs, and to T cells). (**a**) Total OT-I numbers on day 2, 3 and 4 in absence or presence of the pLN2 TRC line. (**b**) Proliferation of OT-I (black) or polyclonal T cells (gray) as assessed by CFSE dilution on day 3 or 4. Histograms (left) show the percentage (± standard deviation) of divided OT-I cells and bar graphs the absolute OT-I cell numbers per CFSE dilution peak (right). (**c**) Dot plots (left) show CFSE dilution versus cell size (FSC) or CD44 expression of OT-I T cells after 3 days. Bar graphs (right) indicate the median FSC values or fluorescence intensity. (**d**) Histograms show CD62L expression and bar graphs the percentage of $CD62L^{low}$ OT-I T cells. (**e**) As c, but showing CD25 expression on OT-I T cells after 4 days. (**f,g**) Bar graphs show the percentage inhibition of OT-I T cell proliferation as based on the proliferating OT-I cell numbers after 3 days of co-culture with different TRC lines (**f**) or *ex vivo* isolated and enriched TRC (**g**). The latter are derived from pLN of un-manipulated B6 mice or from mice s.c. injected with NP-CGG/Montanide 3 days prior to the TRC harvest ('activated TRC'). Different symbols indicate different experiments. Data are representative of >10 (**a-d**), 3 (**e-g**), 2-3 (**f**) experiments; different symbols indicate different experiments. * $p < 0.05$, ** $p < 0.01$, *** $p < 0.001$, p-values relate to 'no stroma' controls.

Importantly, several other fibroblast lines established independently from LN and spleen (Hou et al., 2010) not only shared the same surface phenotype (figure. 2.1.6 and 2.2.2) but also the inhibitory effect on T cell expansion with a reduction in proliferating OT-I T cell numbers of 60-90% (figure. 2.2.1f). Importantly, primary TRCs isolated from naïve pLN limited T cell expansion at least as strongly as TRC lines (figure. 2.2.1g). Even TRCs isolated from pLN of mice immunized 3 days earlier with NP-CGG in Montanide adjuvant maintained these inhibitory properties (figure. 2.2.1g).

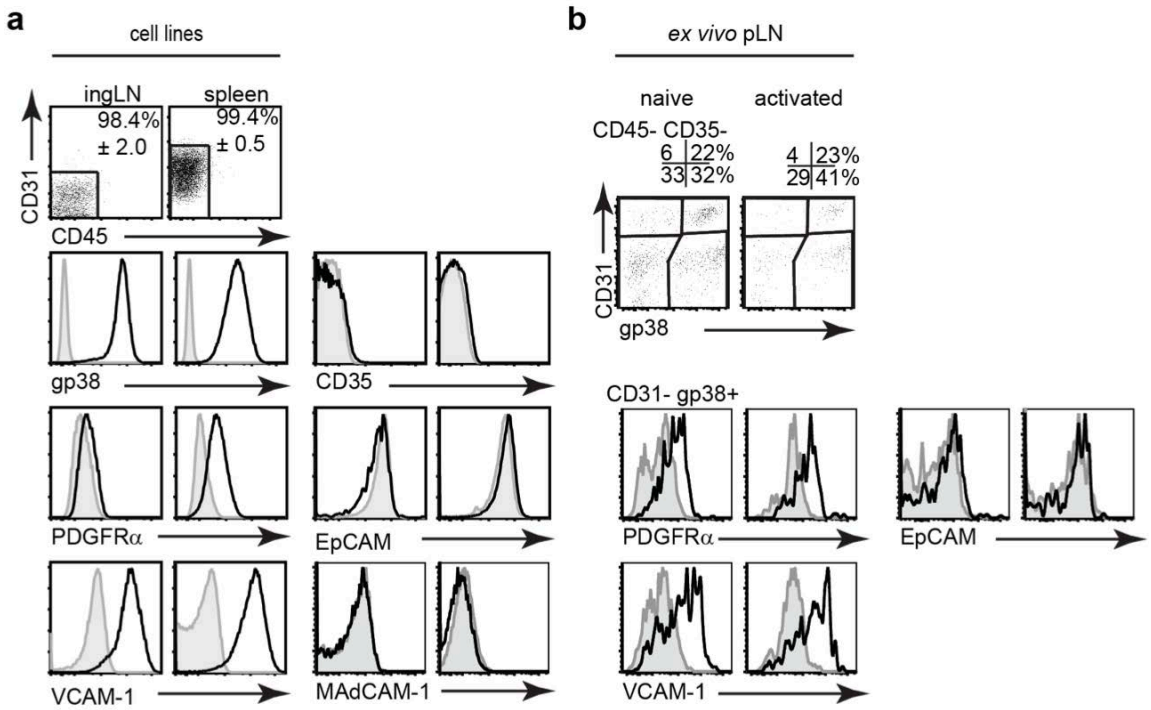

Figure 2.2.2: Surface phenotype of ingLN and splenic TRC lines as well as *ex vivo* TRCs
Flow cytometric analysis of the surface phenotype of (**a**) TRC lines from ingLN and (b) *ex vivo* isolated TRCs from pLN, used in the T cell activation assay shown in figure 2.2.1. (**a**) The first row shows dot plots for CD31 versus CD45 expression and the percentage of $CD31^-$ $CD45^-$ cells (± standard deviation). Following rows show histograms with the indicated surfaces markers on $CD45^-$ $CD31^-$ cells. Lines were established by S. Essex in the laboratory of C. Buckley, Birmingham, UK. (**b**) $CD45^-$ $CD31^-$ cells were analyzed in dot plots for CD31 versus gp38 expression (first row). The following rows show the indicated surface markers on $CD45^-$ $CD35^-$ $CD31^-$ $gp38^+$ cells Grey shadowed curves show the 'no primary antibody control'. (**a,b**) representative for ≥ 3 experiments

Next, we examined the effect of TRCs on CD8+ T cell differentiation. OT-I T cells primed in the presence of TRCs expressed intracellular interferon gamma (IFNγ) protein (figure 2.2.3a) and killed target cells (figure 2.2.3b), although with markedly reduced efficiency. Together these results demonstrate that the presence of TRCs during T cell activation diminishes the expansion or survival of CD8+ T cells and to a lesser extent their differentiation into effector cells.

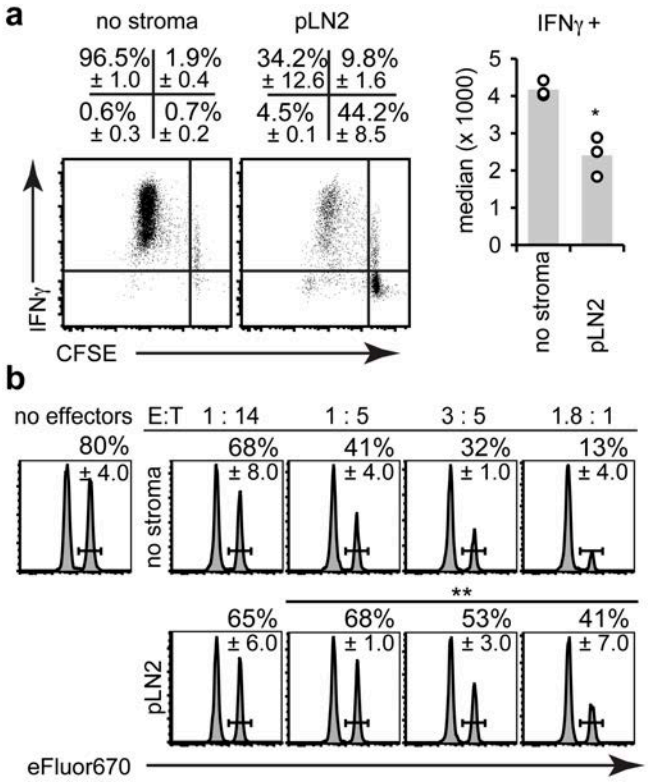

Figure 2.2.3: CD8+ T cell primed in presence of TRCs still produce IFNγ and kill target cells
The T cell activation assay (see legend of figure. 2.2.1) was performed without stroma ('no stroma') or in presence of the pLN2 TRC line for 4 days followed by flow cytometric analysis of OT-I T cell effector function. (a) Dot plots (left) show intracellular IFNg versus CFSE dilution in OT-I T cells after in vitro re-stimulation with 1μM SIINFEKL peptide in presence of Brefeldin A. The right panel shows the median fluorescence intensity of IFNg expression in OT-I T cells. (b) The cytotoxic capacity of OT-I T cells was assessed by co-incubating OT-I T cells (= effector cells, E) from the T cell activation assay in the indicated E:T ratios with SIINFEKL-pulsed-eFluor670high-labelled splenocytes (= target cells, T) mixed 1:1 with unpulsed-eFluor670low-labelled splenocytes (=internal control). After overnight culture the percentage of eFluor670high versus eFluor670low splenocytes was analysed and plotted as histograms. Indicated as percentage is the survival index for the target cells, as based on the ratio of peptide-pulsed eFluor670high relative to un-pulsed eFluor670low cells (± standard deviation). (a,b): n = 3, representative of 3 independent experiments. * $p < 0.05$, ** $p < 0.01$, *** $p < 0.001$, p -values are relative to 'no stroma'.

2.2.2. Fibroblasts from non-lymphoid organs also attenuate T cell proliferation

It has been reported that murine and human fibroblasts can have anti-proliferative effects on activated T cells, similar to mesenchymal stem cells (MSCs) and certain tumour lines (Jones et al., 2007; Haniffa et al., 2009, 2007; Bouffi et al., 2011; Nauta and Fibbe, 2007; Uccelli et al., 2008). Therefore we tested in our system the inhibitory potential of several fibroblastic cell lines established *de novo* from different non-lymphoid organs, as well as their *ex vivo* equivalents (CD45$^-$CD35$^-$CD31$^-$EpCAM$^-$gp38$^+$; figure 2.2.4), and compared them to our pLN2 line. In addition, epithelial-like cells from the epidermis and kidney, a MSC line and two tumour cell lines (MC38 colon carcinoma and B16-F10 melanoma) were tested.

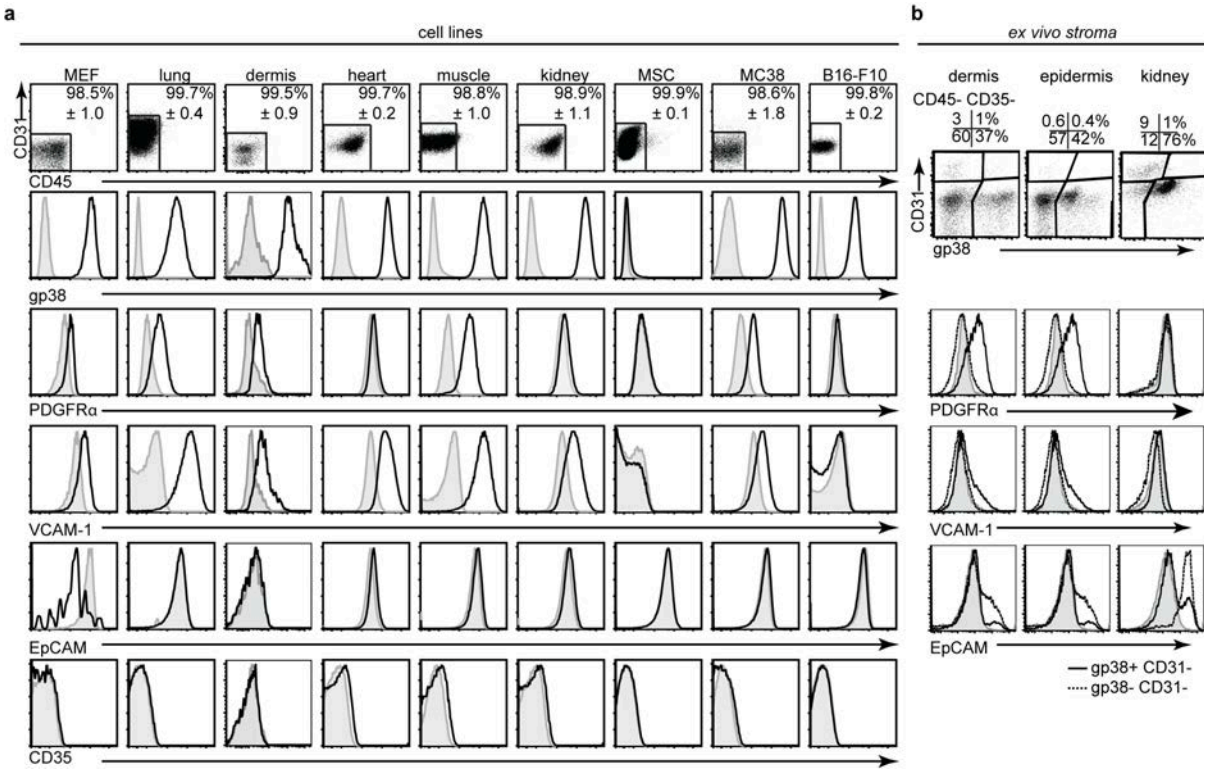

Figure 2.2.4: Surface phenotype of non-lymphoid cell lines as well as *ex vivo* stromal cells from non-lymphoid organs

Flow cytometric analysis of the surface phenotype of (**a**) non-lymphoid cell lines or (**b**) *ex vivo* stromal cells isolated from dermis, epidermis and kidney used in the T cell activation assay shown in figure 2.2.5. (**a**) The first row shows dot plots for CD31 versus CD45 expression and the percentage of CD31$^-$ CD45$^-$ cells (± standard deviation). Following rows show histograms with the indicated surfaces markers on CD45$^-$ CD31$^-$ cells. Lines from lung were established by S. Essex in the laboratory of C. Buckley, Birmingham, UK. MEFs were a kind gift from M. Heikenwalder, Munich, Germany. The MC38 and B16-F10 lines were a kind gift from A. Donda, Lausanne, Switzerland. All other lines were de novo established. (**b**) CD45$^-$ CD31$^-$ cells were analyzed in dot plots for CD31 versus gp38 expression (first row). The following rows show the indicated surface markers on CD45$^-$ CD35$^-$ CD31$^-$ gp38$^+$ cells as black line, and gp38$^-$ CD31$^-$ cells as dotted line (includes epithelial cells). Grey shadowed curves show the 'no primary antibody control'. (a,b) representative for 2-3 experiments

All cell lines inhibited OT-1 T cell proliferation to an extent comparable with pLN2 (figure. 2.2.5), highlighting that inhibition of T cell expansion is a property common to many cell types, including fibroblasts from various non-lymphoid organs.

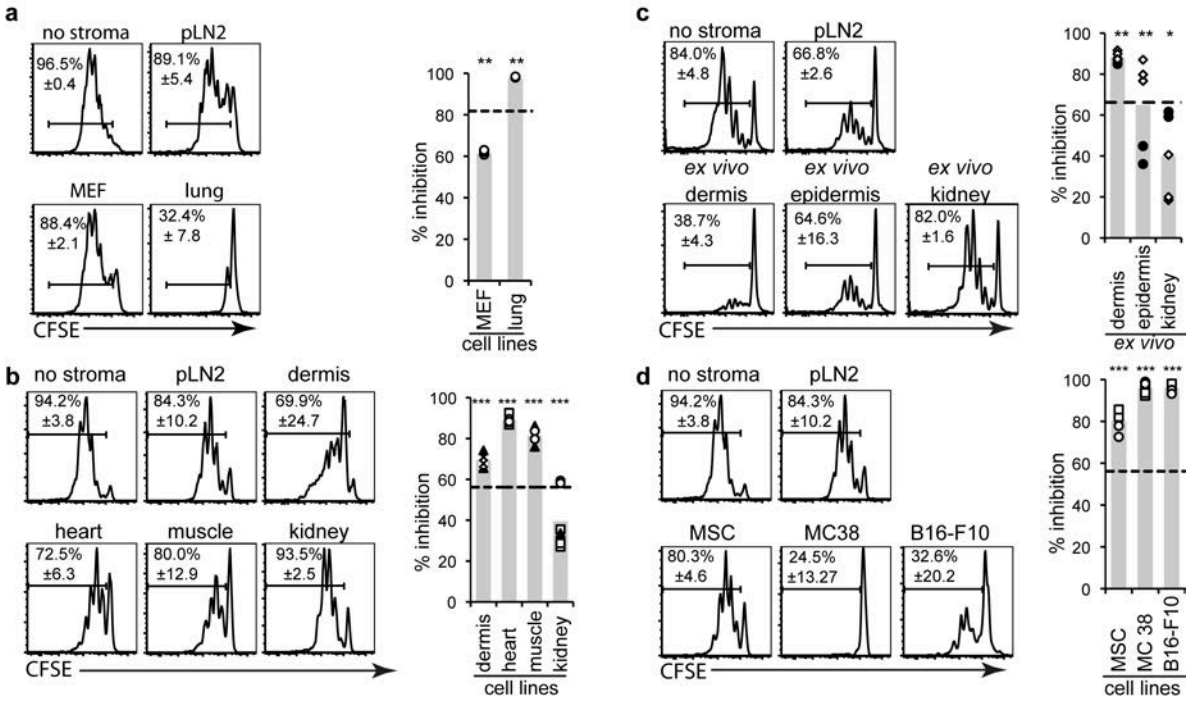

Figure 2.2.5: Stromal cells from various non-lymphoid organs decrease antigen-specific T cell proliferation

The T cell activation assay (see legend of figure. 2.2.1) was performed in presence of either stromal cell lines (**a,b,d**) or *ex vivo* isolated stromal cells (**c**). OT-I T cells co-cultured for 3 days were analyzed for CFSE dilution using flow cytometry. Representative histograms of CFSE dilution (left panel) and the number of proliferating OT-I cells as percentage inhibition are presented (right panel, as in figure. 2.2.1). Shown are assays with a (**a**) mouse embryonic fibroblast line (MEFs) and lung fibroblast line, (**b**) lines derived from different non-lymphoid organs (dermis, heart, femoral muscle, kidney), (**c**) *ex vivo* isolated adherent cells from the dermis, epidermis or kidney, (**d**) Mesenchymal stem/stromal cell (MSC) line and the tumour cell lines B16-F10 (melanoma) and MC-38 (colon carcinoma). (**a-d**) n ≥ 3, representative for ≥ 2 experiments. Different symbols indicate different experiments. * $p < 0.05$, ** $p < 0.01$, *** $p < 0.001$, if not indicated otherwise p-values are relative to 'no stroma'. The dotted line indicates the inhibition observed by pLN2 cells within the same experiment

2.2.3. TRCs directly inhibit T cell proliferation and render DCs less stimulatory

MSCs have been shown to inhibit T cell proliferation by intracellular expression of enzymes such as indoleamine 2,3-dioxygenase (IDO) and arginase-1, surface expression of PD-L1 or by secretion of molecules like NO, prostaglandin E_2 (PGE_2), IL-10 and TGF-β and (Nauta and Fibbe, 2007; Uccelli et al., 2008). The proposed pathways included direct inhibition of T cell proliferation or conversion of DCs to a non-stimulatory or suppressive phenotype (Svensson and Kaye, 2006; Uccelli et al., 2008). To examine whether TRCs can directly interfere with T cell proliferation pLN2 were co-cultured with anti-CD3/CD28 bead-stimulated T cells. Clearly, TRCs diminished the number of dividing T cells but the inhibitory effect was only half of what we had observed in the BMDC-induced T cell activation assay (figure. 2.2.6a). Next, potential effects of TRCs on the stimulatory capacity of antigen-pulsed BMDCs were investigated by co-culturing first pLN2 with BMDCs before incubating these 'TRC-conditioned' BMDCs alone with T cells. The capacity to stimulate T cell proliferation was reduced by half in conditioned relative to unconditioned BMDCs (figure. 2.2.6b). Together these results indicate that TRCs

limit T cell expansion in two additive ways, by making DCs less immunogenic and by directly inhibiting T cell proliferation or survival.

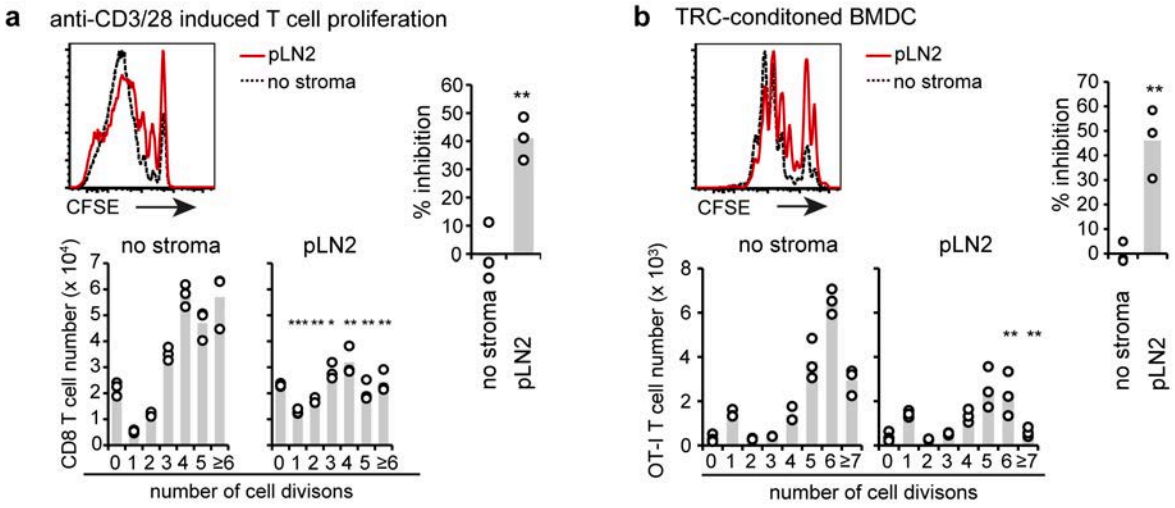

Figure 2.2.6. TRCs dampen T cell proliferation by modifying both T cells as well as BMDCs
(**a**) Flow cytometric analysis of T cell proliferation induced by anti-CD3/CD28 beads as based on CFSE dilution after 3 days of culture. WT T cells were cultured with beads and in presence of the pLN2 TRC line (T cell to TRC ratio of 100:1) or their absence ('no stroma'). Representative histograms (top) show the percentage (± standard deviation) of divided $CD8^+$ T cells and bar graphs (bottom) the absolute $CD8^+$ T cell numbers per division. The bar graph (right) shows percentage of inhibition (as in figure. 2.2.1). Similar data were obtained for $CD4^+$ T cells suggesting TRCs may also suppress their expansion (data not shown). (**b**) Flow cytometric analysis of cell proliferation induced by TRC-conditioned BMDCs. LPS-activated and SIINFEKL-pulsed BMDCs were co-cultured with pLN2 TRCs at a ratio of 1:1, or cultured alone. After overnight culture TRC-conditioned-BMDCs were re-isolated by MACS, counted and subsequently co-cultured for 3 days with CFSE labelled OT-I cells mixed 1:50 with unspecific WT T cells (of which 50% are CFSE labelled). Representative histograms (top) show the percentage (± standard deviation) of divided OT-I cells and bar graphs (bottom) the absolute cell numbers per CFSE dilution peak. Percentage of inhibition (as in figure. 2.2.1) is shown in the bar graph on the right. (**a,b**) n = 3, (**a**) representative for ≥ 3 experiments, (**b**) representative for 2 experiments. * $p < 0.05$, ** $p < 0.01$, *** $p < 0.001$, if not indicated otherwise p-values are relative to 'no stroma'.

2.2.4. TRCs limit T cell expansion by producing NO

To gain insight into the nature of the TRC-derived inhibitory factor T cells and BMDCs were either separated from the pLN2 by a permeable-membrane (transwell) or simply incubated with supernatant (SN) from pLN2. Both settings led to a decrease in T cell expansion, but this was smaller than in co-cultures where all the three cell types are intermingled (figure. 2.2.7a). These results suggest a role for either a soluble factor which acts only efficiently at short distance, or for at least two inhibitory factors, one being soluble and the other being cell-cell contact dependent. It also argues against a role for TRCs in presenting antigen to T cells and thereby inhibiting T cell proliferation. To identify the molecules responsible for suppressing T cell expansion in our assay several candidates or their synthesis pathway were blocked, including PD-L1, TGFβ, IL-10, IDO and arginase-1 but none of them neutralized the TRC-mediated inhibition (figure 2.2.7b).

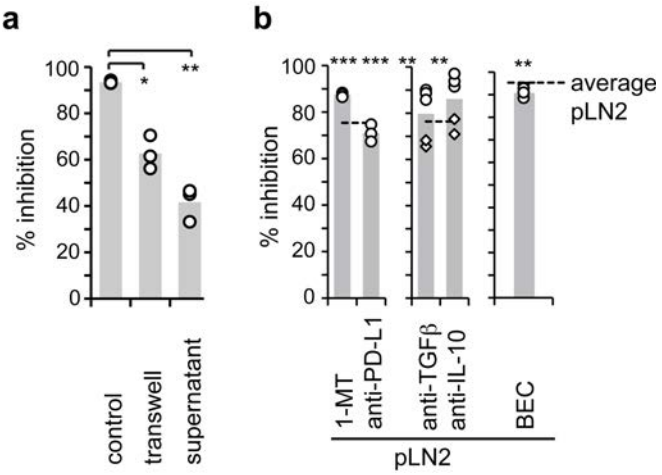

Figure 2.2.7: Inhibition of T cell proliferation by TRCs is mediated by a soluble factor
Flow cytometric analysis of the T cell activation assay (as described in figure. 2.2.1): bar graphs show percentage of inhibition. (**a**) pLN2-TRCs in the assay were present in the same well ('control') or separated by a permeable membrane (transwell). Or 30% pLN2-TRC-conditioned- supernatant taken after 72h from subconfluent irradiated cultures was added to the cultures (**b**) Pharmacological inhibitors against IDO (1MT, 1mM), arginase-1 (BEC, 200μM) or blocking antibodies against PDL1 (20μg/ml), TGFβ (30μg/ml) or IL-10 (20μg/ml) were added to co-cultures. One out of several tested inhibitor concentrations is shown along with the percentage of inhibition. The dotted line shows the average inhibition by pLN2 TRCs without inhibitor/blocking antibodies. (a,b) n≥ 3; representative for 2 experiments. * $p < 0.05$, ** $p < 0.01$, *** $p < 0.001$, if not indicated otherwise p-values are relative to 'no stroma'

However, blocking the enzymatic activity of iNOS (NOS2) or cyclooxygenase (Cox) -1 and -2 partially rescued T cell proliferation with the effects of the two pharmacological inhibitors used being partially additive (figure. 2.2.8a). This result demonstrates that iNOS-dependent NO and COX-1/2 dependant factors are responsible for most of the inhibitory effect observed. We focused our attention on iNOS as transcripts for *Inos* but not *Cox2* were enhanced in stimulated TRCs (as shown later). Strikingly, *Inos*$^{-/-}$ TRCs had lost all suppressive activity and showed even an enhancement of T cell proliferation, in contrast to the inhibitor 1400W that partially abolished the suppressive effect of *ex vivo* WT TRCs (figure. 2.2.8b), reminiscent of the effects seen for the pLN2 line (figure. 2.2.8a). To show directly the expression of iNOS protein in TRCs and assess the frequency of iNOS-expressing cells, antibodies to iNOS were used in immunofluorescence microscopy. iNOS protein could only be detected in pLN2 co-cultures with BMDCs and activated T cells. However, iNOS was only detected in a small fraction of gp38^{+} TRCs (figure. 2.2.8c). Occasionally, iNOS protein staining was observed in BMDCs-like cells (gp38^{-}) but never in lymphocytes (not shown). These experiments establish that TRCs are a source of iNOS that inhibits T cell proliferation. They also demonstrate that the inhibitory activity of TRCs on T cell expansion is not due to metabolic effects of co-culture.

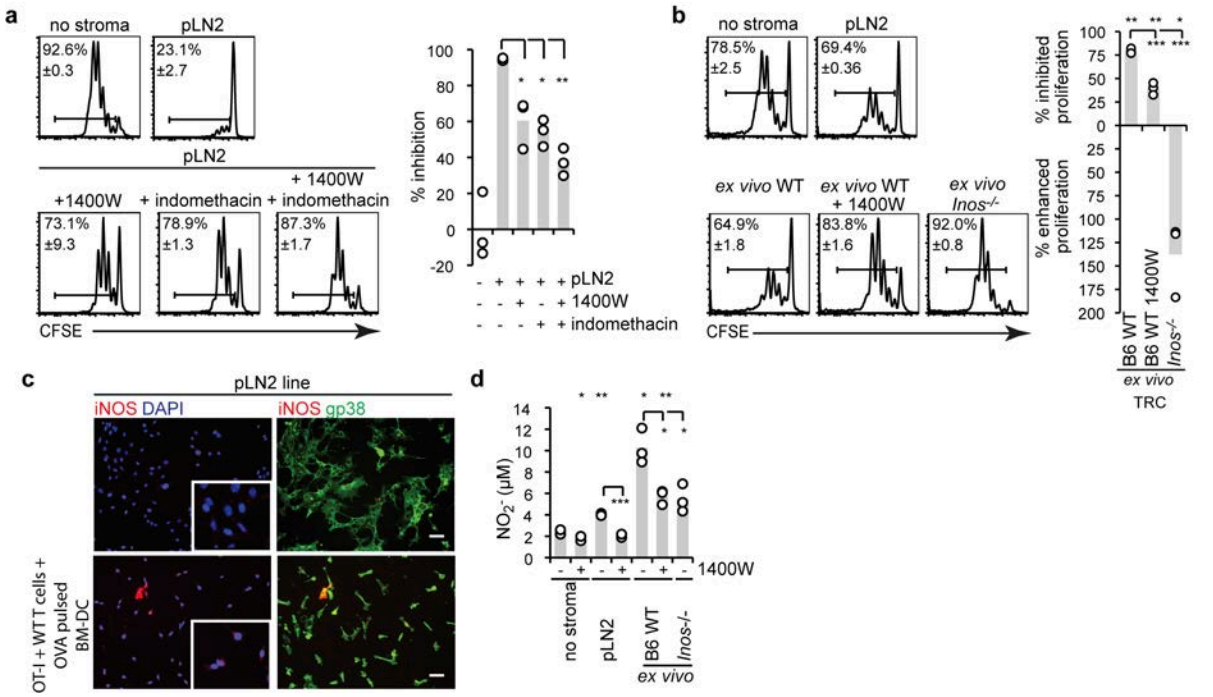

Figure 2.2.8: Inhibition by TRCs is mediated via NO and COX-1/2 dependant factors
Flow cytometric analysis of the T cell activation assay (as described in figure. 2.2.1): (**a**) Pharmacological inhibitors against iNOS (1400W, 1 μM) and/or COX-1/2 (indomethacin, 10 μM) were added to the co-cultures after optimization of their concentrations (tested range for 1400W: 1-10 μM; for indomethacin: 1-10 μM). The histograms show the percentage of divided OT-I cells (± standard deviation) and the bar graph (right) shows the percentage of inhibition. (**b**) T cell activation assay was carried out in the presence of *ex vivo* isolated enriched TRCs from WT or *Inos*$^{-/-}$ mice along with the indicated inhibitors. The histograms show the percentage of divided OT-I cells (± standard deviation) and the bar graph (middle) shows the percentage of inhibition. (**c**) Immunohistochemical analysis of iNOS expression in pLN2 TRC lines. pLN2 cells were cultured alone (top) or in presence of OT-I and WT T cells together with LPS activated, SIINFEKL-pulsed BMDCs (ratios as in figure. 2.2.1) (bottom). Insets of higher resolution images are shown to indicate the generally increased iNOS expression level in pLN2 cocultured with BMDCs, antigen and T cells. (**d**) Bar graph showing NO_2^- levels in the co-culture supernatant from the T cell activation assay shown in (**b,c**) as determined using a Griess assay. (**a-d**) n ≥ 3, (**a**) representative for ≥ 3 experiments, (**b,d**) representative for 2, (**c**) 1 experiment; * $p < 0.05$, ** $p < 0.01$, *** $p < 0.001$, if not indicated otherwise *p*-values are relative 'no stroma'.

As readout of iNOS activity, we measured extracellular nitrite levels in the SN. In absence of TRCs the SN of T cells activated by BMDCs contained very low levels of nitrite. Presence of pLN2 or *ex vivo* TRCs in this assay increased the NO_2^- concentration 2- and 5-fold, respectively (figure. 2.2.8d), further strengthening the notion that NO production by TRCs leads to inhibition of T cell proliferation or survival. In the case of *ex vivo* TRCs approximately half of the nitrite was due to iNOS activity in TRCs as suggested by the use of 1400W or *Inos*$^{-/-}$ TRCs. They also suggest a contribution of NO production by one of the two other NOS isoforms which are insensitive to concentrations of 1400W used and possibly expressed in TRCs or in the few endothelial cells found within the adherent cell fraction. As the levels of iNOS protein correlate better with NO-mediated inhibition of T cell expansion than those of extracellular nitrite, the subsequent analysis was focused on the factors inducing iNOS expression in TRCs.

2.2.5. IFNγ and other T cell derived cytokines induce iNOS protein expression in TRCs

To look at the role of T cells in inducing iNOS protein in TRCs, pLN2 were co-cultured with T cells and fixed cells analysed for intracellular iNOS protein by immunohistology. Non-activated T cells induced iNOS in only a few TRCs whereas T cells activated with anti-CD3/CD28 beads up-regulated iNOS in a large proportion of TRCs (figure. 2.2.9a). This suggests that most TRCs have the potential to express iNOS upon activation but typically only a small proportion shows detectable protein. IFNγ is a T cell-derived cytokine known to induce iNOS expression in various cell types (Lavnikova and Laskin, 1995; Bogdan et al., 2000; Bogdan, 2001; Ren et al., 2008). Indeed, adding recombinant IFNγ was sufficient to induce iNOS expression in a fraction of pLN2 (figure. 2.2.9a). Comparable results were obtained with *ex vivo* LN cells when the adherent cells enriched for $gp38^{+}CD31^{-}$ TRCs were used in presence of naïve or activated T cells or IFNγ (figure. 2.2.9a). Consistent with these data a significant increase in nitrite was observed in the SN of TRC lines or *ex vivo* TRCs upon IFNγ stimulation or upon addition of T cells with or without anti-CD3/28 activation (figure. 2.2.9b).

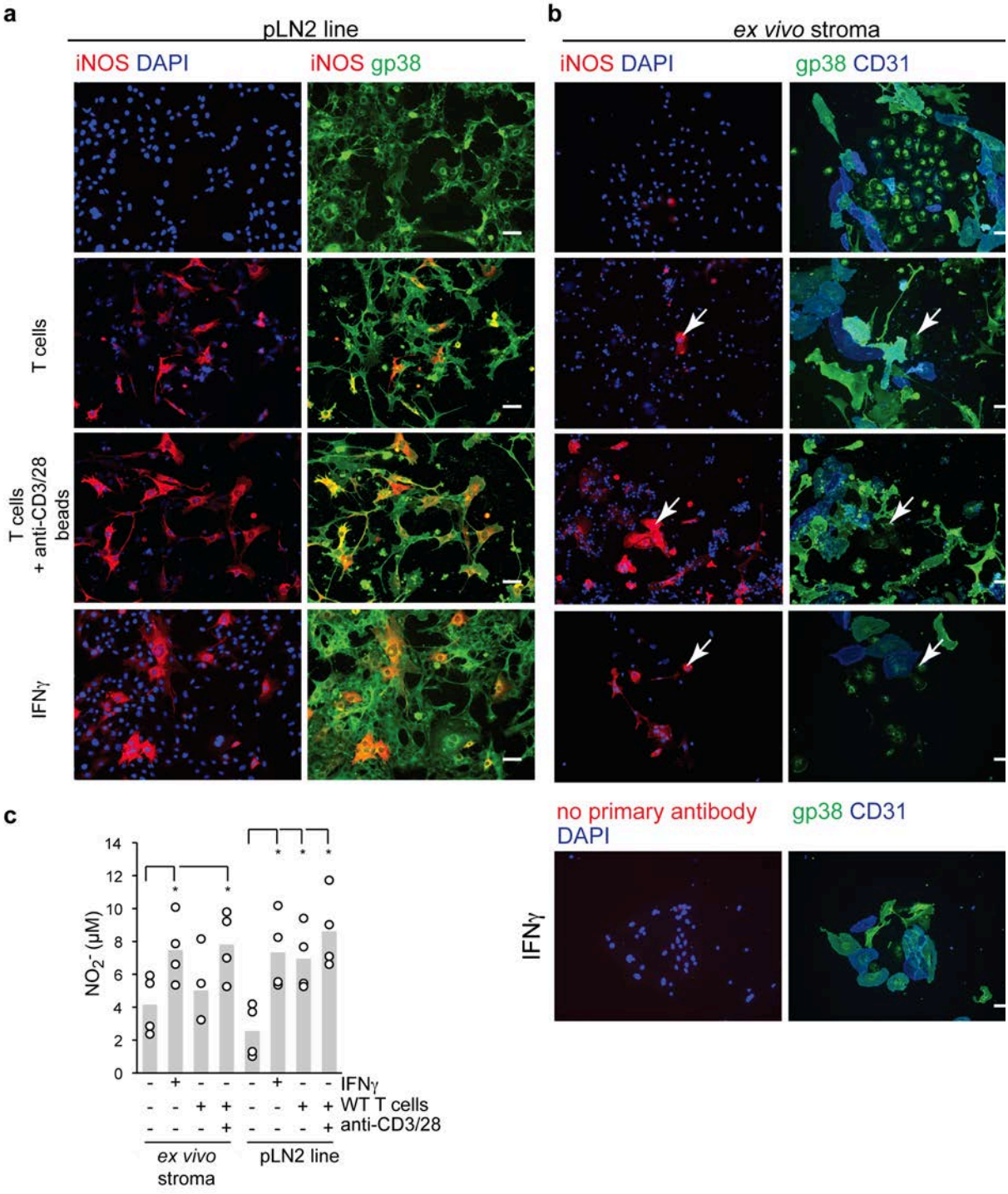

Figure 2.2.9: IFNγ or activated T cells induce iNOS expression in TRCs
Immunohistochemical analysis of iNOS expression in pLN2 TRC lines (**a**) or *ex vivo* (**b**). pLN2 TRCs or TRC-enriched cells from pLN of WT mice were cultured for 2 days either alone (first row), in the presence of WT T cells without (2nd row), with anti-CD3/28 beads (3rd row), or in the presence of 10ng/ml recombinant IFNγ (4th row). (**a**) iNOS is shown in red and gp38 TRCs in green. Blue shows DAPI+ nuclei. Tiny nuclei are from T cells, larger nuclei from BMDCs and pLN2. (**b**) The first column shows iNOS in red and DAPI in blue, except the last row that shows the 'no primary antibody' control in red. The second column shows gp38+ CD31- TRCs and gp38+ CD31+ lymphatic cells. Arrows show examples of gp38+ CD31- TRCs expressing iNOS. Scale bar 50μm. (**c**) Analysis of the NO_2^- concentration in the supernatants from co-cultures shown in a and b. (**a-c**) n= 3-5, representative for 2 experiments. * * $p < 0.05$, ** $p < 0.01$, *** $p < 0.001$

To obtain a more quantitative assessment of iNOS-expressing TRCs, iNOS-expressing cells were measured using intracellular staining and flow cytometry. This analysis showed that while IFNγ induced few TRCs to become iNOS-positive, there was a strong synergistic effect when both IFNγ and BMDCs were present in the co-culture with up to 25% TRCs being positive (figure. 2.2.10a). Given that BMDCs were occasionally observed to express iNOS in the co-cultures, we assessed the influence of IFNγ and TRCs on the ability of BMDCs to express iNOS. Interestingly, both IFNγ and TRCs induced iNOS protein expression in around 3% of BMDCs, but having both IFNγ and TRCs in the co-culture led to a strong synergistic iNOS expression in up to 30% of BMDCs (figure. 2.2.10a). This synergy was reflected in the almost 10-fold increase in extracellular nitrite levels detectable in the SN (figure. 2.2.10b). Interestingly, more than 50% of the nitrite seemed to be due to iNOS expression in TRCs rather than BMDCs as assessed using *Inos*$^{-/-}$ BMDCs. At present, a contribution by the two other NOS isoforms to nitrite production can not be excluded.

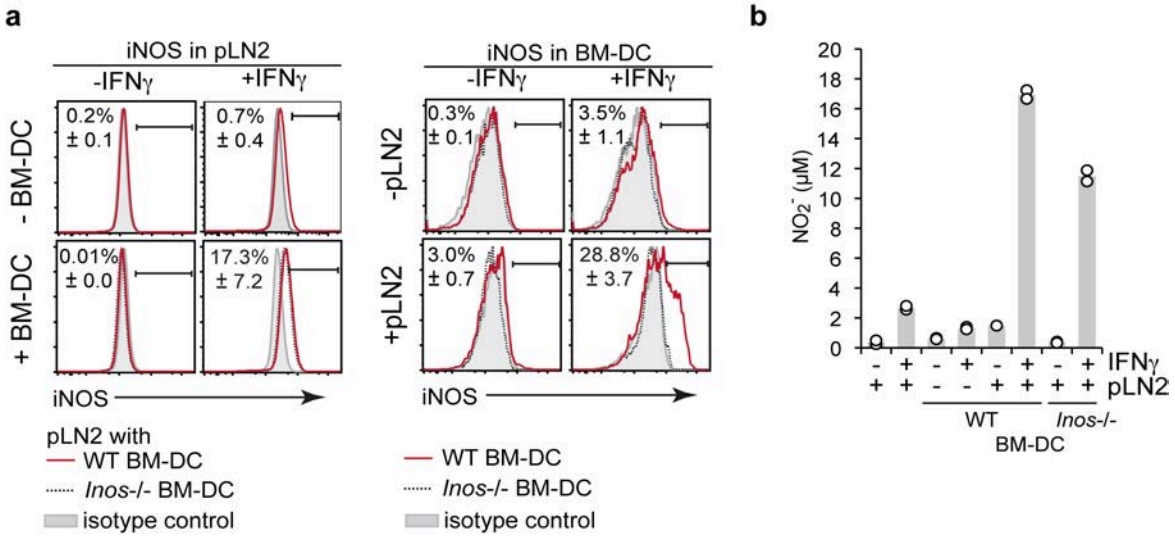

Figure 2.2.10: iNOS and NO production is highest when TRCs, BMDCs and IFNγ are present
(**a**) Flow cytometric analysis of intracellular iNOS expression in pLN2 TRCs or BMDCs, cultured for 2 days either alone or together and with or without 10ng/ml recombinant IFNγ. The histograms show the percentage of iNOS-expressing TRCs (gp38^{+} CD45^{-} CD31^{-}; panel on the left) or BMDCs (CD45^{+}; panel on the right) (± standard deviation). (**b**) NO_2^- concentration in the supernatant from the co-cultures in a; (**a,b**) n= 2, representative for 2 experiments.

Next we analyzed the speed of iNOS induction in pLN2 by looking at transcript levels. Already 7h after IFNγ stimulation *Inos* mRNA was induced 10-fold and further increased after 24h indicating direct transcriptional regulation of the *Inos* promoter (figure. 2.2.11). Interestingly, several pro-inflammatory cytokines (IFNγ, TNFα, LTα3) or LPS showed a similarly rapid and strong induction of *Inos* transcripts while their maintenance at 24h differed. TRCs constitutively expressed *Cox2*, which was slightly elevated after stimulation with IL-1β, TNFα, LTα3 or LPS. In summary, these results demonstrate that a subset of both TRCs and BMDCs can be triggered to express *Inos* transcripts and proteins leading to the release of NO. Various pro-inflammatory signals can serve as triggers in TRCs, including signals derived from

newly primed T cells suggesting the possibility of a negative feedback loop leading to inhibition of T cell expansion in our *in vitro* co-culture assay.

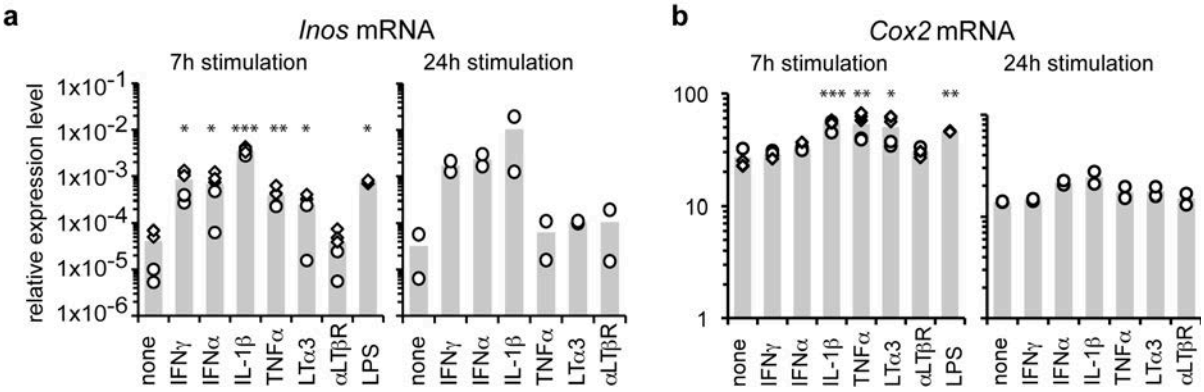

Figure 2.2.11: Various pro-inflammatory cytokines induce iNOS expression in TRC line
Quantitative RT-PCR analysis for *Inos* mRNA (**a**) or *Cox2* mRNA (**b**) of pLN2 cells stimulated with various cytokines, the agonistic anti-LTβR (αLTβR) or the TLR4 ligand LPS for 7h or 24h. The expression levels relative to two housekeeping (*Hprt* and *Tbp*) genes are shown. Different symbols indicate different experiments. (**a,b**) n=2-3, representative for 2 experiments. * $p < 0.05$, ** $p < 0.01$, *** $p < 0.001$

2.2.6. *Inos* deficiency leads to exaggerated CD8$^+$ T cell responses *in vivo*

To characterize the expression of iNOS during immune response *in vivo*, mice adoptively transferred with OT-I T cells were immunized with OVA-expressing vesicular stomatitis virus (VSV-OVA) and draining LN analyzed. By pressing LN across a 40 μm mesh a soluble fraction containing most hematopoietic cells was obtained as well as a non-soluble stromal cell fraction, including TRCs and part of the DCs (Luther et al., 2000; Link et al., 2007). Interestingly, one day after immunization *Inos* transcripts were induced in both fractions and dropped back to pre-immunization levels on day 2 and 4 (figure. 2.2.12a). These levels were always 5-10-fold higher in the fraction enriched in stromal relative to hematopoietic cells. To identify more precisely the cell type and frequency of iNOS expressing cells in the draining LN intracellular iNOS protein expression was analyzed by flow cytometry along with lineage markers. A subset of at least 2.6% TRCs were identified as major iNOS source appearing on day 1 and being again undetectable on day 2 and 4 post infection (figure. 2.2.12b). DCs showed a weak induction of iNOS expression on day 1 without reaching statistical significance relative to day 0. Few macrophages (CD11b$^+$ CD11c$^-$) were also found to express iNOS protein (data not shown). This result emphasizes the inducible and transient activation of iNOS both at the mRNA and protein level, consistent with pro-inflammatory molecules inducing it. It also strengthens the notion of more than one cell type expressing iNOS within the T zone of draining LN, most notably TRCs and DCs. Our attempts to identify and localize iNOS protein-expressing cells in situ were not successful (data not shown), consistent with the low iNOS expression detected by flow cytometry.

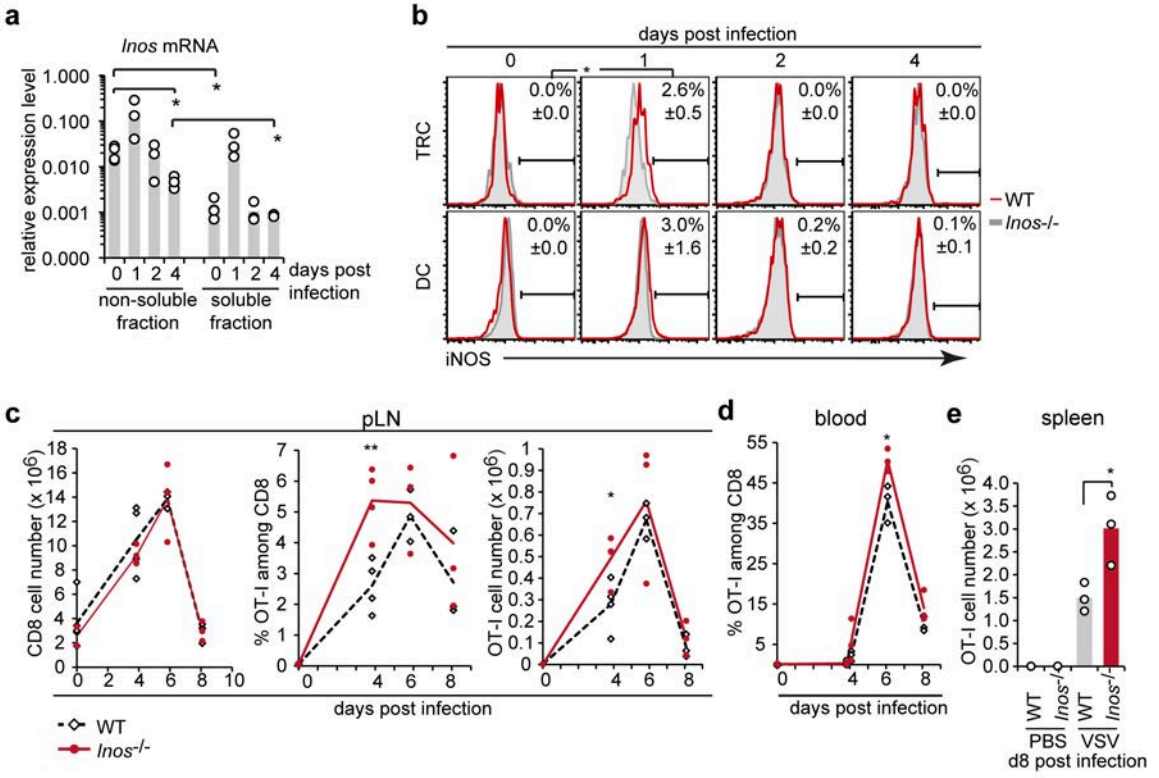

Figure 2.2.12: Lack of iNOS *in vivo* leads to an increased primary T cell response after viral infection
WT or *Inos*$^{-/-}$ mice were retro-orbitally grafted with 100'000 splenocytes from OT-I transgenic mice one day prior to subcutaneous infection with VSV-OVA. (**a,b**) Regional pLN from infected mice were harvested 1, 2 or 4 days after infection. (**a**) Normalized *Inos* mRNA levels as analyzed by quantitative real time-PCR on crude fractions of LN. (**b**) Intracellular iNOS protein expression in TRCs (gp38^{+}CD45^{-}CD31^{-}CD35^{-}) or DCs (CD11c^{+}MHCII^{+}CD45^{+}) as analysed by flow cytometry on collagenase-digested LN. Representative histograms show the percentage (± standard deviation) of iNOS expressing TRCs (top) and DCs (bottom) in WT versus *Inos*$^{-/-}$ mice. (**c**) A pool of 6 draining pLN harvested after 4, 6 or 8 days after infection were homogenized and analyzed by flow cytometry. The graph on the left side shows the total CD8^{+} T cell numbers in pLN, the graph in the middle the percentage of OT-I T cells among the CD8^{+} T cells and the graph on the right side the total OT-I number. No significant difference was observed in total CD8^{+} T cell numbers between immunized WT and *Inos*$^{-/-}$ mice. (**d,e**) Blood of VSV infected mice collected 4, 6 and 8 days after infection (**d**) and spleen harvested on day 8 (**e**) were analyzed by flow cytometry for the presence of OT-I T cells. (**d**) shows the percentage of OT-I T cells among the CD8^{+} T cells in the blood, (**e**) shows the total number of OT-I T cells in the spleen. (**a-e**) n ≥ 3. (**b-e**) 1 out of 2 independent experiments is shown. * $p < 0.05$, ** $p < 0.01$, *** $p < 0.001$

As a next step the impact of *Inos*-deficiency on OVA-specific T cell expansion and survival was measured in the LN draining the site of VSV-OVA injection. While on day 4 after immunization the total CD8^{+} T cell number was similar in both mouse strains the percentage and number of OT-I T cells was 2-fold higher in *Inos*$^{-/-}$ relative to WT mice (figure. 2.2.12c). On day 6 and 8 after immunization, the difference in OT-I T cell numbers was minimal between the two strains presumably due to many effector cells having left the LN between day 5 and 8. This scenario is supported by the strong increase in OT-I cells in blood between day 4 and 6 as well as by the significantly higher frequency of OT-I cells in blood of *Inos*$^{-/-}$ relative to WT mice (figure. 2.2.12d). As a consequence 2-fold more effector OT-I T cells accumulated within day 8 spleen in *Inos*$^{-/-}$ relative to WT mice (figure. 2.2.12e). Interestingly, the differentiation into effector cells occurred efficiently in the absence of iNOS, as based on the analysis of IFNγ expression and *in vitro* killing activity of effector CD8^{+} T cells from LN and spleen (figure. 2.2.13).

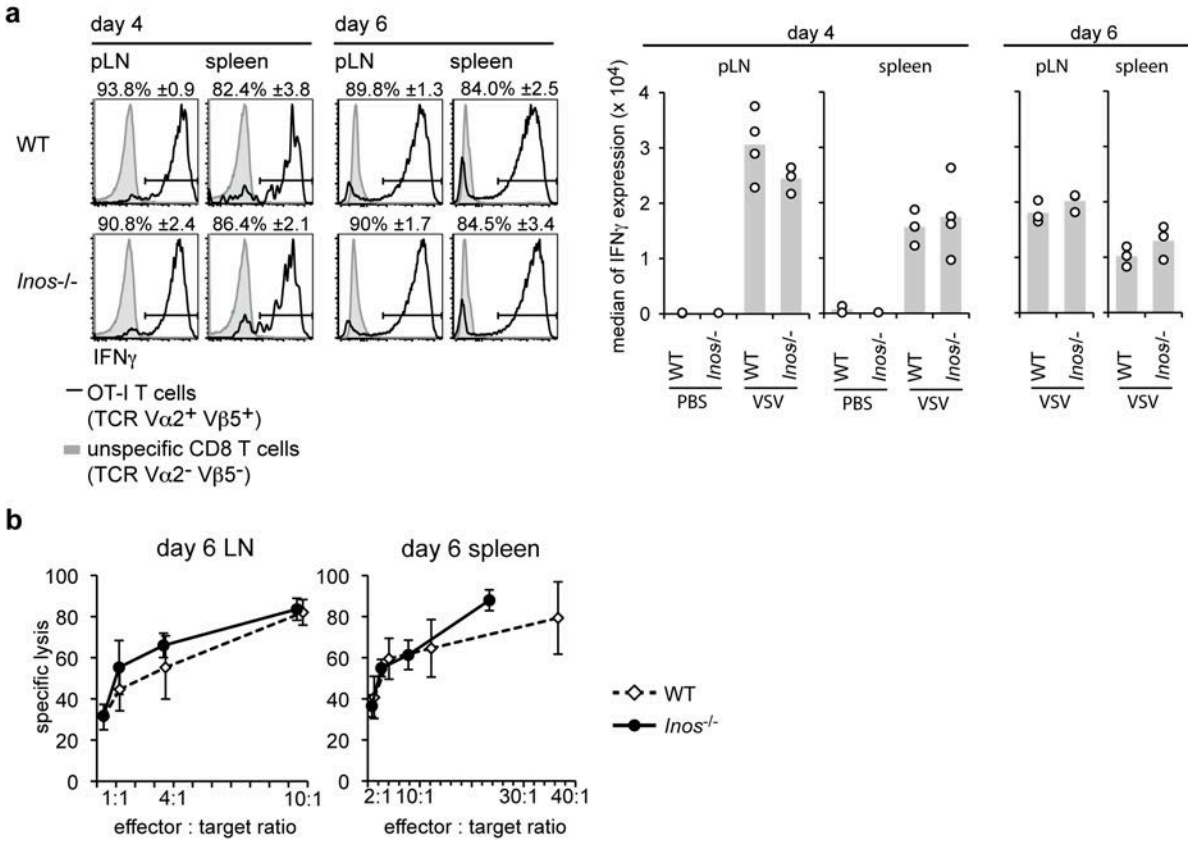

Figure 2.2.13: CD8 effector cells generated in VSV-OVA infected WT or *Inos-/-* mice show no difference in killing ability or IFNγ expression

WT or *Inos-/-* mice received 0.1 x 10^6 OT-I splenocytes by retro-orbital injection 1 day prior to infection with VSV-OVA. Draining pLN and spleen were harvested on day 4 and 6 after infection, homogenized and analyzed for IFNγ protein expression in OT-I T cells using flow cytometry (**a**) or for killing activity (**b**). (**a**) Histograms show the percentage of OT-I T cells (standard deviation) expressing intracellular IFNγ. Bar graphs show the fluorescence intensity of the IFNγ staining within OT-I T cells. (**b**) Cells from day 6 were used in an in vitro killing assay. The specific lysis of target cells is shown for the respective effector to target ratios. (**a,b**) n= 3. (**a**) representative for 2 experiments. (**b**) 1 experiment (but similar data were obtained for day 8 LN and spleen, not shown)

To address whether iNOS expression is critical in hematopoietic or non-hematopoietic cells bone marrow chimeras were generated. Unfortunately, a cell trapping defect was observed in inflamed LN if the stromal cell compartment was *Inos*-deficient, presumable due to a role of NO in vasodilatation in irradiated mice but not straight *Inos*$^{-/-}$ mice (figure 2.2.14). Therefore, no conclusions could be drawn from these experiments. In summary, the *in vivo* data indicate that acute inflammation associated with a viral infection leads to the transient expression of NO by TRCs and BMDCs found within the LN T zone, which slows down and lowers the antigen-specific T cell expansion but does not seem to impact on the differentiation and migration of effector T cells.

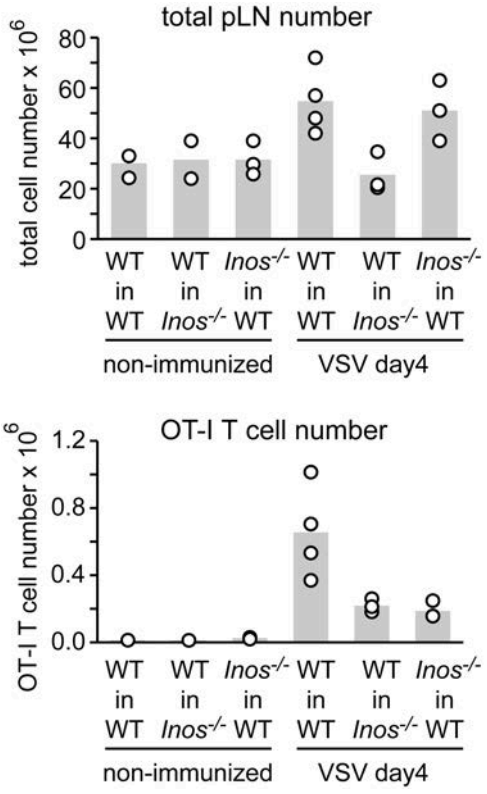

Figure 2.2.14: Bone marrow chimeras lacking *Inos* in the non-hematopoietic system show a lymphocyte trapping defect in immunized lymph nodes
To assess the relative contribution of hematopoietic versus non-hematopoietic cells as iNOS source, BM chimeras were generated having *Inos*-deficiency in either the hematopoietic system (*Inos*$^{-/-}$ BM into WT hosts) or non-hematopoietic system (WT in *Inos*$^{-/-}$) and were compared with control chimeras (WT into WT). 2 month after reconstitution, BM-chimeras were infected with VSV-OVA (as described in figure 2.2.12) and 4 days after infection pLN were collected, single cell suspensions counted and stained before analysis using flow cytometry. As comparison non-immunized BM-chimeras are shown. *Inos*$^{-/-}$ into *Inos*$^{-/-}$ chimeras have not been made. Surprisingly, none of the chimeras showed an increased OT-I expansion. Rather, *Inos*-deficiency in either the hematopoietic or the non-hematopoietic system led to a strong decreased OT-I expansion. Surprisingly, lymphocyte trapping did not occur in the case of *Inos*-deficiency in the non-hematopoietic compartment, in contrast to the other two groups and the non-chimeric *Inos*$^{-/-}$ mice (figure 2.2.12). Therefore, the expansion of OT-I T cells cannot be interpreted for that group of mice. The lack of OT-I expansion in the group of mice having *Inos* deleted in the hematopoietic system indicates also a positive role of *Inos* in T cell proliferation, presumably in a low but not high concentration, as previously suggested (Niedbala et al., 2006). In all BM chimeras the chimerism was >85% as assessed by measuring ratio's of CD45.1 (WT) versus CD45.1 (*Inos*$^{-/-}$ or WT) expression on total LN cells using flow cytometry. 2-4 mice per group, one experiment.

2.2.7. Contribution by others

S.S. generated most cell lines, did most *in vitro* and *in vivo* experiments, made the figures, and contributed to the manuscript writing; **H-Y.H.** developed new methods, performed intracellular iNOS stainings and contributed to transcript analysis, *in vivo* experiments and figure making; **C-Y.Y.** contributed to *in vivo* experiments; **L.S.** contributed to cell line generation, transcript analysis, *in vitro* and *in vivo* assays; **S.F., C.D.B, P.J.N., M.H., H.A.-O., and B.J.M.** contributed key reagents; **D.Z.** contributed VSV-OVA particles and advice, and participated in the writing; **S.A.L.** conceived and directed the study, wrote the manuscript and provided most funding. All authors contributed with advice and discussions and critically reviewed the manuscript. **Fabienne Tacchini-Cottier** contributed with discussions and critical reading of the manuscript; **Alena Donda, Greta Guarda, Catherine Ronet, Carl Ware** and **Anne Wilson** with reagents and valuable advice.

2.2.8. Discussion

Inflamed LN as well as the TRC network are generally considered as strongly immune-stimulatory for T cell immunity. Surprisingly, we obtained several lines of evidence demonstrating an inhibitory role of TRCs in early T cell activation: 1) *In vitro* TRCs limit the expansion of $CD8^+$ T cells primed by antigen-pulsed BMDCs or anti-CD3/28 beads at TRC-T cell ratio's as low as 1:100 with T cell effector function being reduced as well. 2) TRCs reduce the T cell activation potential of antigen-loaded BMDCs. 3) TRCs constitutively express transcripts for *Cox-2*, the enzyme required for the synthesis of PGE_2 and related factors (Tsatsanis et al., 2006). Inhibition of *Cox-1/2* markedly reduces this suppressive effect. 4) When exposed to pro-inflammatory cytokines pLN2 and *ex vivo* TRCs transiently express iNOS protein leading to NO_2^- synthesis. This correlates with rapid induction of *Inos* transcripts in activated pLN2. Inhibition of iNOS or use of *Inos*-deficient TRCs markedly reduces the suppression with this effect being enhanced by a *Cox-2*-inhibitor. 5) Upon immunization, iNOS protein gets transiently expressed in TRCs and DCs within the draining LN. 6) Absence of iNOS *in vivo* correlates with an exaggerated primary $CD8^+$ T cell response, consistent with the previous observation of an exaggerated memory T cell response in $Inos^{-/-}$ mice (Vig et al., 2004). Thus, while TRCs may have several ways of enhancing T cell activation, our assays have only revealed attenuating effects.

Attenuating effects of TRCs on T cell immunity have been reported recently based on the expression of self-antigen in the context of MHC I as well as PD-L1 expression on TRCs leading to modulation of $CD8^+$ T cell responses (Mueller et al., 2007; Lee et al., 2007; Fletcher et al., 2010). Here we have used fibroblasts of the LN T zone to show that they are a source of soluble immunomodulators such as NO and COX-1/2 dependent factors strongly inhibiting T cell expansion in response to a foreign antigen, with no role observed for PD-L1. Another study had noted iNOS expression in reticular LN fibroblasts upon infection with *Leishmania major* parasites, but the precise nature and localization of these cells have remained unclear. In addition, NO was in that case shown to be important for the control of the parasite rather than for adaptive immunity (Bogdan et al., 2000). Together these data suggest TRCs may help control $CD8^+$ T cell responses to both self- and foreign-antigens. Whether they also modulate the deletion of self-reactive T cells still needs to be tested.

Two previous reports have highlighted the capacity of spleen-derived stromal cells in inhibiting T cell activation. A mix of adherent stromal cells, possibly including TRCs, was shown to promote development of BM-derived progenitor cells into $IL\text{-}10^+$ regulatory DCs (Svensson et al., 2004) or the conversion of mature BMDCs into NO^+ regulatory DCs (Zhang et al., 2004). We did not observe consistent changes in the surface phenotype of TRC-conditioned DCs, possibly because our co-cultures were less than 16h allowing only short-term changes. In contrast, the previous reports were based on co-cultures of 1-2 weeks allowing developmental changes. While we have not yet identified the reason for the decreased stimulatory capacity of TRC-conditioned DCs it may be due to the rapid induction of iNOS in BMDCs.

Our results are reminiscent of observations with MSCs known to modulate many aspects of innate and adaptive immunity, including T cell proliferation (Nauta and Fibbe, 2007; Uccelli et al., 2008). *In vitro* BM-derived MSCs were shown to block mitogen- and DC-induced T cell proliferation by many different pathways, including NO and PGE_2 production (Aggarwal and Pittenger, 2005; Sato et al., 2007; Ren et al., 2008). In settings of allografts and autoimmune disease large numbers of injected MSCs strongly suppress T cell responses due to their anti-inflammatory properties, and due to their efficient homing to inflammatory sites and lymphoid tissues (Von Luttichau et al., 2005; Nauta and Fibbe, 2007; Uccelli et al., 2008). Interestingly, mature mesenchymal cells such as fibroblasts from various non-lymphoid tissues also dampen T cell expansion (Jones et al., 2007; Haniffa et al., 2007; Uccelli et al., 2008; Bouffi et al., 2011) suggesting mesenchymal cells at several maturation stages share this property. Alternatively, MSCs and fibroblasts may be hard to distinguish (Haniffa et al., 2009). We propose that LN and spleen TRCs have conserved this immunosuppressive property that they share with MSCs and fibroblasts from non-lymphoid tissues. The extent of inhibition was highly dependent on the number of TRCs being present in the culture (unpublished observation) which may explain the difference in the extent of NO-mediated suppression observed *in vitro* versus *in vivo*. Our preliminary results suggest that this inhibitory effect not only affects $CD8^+$ but also $CD4^+$ T cells. Besides affecting T cell expansion and possibly apoptosis, TRC presence partially reduced effector differentiation *in vitro* but not *in vivo*. While the reason for this difference is not known, it may be explained by the presence of lower NO concentrations or additional factors found *in vivo* that positively influence $CD8^+$ T cell differentiation. Given that TRCs and non-lymphoid fibroblasts can be grown easily from many accessible tissues in humans, such as tonsils or skin, they may represent an interesting source of immunomodulatory cells. A very recent study using skin fibroblasts has established their potential in efficiently suppressing the clinical signs of experimental arthritis in mice (Bouffi et al., 2011).

Different mechanisms of suppression have been described for MSCs: they can either directly inhibit T cell activation or reduce the stimulatory capacity of DCs by various means (Nauta and Fibbe, 2007; Uccelli et al., 2008). MSCs can produce high amounts of NO upon contact with T cells which interferes with STAT-5 phosphorylation and therefore IL-2 signalling. MSC-mediated T cell suppression could be partially neutralized using inhibitors of iNOS or COX-2, or using *Inos*$^{-/-}$ MSCs (Sato et al., 2007; Ren et al., 2008) thus showing clear parallels in MSC- and TRC-mediated T cell mechanisms. In our *in vitro* experiments we have obtained evidence for an additive inhibitory effect of NO and COX-1/2 dependent factors (possibly PGE_2), but additional factor(s) probably remain to be identified to explain the entire inhibitory effect. Blocking TGFβ, PD-L1, IL-10, arginase-1 and IDO activity did not influence TRC mediated inhibition, however additional studies will be necessary to fully rule out their contribution. Furthermore, we cannot exclude that the other two NOS isoforms - eNOS and nNOS - are expressed in TRCs and contribute to the TRC mediated inhibition.

The expression and activity of iNOS is tightly controlled at several levels with the best-characterized positive regulators being IFNγ, IFN-α/β, TNFα, IL-1 and LPS (Bogdan, 2001). Indeed, iNOS expression in TRCs was induced by all of these pro-inflammatory cytokines confirming and extending previous data using LN fibroblasts, MEFs and MSCs (Lavnikova and Laskin, 1995; Bogdan et al., 2000; Bogdan, 2001; Ren et al., 2008). Interestingly, only a subset of IFNγ-stimulated TRCs expressed iNOS, even when a TRC clone was used (data not shown), in line with previous reports on other fibroblast types (Lavnikova and Laskin, 1995; Bogdan et al., 2000) as well as our observation on BMDCs reported here. Whether these are distinct cell subsets or whether iNOS expression by some cells prevents expression by others remains to be investigated. Recent results suggest that IFNγ is not restricted to immune synapses but more widely accessible throughout the T zone (Perona-Wright et al., 2010) which may explain why TRCs obtain this signal in the absence of cognate interaction with primed T cells. Several reports showed that IFNγ during T cell priming influences the degree of $CD8^+$ T cell contraction (Haring et al., 2006). While IFNγ signalling within T cells may lead to this outcome (Haring et al., 2006), our results suggest that IFNγ signalling in TRCs and DCs leading to NO production early after infection might not only control the expansion, but also the contraction phase of $CD8^+$ T cells, such as by nitrosylating and thereby altering key proteins of the IL-2 or TCR signalling pathway (Bogdan, 2011; Kasic et al., 2011). More experiments will be necessary to test this hypothesis and to understand the underlying mechanism.

Strikingly, iNOS induction and NO_2^- production was highest when TRCs, activated DCs and IFNγ were present together suggesting only adjacent TRCs become licensed to suppress T cell expansion with this being a highly controlled and transient process. The DC-derived signals leading to iNOS expression in TRCs remain to be identified. Good candidates are IL-1α/β and TNFα which may act synergistically with IFNγ, similar to iNOS expression in MSCs (Ren et al., 2008). NO effects are known to be highly dose-dependent. Low NO doses can enhance T cell proliferation, as possibly suggested by the decreased T cell expansion in some of the BM chimera experiments (*Inos*$^{-/-}$ into WT). Higher NO doses are known to induce cell-cycle arrest and apoptosis of T cells (Bogdan, 2001; Niedbala et al., 2006) indicating that the reduced expansion seen in presence of TRCs may represent a combined effect of reduced proliferation and increased apoptosis of T cells. The dual role of NO may also explain the only two-fold higher expansion of T cells in absence of iNOS. Given that NO is a highly reactive gas close proximity to TRCs is likely to be critical in inhibiting T cells and DC activation. To further improve this process cytokine-stimulated TRCs could actively recruit or retain primed T cells, as suggested for MSCs (Ren et al., 2008). Interestingly, TNFα-stimulated TRCs were shown to express the IFNγ-inducible chemokine CXCL10 that attracts activated but not naïve T cells (Katakai et al., 2004).

Both *in vitro* and *in vivo*, we found not only TRCs but also DCs to express iNOS and produce NO_2-. It is possible that the $iNOS^+$ DC subset identified *in vivo* represents the inflammatory tipDC ($TNF\alpha^+iNOS^+CCR2^+$) which are recruited into the splenic T zone early during infection with *Listeria monocytogenes* a (Serbina et al., 2003) or other pathogens (Dominguez and Ardavin, 2010) as they were also

CD11c^{int} in our analysis (unpublished observation). Interestingly, increased T cell proliferation was also reported for *Ccr2*$^{-/-}$ mice lacking tipDCs (Serbina et al., 2003). *In vitro* we found iNOS expression in BMDCs to be induced in a synergistic manner by IFNγ and TRC presence, similar to synergistic effects of IFNγ and BMDCs on iNOS expression by TRCs. While the factors involved in the cellular crosstalk remain to be identified these findings point to the interdependence of these two cell types in inhibition of T cell expansion, an observation which needs further *in vivo* studies with cell-type specific *Inos* deletion. Our attempts to distinguish between stromal versus hematopoietic sources of iNOS using bone marrow chimeras were unsuccessful due to a cell trapping defect in inflamed LN if the stromal cell compartment was *Inos*-deficient, presumably due to a role of NO in vasodilatation in irradiated mice but not straight *Inos*$^{-/-}$ mice. Based on our current results we propose the following working model (figure 2.2.15): Low levels of iNOS expression are induced in both immigrating DCs and TRCs when they meet in the T zone early during the immune response. This may increase the threshold required for T cell priming and thereby prevent the activation of low-affinity T cells that are often self-reactive. Alternatively, it may help in T cell priming. Once the first T cells are primed and produce IFNγ they may boost iNOS expression in both cell types in a transient fashion thereby inducing a negative feedback loop dampening T cell expansion by either slowing down their proliferation or diminishing their survival. This feedback loop may be activated mainly during a very strong immune response.

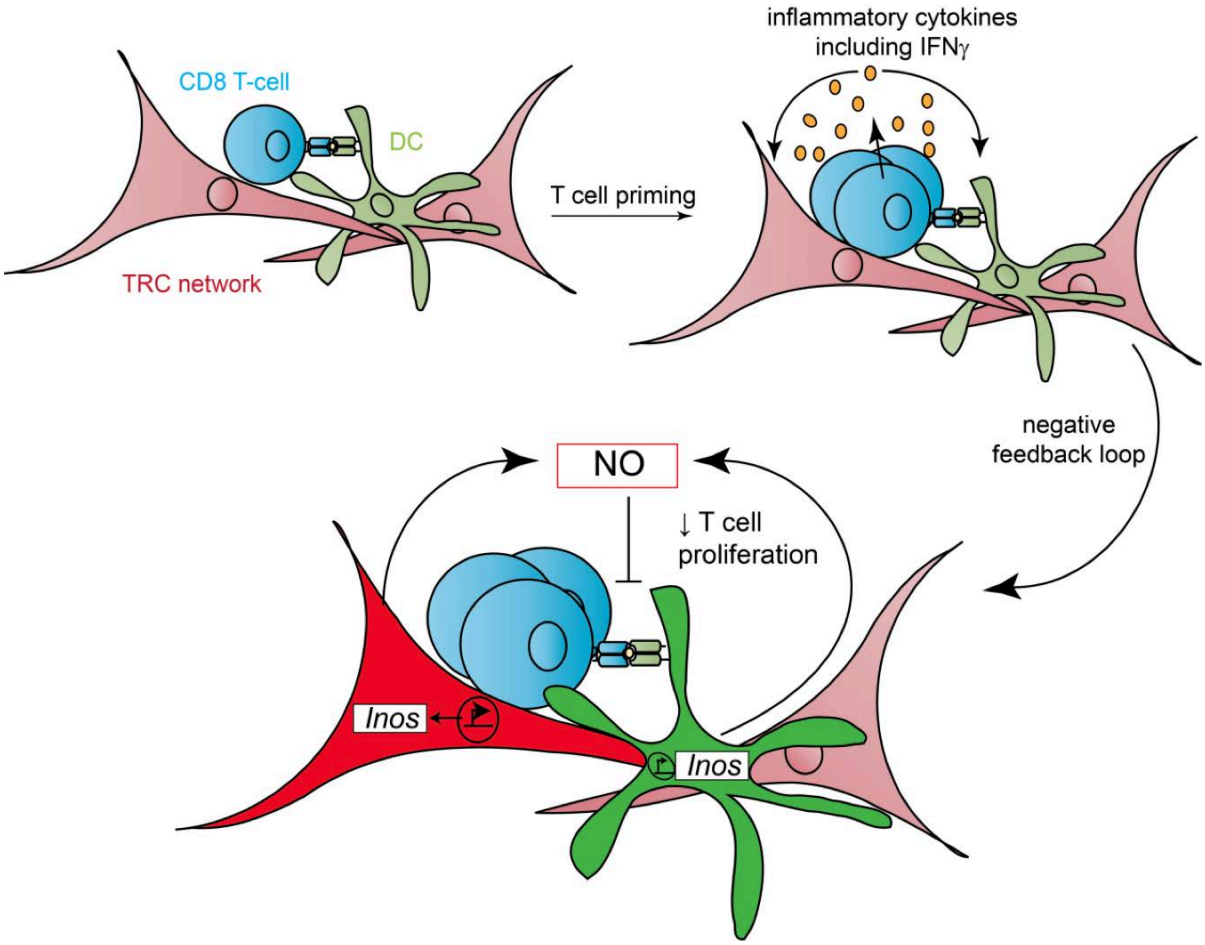

Figure 2.2.15: Model showing how inflammatory cytokines may induce iNOS expression in TRCs and create a negative feedback loop limiting antigen-specific T cell expansion
During the early phase of immune response antigen –specific CD8+ T cells interact with antigen-bearing DCs within the context of the TRCs network within the T zone of the draining LN. Upon prolonged cognate interactions T cells start to produce IFNγ and possible other cytokines that induce strong but transient iNOS expression in the neighbouring TRCs as well as DCs. The local production of NO creates a negative feedback loop in which NO and possibly other inhibitory factors limit the expansion of neighbouring antigen-specific T cells. This effect is due in part to direct inhibition of T cell proliferation or survival, in part to a decrease in the stimulatory capacity of DCs. NO is known to lead to nitrosylation of cysteine- and tyrosine-containing proteins thereby altering their function, including in T cells where reduced T cell proliferation was reported in presence of NO (Bogdan, 2011). High NO concentrations may also reduce T cell survival. An alternative model is that *in vivo* innate immune cells, such as NK cells, become activated early during the response and release IFNγ that induces iNOS in TRCs and DCs. Together, these processes may prevent overshooting antigen-specific T cell expansion while affecting much less T cell differentiation. This selective negative regulation of T cell numbers by TRCs and DCs may allow gradual organ and stromal cell growth thereby achieving a compromise between preservation of functional organ structure and fast effector T cell differentiation. It is reminiscent of the role of TRCs in controlling naive T cell numbers (Link et al., 2007; Zeng et al., 2011). The early and transient induction of iNOS may have also an impact on later aspects of the immune response, such as the contraction phase and memory T cell generation, as they are thought to be controlled by conditions encountered during T cell priming phase (Williams and Bevan, 2007; Haring et al., 2006).

The immunosuppressive feature of mesenchymal cells is intriguing. It raises the question of why these cells have this function, especially when considering TRCs localize to the T zone of SLO where inhibitory effects are less expected but well known from TipDCs and regulatory T cells. We would like to propose two possible reasons: 1) Keeping the LN in a slightly suppressive state might be a mechanism to limit the

activation of potentially auto-reactive cells while allowing strong immune responses to foreign antigens to occur. In line with this hypothesis we found *Cox-2* transcripts to be highly expressed in naïve LN. Others showed that high iNOS and NO_2^- levels are frequently associated with Th1-mediated inflammation, but sometimes also with autoimmune disease (Bogdan, 2001; Niedbala et al., 2006) Consistent with a protective role of this pathway in certain autoimmune diseases, *Inos*$^{-/-}$ and *Ifnγ*$^{-/-}$ mice have a higher incidence, increased severity and less relapses of experimental autoimmune encephalitis that correlate with increased proliferation of auto-reactive T cells relative to WT mice (Fenyk-Melody et al., 1998; Xiao et al., 2008) Similarly, in a mouse model for myasthenia gravis *Inos*$^{-/-}$ mice develop more self-reactive T and B cells, including epitope spreading (Shi et al., 2001). 2) In contrast to recirculating hematopoietic cells fibroblasts resident in lymphoid and non-lymphoid organs have a function for the organ itself: ensure its integrity and functionality. During injury, such as infection or inflammation, fibroblasts perform tissue repair to re-establish homeostasis. LN swelling during immune response can be viewed as a threat to the organ as it is characterized by the dramatic increase in organ size due to the influx of many naïve lymphocytes as well as the rapid expansion of antigen-specific lymphocytes. The strong increase in lymphocyte numbers within the T zone may be harmful for the existing TRC network that functions as the structural platform for T cell priming and probably also T cell differentiation. Destruction of the TRC architecture, such as after LCMV infection, correlates well with immunodeficiency (Scandella et al., 2008; Mueller and Germain, 2009; Svensson and Kaye, 2006). Limiting T cell expansion early in the immune response might be necessary to give TRCs the time to adjust step-wise to the new space demands and to start proliferating thereby increasing the scaffold size accommodating T cells and DCs. Such a process may ensure continuous functionality of the growing organ which is finally also to the benefit of efficient effector T cell generation

.

3. General discussion and perspectives

Overview over the major findings

In the first results part of this thesis, I have described the establishment and characterization of LN TRC clones and lines, the establishment of a special 3D cell culture system for TRCs in which T cells and antigen-bearing DCs can be included. Therefore, I was able for the first time to reproduce a functional T zone microenvironment *in vitro* in which T cell activation could be induced. Much to our surprise, the presence of TRCs appeared to reduce rather than enhance T cell proliferation.

In the second results part of this thesis I have dissected in detail the surprising negative effect of TRCs on T cell activation by antigen-presenting DCs using 2D cultures. I have obtained *in vitro* and *in vivo* evidence for prominent iNOS expression in activated TRCs along with a key role for NO in the attenuation of T cell responses. Therefore, we propose that TRCs act not only as positive but also as negative regulators of T cell immunity within draining LN.

3.1. Establishment and characterization of TRC clones / lines and the reconstruction of the lymphoid T zone *in vitro*

Culturing adherent cells from digested murine LN led to the outgrowth of fibroblastic cells with a morphological and surface phenotype comparable to *ex vivo* isolated TRCs. However, the production of *Ccl19, Ccl21* and *Il-7* is lost and could not be re-stored by stimulation with various cytokines or TLR ligands. One possibility explaining the lack of CCL19, CCL21 and IL-7 expression, might a partial de-differentiation of TRCs *in vitro* and it remains to be clarified whether TRC clones and lines still have the capability to produce these cytokines. Preliminary experiments by Chen-Ying Yang in the lab failed to recover TRCs upon intravenous or subcutaneous cell transfer. It would be interesting to test whether injection of these cells via afferent lymphatic vessels would lead to their re-integration into the stromal network of the draining LN and whether their cytokine expression is restored in the *in vivo* microenvironment.

We have established a 3D culture system for TRCs that corresponds much more to a 3D network forming cell type than conventional 2D cultures. When collagen-only gels were used strong contraction of these was observed (Tomei et al., 2009b; Link et al., 2007), similar to a recent report by Fletcher and colleagues, who cultured *ex vivo* isolated TRCs in a collagen-matrigel matrix. They added the pan Src tyrosine kinase inhibitor PP2 to prevent gel contraction (Fletcher et al., 2011a). As this inhibitor blocks several Src tyrosine kinases including Lck and Fyn it interferes with TCR signalling and would not be appropriate for studies on T cell activation (Salmond et al., 2009; Hanke et al., 1996). To that end, a rigid poly-urethane sponge like used in our experiments appears more appropriate (Tomei et al., 2009a, 2009b). In both studies, TRCs cultured in 3D show *in vivo* like morphology and form 3D networks (Tomei et al., 2009b; Fletcher et al., 2011a). When we added antigen specific T cells and antigen loaded BMDCs to this 3D culture system, antigen-specific T cell activation was observed. Preliminary microscopical analysis, however, indicated that T cells and DCs did not penetrate into the deeper regions of the sponge-collagen culture, which was not altered by embedding CCL19 and CCL21 in the collagen matrix. Therefore, this

likely arises from insufficient oxygen and nutrient transport due to the thickness of our 3D culture system (Haycock, 2011). When Fletcher and colleagues added T cells and DCs to their 3D cultured TRCs, migration of T cells along TRC networks was observed (Fletcher et al., 2011a). In contrast to our 3D culture, they cultured TRCs in thin gels, in which no problems with oxygen or nutrient supply should occur. However, TRCs rapidly contract these matrices, making long-term culture and imaging of T cell activation almost impossible. The integration of an oxygen-supply into our 3D culture system should allow to perform long-term culture with good gel penetration of cells. An alternative approach to study T cell activation *in vitro* in a more physiological system, would be the use of live vibratome sections, used for example by Aspertini-Boursin and colleagues (Asperti-Boursin et al., 2007). However, in such a system the composition of the slice, for example the presence of certain chemokines, cannot be as easily controlled as in the 3D culture system. More importantly, as no TRC-knock out model is yet described, T cell activation could not be observed in the complete absence of TRCs.

3.2. TRC attenuate T cell proliferation mediated by nitric oxide production

The presence of TRCs in our *in vitro* T cell activation assay strongly reduced T cell proliferation and partially reduced cytotoxic T cell differentiation into effector cells. It was hypothesized that the TRC network helps T cells to efficiently encounter many antigen presenting DCs and in this way positively influences T cell activation (Junt et al., 2008; Mueller and Germain, 2009). However, the T cell activation assay was conducted in 2D co-cultures in which it should be easier for antigen-specific T cells to find antigen-presenting DCs than in 3D, making the described positive influence from TRCs less important in that system. To this end, preliminary experiments were conducted in the 3D culture system where *in vivo* like TRC networks were present but T cell proliferation was similarly inhibited compared to the 'no stroma' control that showed efficient T cell activation. However, as discussed above, the 3D culture system still needs optimization in terms of oxygen supply and it remains to be tested, whether the access of T cells and DCs to the deeper regions of the sponge might change the outcome of T cell activation.

Nevertheless, in accordance with our results, Kaminer-Israeli and colleagues reported that presence of a murine BM-derived stromal cell line inhibits T cell proliferation induced by antigen-pulsed BMDC in a 3D culture system *in vitro* (Kaminer-Israeli et al., 2010). In their report stromal cells were embedded in an alginate scaffold along with BMDC, while proteolipid-protein (PLP) specific T cells were added exogenously. Addition of stromal cells markedly inhibited T cell proliferation and development into Th1 or Th17 cells, possibly due to the high levels of IL-10 and TGF-β found in the system. Furthermore, the BMDC or BMDC/stromal cell seeded alginate constructs could be successfully transplanted under the kidney capsule and were shown to maintain PLP antigen *in vivo*. Transplanted constructs in PLP-TCR transgenic mice were infiltrated by T cells, which subsequently proliferated. Also in the *in vivo* situation, presence of stromal cells inhibited T cell proliferation (Kaminer-Israeli et al., 2010). These findings suggest that upon optimization of our 3D culture system similar results may be obtained.

TRCs *in vivo* are a major source of the three cytokines IL-7, CCL19 and CCL21, which was taken as evidence that TRCs positively regulate T cell responses. In contrast, TRC lines used for most of the experiments lack the production of CCL19, CCL21 and IL-7. For this reason, in initial experiments recombinant CCL19, CCL21 and IL-7 were added without altering the dampened T cell activation observed in presence of TRC lines. Furthermore, freshly isolated *ex vivo* TRCs, which still produce CCL21, CCL19 and IL-7 (Link et al., 2007) (personal communication with T. Vogt) equally inhibited T cell proliferation. In summary, we conclude that it is most likely not the lack of the homeostatic chemokines or IL-7 production by TRC lines that mediates inhibition of T cell proliferation. However, in initial T cell activation assays a considerable number of dying T cells was observed which was ameliorated by addition of low doses of recombinant IL-7 and IL-2. None of the two cytokines had obvious effects on the TRC-mediated inhibition of T cell proliferation and therefore they were routinely added in further experiments to ensure good survival of T cells. This is consistent with previous observations that IL-7 enhances T cell responses to influenza A infection *in vivo*, without having effects on T cell activation *in vitro* (Saini et al., 2009; Pellegrini et al., 2011).

The situation is different for the chemokines CCL21 and CCL19 that are also presented by HEVs and LECs (Förster et al., 2008) thereby guiding both lymphocytes and mature DCs into the LN T zone. As a consequence, immune responses in LN of CCR7-deficient or *plt/plt* (*paucity of lymph node T cell*) mouse mutants is delayed (Förster et al., 2008; Cyster, 2005). In our *in vitro* assay, this role of CCR7 ligands is not necessary. It may, as suggested by several *in vitro* studies, simply increase somewhat T cell motility (Asperti-Boursin et al., 2007) and T cell co-stimulation (Friedman et al., 2006; Flanagan et al., 2004; Gollmer et al., 2009) besides enhancing DC maturation (Sanchez-Sanchez et al., 2006; Marsland et al., 2005). However, CCL19 is completely dispensable for effective T cell activation *in vivo* under the conditions tested (Britschgi et al., 2010). Furthermore, viral infection of $CCR7^{-/-}$ mice still results in efficient formation of cytotoxic T cells (Junt et al., 2004). It is possible that the effects of CCL19 and CCL21 on T cell priming only become detectable in settings of suboptimal stimulation which may not be the case in our co-culture systems where we used relatively high OT-I T cell frequencies and fully matured BMDCs loaded with saturating doses of peptide.

An early working hypothesis was that inhibition of T cell proliferation by TRCs might only occur in naïve mice and in this way represent a mechanism to prevent activation of auto-reactive T cells. Accordingly, stimulation of TRCs with pro-inflammatory signals produced in infections could lead to a functional switch in TRCs and make them non-inhibitory. To this end, various cytokines were added to the T cell activation assay. None of the tested cytokines or agonists (IL-1α, IL-1β, IL-6, IL-13, RANKL, TNFα, LTα3, anti-LTβR) significantly decreased the inhibition of T cell proliferation, or stimulation led to unspecific effects. To draw a definitive conclusion more experiments will be necessary. MSCs were reported to express TLR3 and TLR4 and triggering of these receptors abrogated their ability to suppress T cell proliferation (Liotta et al., 2008). In our hands, stimulation with the TLR ligands Poly I:C (TLR3

ligand), CpG or LPS (TLR9 and TLR4 ligand, respectively) slightly (up to 50% less inhibition) decreased the inhibition of T cell proliferation, but direct effects on DCs could not be excluded. To this end TRCs were pre-stimulated with various cytokines or TLR ligands for 24 hours prior to addition of T cells and DCs. Again, none of the tested cytokines significantly changed T cell proliferation in presence of TRCs. While no effect of LPS pre-stimulation could be observed, pre-stimulation with Poly I:C seemed to reduce the TRCs mediated inhibition (50-100% less inhibition in 3 independent experiments). But considerable variations were observed in different experiments and no definitive conclusion could be drawn. These results are rather puzzling, as LPS stimulation of TRCs induced *Inos* expression and LPS is known to be a strong inducer of *Inos* expression in macrophages and DCs (Bogdan, 2001). However, freshly isolated *ex vivo* TRCs from immunized mice inhibited T cell proliferation to similar extent as *ex vivo* TRCs from naïve LN, rather arguing against a functional switch of TRCs during inflammation. Still, mice in these experiments were immunized with NP-CGG in Montanide, the latter being a water-in-oil-emulsion adjuvant. Although pro-inflammatory cytokines should be produced, no known TLR ligands were added. Therefore, regulation of the inhibitory features of TRCs by TLR-ligands might still represent a possible control mechanism. Experiments with TLR3- and/or TLR4-deficient TRCs would be useful to gain more insight into the role of these pathways.

We show here that indomethacin, a COX inhibitor, and 1400W, an iNOS specific inhibitor, restored partially the T cell activation in presence of TRCs. Interestingly, *Cox-2* is constitutively expressed in TRCs while *Inos* was induced by IFNγ as well as other cytokines such as IL-1β and was highest when IFNγ and activated BMDCs were present. TRC-conditioned supernatant inhibited T cell activation but the extent was significantly decreased compared to physical presence of TRCs. This is most likely not due to NO as TRC conditioned supernatant was derived from TRCs cultured alone and no iNOS expression was detectable without cytokine stimulation. Moreover, NO is a short-lived molecule, which is most likely not stable in cell culture supernatant. Therefore, we attribute the weak inhibitory features of TRC conditioned supernatant mostly to COX-1/2 dependent factors. However, it should be mentioned that also *Cox-2* transcription was enhanced after stimulation with pro-inflammatory stimuli such as IL-1β. This might be partially a consequence of *Inos* induction, as NO is known to positively regulate *Cox-2* transcription (Tsatsanis et al., 2006; Harizi and Gualde, 2006).

Constitutive expression of *Cox-2* in TRCs might be a mechanism to keep the LN in a slightly suppressive state during homeostasis and to prevent activation of auto-reactive T cells by setting an 'activation threshold' (figure 3.1). In that sense it would be interesting to test whether TRC-specific COX-2 deficient mice are more prone to develop auto-immunity compared to WT mice. Interestingly, *Cox-2* was found to be constitutively expressed in thymic stromal cells and seems to be implicated in tolerance induction (Rocca and FitzGerald, 2002). Furthermore similar to thymic stromal cells, TRCs were shown to express peripheral-tissue antigens and to promote peripheral tolerance (Fletcher et al., 2011b). Therefore, it seems worthwhile to test whether COX-2 activity in TRCs contributes to peripheral tolerance induction. In

addition, the transient induction of *Inos* during infection might be a mechanism to increase the 'activation threshold' for T cells to prevent bystander activation of autoreactive T cells during acute inflammation and T cell activation (figure 3.1). If this model were correct, then TRC-specific *Cox-2/Inos* double knockout mice should be more susceptible to experimentally induced autoimmunity than single knockout mice, or even develop spontaneous autoimmune disease.

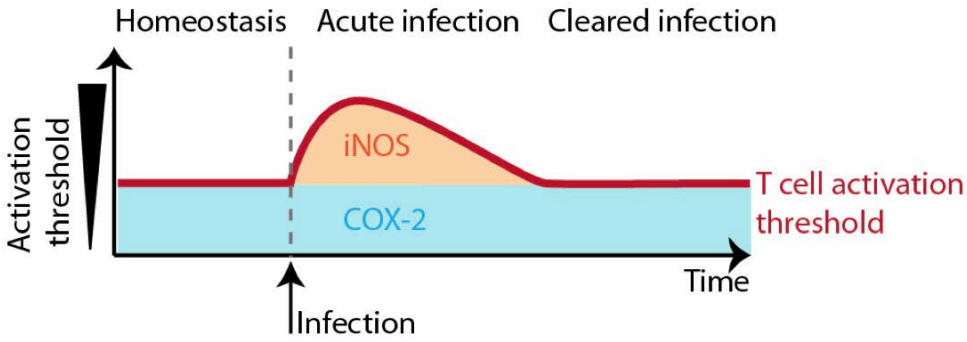

Figure 3.1: Model showing how COX-2 and iNOS expression in TRCs could set a threshold for T cell activation
TRCs constitutively express *Cox-2*, which might keep the LN in a slightly suppressive state during homeostasis. Upon infection, iNOS is transiently induced in TRCs (and DCs), which may increase the threshold for T cell activation. This might be an important mechanism to prevent bystander activation of autoreactive T cells during inflammatory responses.

Upon viral infection of WT mice, *Inos* was transiently induced in a subset of TRCs and DCs. In accordance with previous reports showing that the outcome of a CD8 T cell response is programmed within the first few days after infection (Williams and Bevan, 2007; Haring et al., 2006), this was sufficient to limit T cell expansion, as it was significantly increased in iNOS$^{-/-}$ mice. Unfortunately, it was not possible to dissect the role of iNOS expression in DCs versus TRCs. Experiments with BM-chimeras of WT in iNOS$^{-/-}$ and vice versa were conducted. However, chimeras showed defective cell trapping upon infection and results were therefore not conclusive. Cell type specific iNOS$^{-/-}$ mice will be needed to answer this question more conclusively. To this end, the establishment of mice carrying a floxed iNOS is necessary (ES cells containing floxed *Inos* are available from the Wellcome Trust Sanger Institute, UK) which can then to be crossed with DC or TRC specific cre-recombinase mice. Though DC specific CD11c-cre mice exist (Caton et al., 2007), no such mouse model is available yet for TRCs. One difficulty is that no highly TRC-specific promoter is known. Very recently Onder and colleagues reported the generation of a BAC transgenic mouse expressing the cre-recombinase under the gp38 promoter, but only 15% of LN FRCs were shown to express the transgene. In addition the transgene was also expressed in a subset of LECs (Onder et al., 2011). For this reasons this mouse model is not the ideal to dissect the TRC-specific role of iNOS. Nevertheless, in collaboration with our laboratory B. Ludewig (St. Gallen, Switzerland) has established a transgenic mouse expressing cre-recombinase under control of the CCL19 promoter (abstract, Swiss Immunology meeting, Lugano, 2011), which might prove to be a valuable tool for future experiments.

Although primary T cell expansion was significantly increased in iNOS$^{-/-}$ mice, the magnitude of this effect seems to be smaller compared to the difference in T cell proliferation observed *in vitro* with or without TRCs or 1400W. One major difference is that TRCs were completely absent in our negative control of the *in vitro* assay, while these cells were still present in *Inos*$^{-/-}$ LN, and therefore capable of expressing other suppressive factors such as such as COX-1/2 dependent molecules. It remains to be tested whether blockage of PGE_2 production *in vivo* and/or genetic disruption of the *Cox2* gene will lead to increased primary T cell responses. Furthermore, if the production of PGE_2 partially compensates for the lack of *Inos* in our *in vivo* model, then primary T cell responses should be even more enhanced in *Cox2-Inos* double knock out mice. However, as both iNOS and COX-2 are known to be expressed by DCs and not only TRCs (Harizi and Gualde, 2006; Gualde and Harizi, 2004), again the question will arise about the contribution of DCs and TRCs to this effect *in vivo*. It remains to be tested how much COX-1/2 is expressed by TRCs compared to DCs. More important evidence may be obtained by analysing cell-specific COX-2 knock out mice. PGE_2 is an interesting molecule as it was shown to have anti- and pro-inflammatory features depending on the context. It modulates DC function: While it is co-stimulatory for naïve DCs in the periphery it seems to be suppressive for mature DCs (Gualde and Harizi, 2004). We show that co-culture of TRCs with activated BMDCs reduces the stimulatory capacity of DCs. It is likely that this is mediated by COX-1/2 derived factors, as *Cox-2* is constitutively expressed in TRCs and NO_2^- levels were not elevated in supernatant from TRC BMDC co-cultures in absence of IFNγ. However other factors or cell-cell contact as reported by Zhang and colleagues (Zhang et al., 2004) might play a role as well. Therefore, co-cultures of TRCs and BMDCs in a transwell setting would be useful to further dissect this question. Or to condition BMDCs with supernatant derived from TRCs cultured in presence of the COX-1/2 inhibitor indomethacin.

Strengthening the relevance of the negative regulation of T cell activation by TRCs, two other publications were recently published showing very similar results (Lukacs-Kornek et al., 2011; Khan et al., 2011) (table 3.1).

		Siegert	**Khan**	**Lukacs-Kornek**
Read-out for proliferation based on		Number of proliferating T cells	% T blasts	Number of divisions and % of divided T cells
BMDC stimulated T cells	DC : OT-I TRC : OT-I OT-I :WT	1:4 1:4 1:50	1:10 1:20/40/100 No WT T cells	1:1 = 1:1/5/10 No WT T cells
	Reduction of T cell proliferation by TRC	80%	50-100% (dose-dependent)	50-100% (dose-dependent)
Anti-CD3/28 stimulated T cells	TRC : T	1: 100	1 : 1/5/10/20	1 : 20
	Reduction of T cell proliferation by TRC	40-50%	0-90% (dose-dependent)	30%
further characterization of *in vitro* T cell proliferation in presence of	Stimulation of T cells by	BMDC	BMDC	Anti-CD3/28
	T cells activation markers	CD69 no difference (↓) CD44, CD25; ↑ CD62L	CD69 and CD25 no difference	CD69 and CD25 no difference

TRC	Differentiation into effector T cells	Slightly reduced	No data	No data
	T Cell cycle progression	No data	Blocked by TRC	No data
Transwell	Reduction of T cell proliferation by TRC	50-60%	No reduction	No reduction
TRC supernatant	Reduction of T cell proliferation by TRC	40%	No data	No data
Mechanism of inhibition	Not responsible	Lack of IL-2 PD-L1, Il-10 TGFβ, IDO, Arginase-1,	Lack of IL-2 PD-L1, CD80 CD86, IL-4, IL-12	Lack of IL-2 PD-L1, IDO, Arginase-1
	Block of iNOS activity	1400W rescues about 50% of T cell proliferation	Complete rescue by 1400W and L-NMMA	Complete rescue by L-NMMA
	iNOS induction in TRC	By IFNγ and other pro-inflammatory cytokines; highest in presence of DC and IFNγ	Highest in presence of DC and IFNγ	Induced by IFNγ and TNFα;
	Block of IFNγ activity	No data	Complete rescue	Complete rescue, IFNγ is derived from T cells and reacts on TRC
	Block of Cox2 activity	Indomethacin recues about 50% of T cell proliferation	No data	No data
In vivo relevance	Model	Transfer of OT-I cells and VSV-OVA infection	Antigen-loaded DC injection or antigen-targeting via anti-DEC205	Transfer of OT-I cells into iFABP-tOVA mice
	iNOS expression	Transient in TRC and DC	No data	In TRC and LEC
	$iNOS^{-/-}$ mice	↑ Primary T cell expansion (inflammatory conditions)	↑ Primary T cell expansion with inflammatory DC ↓ Primary T cell expansion in non-inflammatory condition	↑ OT-I proliferation in response to antigen presented by TRC in non-inflammatory condition
Reduced T cell proliferation in presence of other stromal cells		Various fibroblasts lines, MSC and tumour cells	MEF, NIH-3T3, BEC, LEC	LEC

Table 3.1: comparison of our results to two similar reports
All three publications report that TRC presence inhibits T cell proliferation in vitro. This is mediated by NO production of TRCs induced by IFNγ. Despite remarkable resemblance of the results, some difference exist between the different reports, which might be largely explained by different ratios of TRCs to T cells, stimulating methods and reads-outs used to assess T cell proliferation. Interestingly, in all three reports the primary T cell response was about 2 times increased in Inos-deficient mice. Also the decrease of the primary T cell response in *Inos*$^{-/-}$ mice in non-inflammatory conditions reported by Khan and colleagues was in this range. (Khan et al., 2011; Lukacs-Kornek et al., 2011).

Both reports show that presence of TRC lines but also *ex vivo* isolated TRCs dampens T cell proliferation stimulated by peptide-loaded DC or anti-CD3/28 in a dose-dependent manner. This inhibition is mediated via NO production by iNOS, which is induced in TRCs by IFNγ (figure 3.2a) (Lukacs-Kornek et al., 2011; Khan et al., 2011). Similar to our results, Khan and colleagues show that other fibroblasts –

MEFs and NIH-3T3 cells - inhibited T cell proliferation, but also endothelial cells –BEC and LEC lines - had the same effects, the later confirmed by Lucas-Kornek and colleagues (Lukacs-Kornek et al., 2011). This substantiates our findings that inhibition of T cell proliferation seems to be a common fibroblastic feature and extends this observation to endothelial cells found in LN. In addition, endothelial cell seem to suppress T cell activation as well via an IFNγ/NO dependant mechanism (Khan et al., 2011; Lukacs-Kornek et al., 2011). This is an interesting finding as MSCs and adult fibroblasts from non-lymphoid tissues were shown to be strongly immune-suppressive in murine disease models or human patients (Haniffa et al., 2007; Jones et al., 2007; Uccelli et al., 2008; Sato et al., 2010). As TRCs display very similar feature and as they are easy to obtain from tonsils (Amé-Thomas et al., 2007) and to maintain in culture they might provide another source of cells that could be used for that purpose. The established TRC lines would be a valuable tool to test how long TRCs infused in mice stay alive, where they home and whether their presence could ameliorate graft-versus-host disease, auto-immune diseases such as EAE or chronic inflammation such as arthritis. An intriguing aspect of MSCs is that allogeneic cells have been successfully used to ameliorate graft-versus-host disease in human patients (Sato et al., 2010). It would be interesting to test whether the same holds true for TRCs. This could be tested by infusion of the TRC lines that originate from C57BL/6 mice into BALB/c mice. The GFP-expressing TRC lines would thereby provide a tool for easy tracking of infused TRCs in mice.

Both, Khan and Lukacs-Kornek show that IFNγ is needed for TRC-mediated inhibition (figure 3.2). In a series of experiments using IFNγ$^{-/-}$ T cells or IFNγ–R$^{-/-}$ TRCs, Lukacs-Kornek and colleagues establish that in their *in vitro* co-culture IFNγ is produced by T cells and acts on the TRCs (figure 3.2a) (Lukacs-Kornek et al., 2011). Consistent with our results, inhibition of T cell proliferation by TRCs was not mediated by PD-L1, IL-4, IL-12, IDO or arginase but blocking of iNOS activity restored T cell proliferation (Lukacs-Kornek et al., 2011; Khan et al., 2011). Unlike the two reports, we did not observe complete rescue of T cell proliferation by blocking iNOS activity. This might be explained by the use of different read-outs: while we used absolute numbers of proliferated T cells to assess the amount of inhibition, both other groups used only the percentage of proliferated T cells (table 3.1). If we only took the percentage of proliferated T cells into account, we would as well see a complete rescue of T cell proliferation by blocking iNOS; however, the absolute numbers were still reduced. Besides different presentation and interpretation of the data, another reason for this discrepancy might be the use of different assay conditions (table 3.1). By increasing the iNOS inhibitor concentration we could completely restore T cell proliferation, but unspecific effects in the 'no stroma' control were observed making these data non-conclusive (data not shown). Similarly to our results, when Lukacs-Kornek used iNOS$^{-/-}$ TRCs the inhibition of T cell proliferation was not only ablated but CD8 T cell proliferation was even increased. The reason for this phenomenon is unknown. One may speculate that in the absence of iNOS/NO factors are induced in TRCs that positive regulate T cell activation. To elaborate on this, a large screening of factors produced by WT versus iNOS$^{-/-}$ would be interesting. Furthermore, it should be tested whether and how TRCs respond to NO themselves leading potentially to inactivation of positive regulators. In

contrast to our results, both Khan and Lukacs-Kornek do not mention experiments in which COX-2 activity was blocked. Nevertheless, in a recent report from Fletcher and colleagues reporting microarray analysis of *ex vivo* sorted TRCs, *Cox-2* (also named *Ptgs-2*) was found to be expressed in TRCs (Fletcher et al., 2011a).

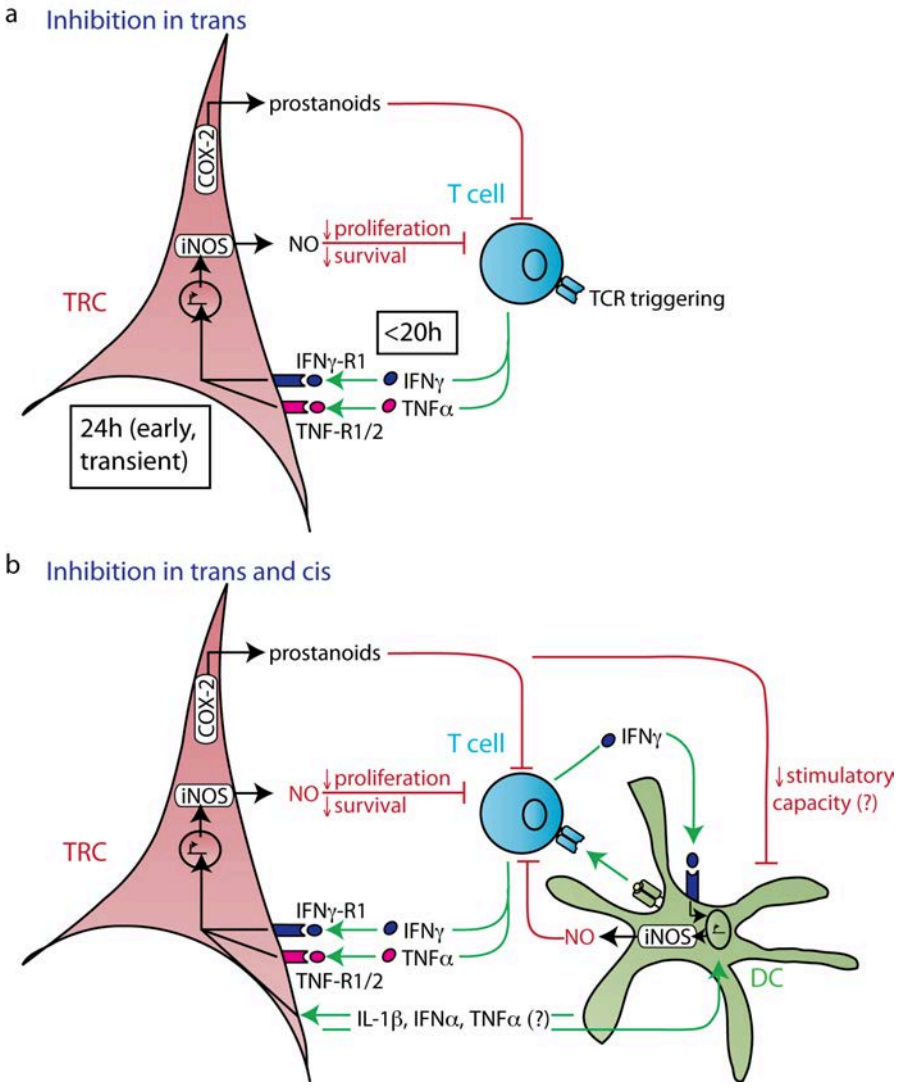

Figure 3.2: Mechanism of TRC mediated inhibition of T cell proliferation
(**a**) Interaction between TRCs and T cells: upon polyclonal TCR triggering T cells produce IFNγ and TNFα, which together induce *Inos* expression in TRCs. *Cox-2* is constitutively expressed in TRCs. NO and COX-2 dependent factors, such as PGE_2, decrease T cell proliferation. (**b**) Interactions between TRCs, DCs and T cells: T cells primed by antigen-presenting DCs produce IFNγ that stimulates *Inos* expression and NO production in DCs and TRCs. Also other factors, such as IL-1β or LPS can induce *Inos* expression in TRCs and possibly DC (Khan et al., 2011; Lukacs-Kornek et al., 2011; Siegert et al., 2011). In addition, TRCs decrease the stimulatory capacity of DCs, (Siegert et al., 2011), most likely at least in part by COX-1/2 dependent factors. It is likely that NO here also negatively influences DCs (Bogdan, 2011) and possibly also TRCs.

To confirm the *in vitro* findings in a more physiological setting, both reports show experiments comparing WT with iNOS$^{-/-}$ mice (table 3.1). Similar to our observations, Khan and colleagues report unexpected defects in the lymphoid compartment of BM chimeras (iNOS$^{-/-}$- into WT) and results were therefore not

conclusive. However, when iNOS$^{-/-}$ mice were immunized with peptide loaded BMDC, a significant increase in antigen-specific T cells could be observed in comparison to WT mice three days after immunization (Khan et al., 2011). This is consistent with our unpublished observations using the same system. In contrast, when OVA was directly targeted to LN resident non-inflammatory DC using the anti-DEC205 antibody, a decrease in antigen-specific T cell expansion was observed (Khan et al., 2011). This shows that TRC mediated inhibition might only be relevant in specific types of immune responses, for example in which very large amounts of IFNγ are produced. Lukacs-Kornek and colleagues used the iFABP-tOVA model in which a truncated form of OVA is expressed under the control of the intestinal fatty acid binding promoter. In a previous report, Fletcher and colleagues showed that TRCs in pLN express tOVA, leading to peripheral tolerance induction by clonal deletion (Fletcher et al., 2010). After transfer of OT-I T cells into iNOS$^{-/-}$ iFABP-tOVA mice the T cells expanded and proliferated more than in WT iFABP-tOVA mice. It was accompanied by increased iNOS expression in TRCs and LECs, but probably not in DCs (Lukacs-Kornek et al., 2011). The discrepancy to our results is very likely due to the use of different model systems. While Lukacs-Kornek and colleagues use a model, in which antigen is presented by TRCs and no inflammation is induced, we use a viral infection model in which antigen should be mainly presented by DCs and which should be accompanied by massive inflammation (table 3.1). This leads to activation of DCs and possibly other myeloid cells and induces iNOS expression in these cells (figure 3.2b). In contrast to Lukacs-Kornek and colleagues, Khan and colleagues observed decreased T cell expansion under non-inflammatory conditions, when iNOS was absent. This discrepancy might be explained be the different cell types that present antigen in the two different models: While Khan and colleagues target antigen to non-inflammatory DCs, Lukacs-Kornek and colleagues use a model in which antigen is presented by TRCs themselves. The observations by us and Khan et al. suggests a role in trans for TRCs with no evidence for antigen presentation by TRCs. Furthermore, Khan and colleagues evaluated the proliferation of endogenous T cells in response to the OVA-SL8 peptide and did, in contrast to us or Lukacs-Kornek and colleagues, not adoptively transfer OT-I T cells (Lukacs-Kornek et al., 2011; Khan et al., 2011). Therefore, the percentage of antigen-specific cells should be much lower for Khan and colleagues. In addition, it was shown, that naïve OT-I T cells very rapidly produce TNFα upon TCR triggering and IFNγ after entering cell cycle (Denton et al., 2011). Therefore, one can assume that in the anti-DEC205 model used by Khan and colleagues, much less TNFα and IFNγ are present in the LN leading to less iNOS expression in TRCs (figure 3.2).

Together, these three reports (Lukacs-Kornek et al., 2011; Khan et al., 2011) show that TRCs have besides their established positive role a negative influence on T cell proliferation. However, the different *in vivo* systems suggest that the dampening of T cell proliferation might be only important in certain type of immune responses. TRCs mediated attenuation may be particularly important when high amounts of IFNγ are produced. Traditionally, IFNγ is regarded as a pro-inflammatory cytokine, and it plays an essential role in various aspects of the immune response, such as for the activation of macrophages, clearance of intracellular pathogens or the promotion of T_{H1} responses. However, IFNγ was shown to

have immune-regulatory features, thereby limiting tissue damage associated with inflammation. Interestingly, depending on the context IFNγ can augment or suppress auto-immunity, such as in experimental autoimmune encephalomyelitis (EAE) (Hu and Ivashkiv, 2009; Kelchtermans et al., 2008). Several mechanisms have been shown to play a role: IFNγ modulates expression of tissue-destructive enzymes, alters the recruitment of inflammatory cells, such as neutrophils, suppresses T_{H17} differentiation and positively regulates T_{REG} differentiation (Hu and Ivashkiv, 2009; Kelchtermans et al., 2008). Interestingly in an EAE model, in which disease is enhanced in IFNγ-/- mice, an increase of proliferating T cells was shown in spleen and the central nervous system when IFNγ was absent (Chu et al., 2000). In addition, Feurer and colleagues showed that IFNγ produced by T_{H1} T cells limits their own expansion in the later phase of the immune response dependent on NO production by host cells (Feuerer et al., 2006). We propose that TRC-produced NO is at least partially responsible for inhibition of T cell expansion in IFNγ$^{-/-}$ mice. Therefore, it would be worthwhile to test whether TRC-specific IFNγ-R$^{-/-}$ mice show similar results after EAE induction as reported for complete IFNγ$^{-/-}$ mice. Interestingly, another inducer of *Inos* in TRCs, TNFα, was also shown to have a dual role in autoimmunity: it promotes autoimmune disease, such as in rheumatoid arthritis or multiple sclerosis, but surprisingly anti-TNF therapy in MS patients aggravates disease and consistent with this finding, several autoimmune mouse models show higher incidence and severity when TNFα is absent (Kassiotis and Kollias, 2001a, 2001b; Campbell et al., 2001). Another positive regulator of *Inos* in TRCs is IL-1β, which is known to promote the development of autoimmune disease (Lachmann et al., 2011). However, unlike IFNγ or TNFα no dual role has been described for IL-1β in autoimmunity.

Nevertheless, the biological reason of TRC mediated inhibition of T cell proliferation is only speculative so far. We assume that this is a mechanism to prevent overshooting T cell responses and the potentially accompanied tissue disruption. During an immune response the LN size increases dramatically. T. Vogt and CY. Yang observed that at the peak of the immune response, the TRC network is still intact and that this is achieved by extensive TRC proliferation after immunization. Interestingly, TRC proliferation only starts 3 days after immunization, when the total LN cellularity is already increased. This might indicate that TRCs need some time to adapt to the new situation and slowing down the T cell proliferation might be mechanism to buy this time preventing disruption of the TRC network (poster CY Yang and S Luther, Swiss Society for Allergology and Immunology, Lugano 2011). In addition, it should be stressed that iNOS induction in TRCs is only very transient which indicates a tight regulation of this immunoregulatory mechanism. It is also intriguing that iNOS was only induced in a subset of TRCs. This might be an evidence for the existence of a special "regulatory" TRC subset, similar to T_{REG} or regulatory DCs. Another possibility is that within the T zone special "regulatory" niches are induced in which T cell proliferation is inhibited. This might be a mechanism to facilitate tight control the T cell proliferation within the LN. It would be interesting to further characterize the immune response in TRC-specific *Inos*$^{-/-}$ mice after VSV-infections when treated or not with Cox-2 inhibitors. If our assumption is true, these mice should show disruption of the stromal cell network in the pLN. Scandella and colleagues showed

that destruction of the TRC network leads to infection-associated immunodeficiency (Scandella et al., 2008). Therefore one should investigate whether this is also the case in TRC-specific *Inos*/*Cox2* double knockout mice.

The summary of results obtained during this thesis clearly show that TRCs are far from being only inert structural cells in the LN. In contrast, these cells influence the immune response in several ways and are implicated in tolerance induction. The further characterization of these cells, especially in the context of tolerance induction, will be of great interest, as these cells might prove to be a potential target in the therapy of auto-immune disease and chronic inflammation. In addition, the new tools established during my thesis work, the TRC lines and co-culture systems, should be of great help to advance our knowledge on these still poorly defined LN fibroblasts.

4. Materials and Methods

4.1. Mice and immunizations

C57BL/6 (B6, CD45.2$^+$) mice were from Janvier (France). B6 OT-I CD45.1$^+$, *Ubiquitin-gfp* transgenic and *Inos*$^{-/-}$ mice were from the Jackson laboratories. p19$^{arf-/-}$ and p53$^{-/-}$ mice were previously described (Kamijo et al., 1997; Zheng et al., 2002). Immunizations: For both -the NP-CGG immunization and the VSV-infection model- mice were subcutaneously (s.c.) injected at six sites in the back to target six peripheral lymph nodes (pLN; 2x axillary, 2x brachial, 2x inguinal). NP-CGG model: 25μg NP-CGG (Biosearch Technology) diluted in PBS and Montanide ISA 25 (25%; Seppic) were injected per site. VSV infection model: 0.1 x 10^6 OT-I splenocytes were retro-orbitally grafted into mice 1-3 days prior to viral infection. Per site 0.33 x 10^6 pfu VSV-OVA (Kim et al., 1998) were injected. Bone marrow (BM)-chimeras: BM from donor-mice was obtained from femur and tibia by crushing bones with a mortar. 15 x 10^6 BM cells were injected retro-orbitally into recipient mice irradiated twice with 450 rad in a 4h interval. The following 4 weeks mice received the antibiotic 'Baytril 10%' (1/1000) in the drinking water. WT mice used were either CD45.2$^+$ or CD45.1$^+$ while *Inos* mice were CD45.1$^+$. All mice were maintained in specific pathogen-free conditions. All mouse experiments were authorized by the Swiss Federal Veterinary Office (Bern, Switzerland).

4.2. Flow cytometry

Groups of 1 x 10^5 to 2 x 10^6 cells were stained in 96-well V-bottom plates (Falcon). Cells were blocked with 2% normal mouse serum (Sigma) or Fc-receptor block (anti-CD16/32 antibodies from the hybridoma 2.4G2) for 20 min on ice and then stained with antibodies in 25 μl FACS buffer (PBS containing 2% fetal calf serum (FCS; PAA), 2 mM EDTA and 0.1% NaN_3) for 30 min on ice. After 2 times washing, cells were incubated with secondary reagents in 25μl FACS buffer. Antibodies and secondary reagents used are listed in the table 4.1. OT-I T cells were identified as CD8$^+$B220$^-$ cells expressing CD45.1 (and in some cases TCR Vα2 and Vβ5). Dead cells were excluded using 7-AAD (7-Aminoactinomycin D) or DAPI (4,6-diamidino-2-phenylindole), or using Aqua (all from Invitrogen) in case of 4% paraformaldehyde (PFA)-fixed cells from VSV-infected mice. Intracellular IFNγ staining: cells were re-stimulated *in vitro* with 1μM SIINFEKL peptide in the presence of Brefeldin-A (10 μg/ml, AppliChem) for 3-4h at 37°C. Then cells were fixed with BD-cytofix (BectonDickinson) for 10 min at RT. After permeabilization with BD-Permwash (BectonDickinson) for 30 min, cells were incubated 45 min with the anti-IFNγ antibody (XMG1.2) diluted in BD-Permwash at RT. In case of VSV-infected tissues, cells were fixed in 4% PFA followed by permeabilization with 0.1% saponin (Sigma). Intracellular iNOS staining: Cells fixed with 4% PFA were washed, permeabilized with FACS buffer containing 0.1% saponin, then anti-iNOS antibody (rabbit antibody; Millipore) or as a control anti-LYVE-1 antibody (RELIAtech) was added followed by donkey-anti-rabbit IgG coupled to Alexa488 (Molecular Probes). For cell cycle analysis cells were fixed and permeabilized, then incubated with Hoechst 33342 (20 μg/ml; Invitrogen) for 5 min at RT. Data were acquired on a FACSCanto or LSR II flow cytometer (both BectonDickinson) and were analysed with FlowJo software (TreeStar).

Primary reagents				
Target	**Species**	**Clone or designation**	**Conjugate**	**Supplier**
CD105 (Endoglin)	Rat	MJ7/18	FITC	Hybridoma
CD106 (VCAM-1)	Rat	429	eFluor450 or biotin or FITC	eBioscience or hybridoma
CD11b	Rat	M1/70	Alexa700 or FITC or biotin	eBioscience or bioLegend
CD11c	Rat	N418	PE-Cy5.5 or FITC	eBioscience or hybridoma
CD140a (PDGFRα)	Rat	APA5	FITC or biotin	Hybridoma
CD140b (PDGFRβ)	Rat	APB5	FITC or biotin	Hybridoma
CD120a (TNF-R1)	A. Hamster	55R-170	Biotin	BioLegend
CD157 (BP-3)	Mouse	BP-3	Biotin or PE	BD Pharmingen
CD19	Rat	ID3	FITC	Hybridoma
CD25	Rat	PC61	Biotin	eBioscience
CD31 (PECAM1)	Rat	390	PE or PerCP-eFluor710	BioLegend/eBioscience
CD326 (EpCAM)	Rat	G8.8	Biotin	BioLegend
CD35/21	Rat	7E9	PE-Cy7	BioLegend
CD4	Rat	RM-4-6	PE-Cy5.5 or eFluor450	eBioscience
CD40	Rat	FGK-45	FITC	Hybridoma
CD44	Rat	IM7	Biotin	eBioscience
CD45	Rat	30-F11	PE-Cy7	eBioscience
CD45.1	Mouse	A20.1	Alexa647	hybridoma
CD45R (B220)	Rat	RA3-6B2	PE-Texas Red	BD Pharmingen
CD54 (ICAM-1)	Rat	YN1/1.7.4	FITC or biotin	Hybridoma
CD62L (L-selectin)	Rat	MEL-14	Alexa700	eBioscience
CD71	Rat	R17217	PE	eBioscience
CD80 (B7-1)	A. Hamster	16-10A1	Biotin	BioLegend
CD86 (B7-2)	Rat	GL-1	PE	eBioscience
CD8α	Rat	53-6.7	PE-Cy7	BioLegend
IFNγ	Rat	XMG1.2	PE	eBioscience
iNOS	Rabbit	Polyclonal, cat nbr. 06-573	Purified	Millipore
gp38 (podoplanin)	S. hamster	8.1.1	Alexa647	Hybridoma
LYVE-1	Rabbit	Polyclonal	Purified	RELIATech
LTβR	rat	3C8	Biotin	eBioscience
MAdCAM-1	Rat	Meca-89	FITC	Hybridoma
MHCI (H-2kb)	Mouse	AF6	Biotin	eBioscience
MHCI-SIINFEKL	Mouse	eBio25-D1.16	PE	eBioscience
MHCII I-A/I-E	Rat	M5/114.15.2	Alexa647	Hybridoma
PD-1 (CD279)	A. Hamster	J43	Biotin	eBioscience
PD-L1 (CD274)	Rat	MIH5	biotin	eBioscience
TCR Vα2	Rat	B20.1	FITC	Hybridoma
TCR Vβ5	Mouse	MR9-4	PE	BD Pharmingen
Secondary reagents				
Streptavidin			PE or APC-Cy7 or APC-eFluor780	eBioscience
Streptavidin			Alexa700	Invitrogen
Rabbit IgG	donkey		Alexa488	Molecular Probes

Table 4.1: Primary and secondary reagents used for flow cytometry
A. =Armenian; S. = Syrian

4.3. *Ex vivo* stromal cell isolation

To isolate stromal cells from LN, axillary, brachial and inguinal LN were isolated from CO_2-killed mice, their capsule opened with a 26-gauge needle and the organs digested for 30 minutes at 37°C in DMEM (Invitrogen) containing collagenase IV (3mg/ml; Worthington), DNAse I (40mg/ml; Roche), 2.5% (vol/vol) FCS, 1.2 mM $CaCl_2$, 10 mM HEPES and 50IU/ml Penicillin, 50μg/ml streptomycin.

Subsequently, EDTA was added (5mM final) and remaining clumps dissolved by pipetting, passed through a 40-μm mesh, washed twice, and re-suspended in complete RPMI. Complete RPMI contained: RPMI 1640 plus GlutaMAX-I (Invitrogen) supplemented with 10% FCS (PAA), 10mM HEPES (Sigma), 50IU/ml penicillin, 50μg/ml streptomycin (Sigma) and 50μM β-mercaptoethanol (Sigma). For stromal cell isolation from femoral muscle, kidney and heart, the respective organs were dissected, then cut into small pieces using razor blades and digested as described above for 1h at 37°C. For stromal cell isolation from ears: Ears were split with forceps and incubated in phosphate-buffered saline (PBS) with 0.5% trypsin (Sigma-Aldrich) and 5mM EDTA for 20 minutes at 37°C to separate dermal and epidermal sheets. The separation was done under a stereomicroscope using forceps. Then both sheets were cut into small pieces using razor blades and digested for 2h with collagenase IV as described above. After digestion, stromal cells were enriched by panning on 10 or 15cm dishes coated with antibodies against CD45 (5μg/ml; clone M1/9.4.3), CD31 (1.5μg/ml; clone GC-51), CD11c (1μg/ml; clone N418) and CD11b (1μg/ml; clone M1/70). Cells were added on the panning plates in 5ml (for 10cm dish) or in 10ml (for 15cm dish) complete RPMI and incubated for 30 min at 4°C. Panning was done 2 times. Live cells were counted by using trypan blue dye to exclude dead cells and using an automated cell counter (Countess, Invitrogen).

4.4. TRC clone generation

Peripheral LNs (pool of axillary, brachial, and inguinal) were isolated from adult $p53^{-/-}$ mice or $p19^{-/-}$(mix of C57BL/6 and 129 background) (Zheng et al., 2002), digested as previously described (Link et al., 2007), and cultured at 37°C with 4.5% CO_2 in complete RPMI. After 24 h, non-adherent cells were removed and the adherent fibroblastic cells were cultured for several weeks and then subcloned using limited dilution. Outgrowth over 2–3 months yielded only $CD45^-CD31^-$ $podoplanin^+$ clones.

4.5. Fibroblastic cell line generation

To generate stromal cell lines stromal cells were isolated by collagenase digest (described above) of pLN, mLN heart, dermis, epidermis and kidney of naïve B6 mice and from pLN of naïve *Ubiquitin-gfp* mice. After overnight culture in complete RPMI non-adherent cells were washed away. Adherent cells were cultured at 37°C with 4.5% CO_2 until they reached confluency, then split on new dishes. Cells were used between passage 8 and 25. Other cell lines used: B16-F10 and MC-38 tumour lines (kindly provided by A.Donda, Lausanne), spleen and lung fibroblasts (C.Buckley (Hou et al., 2010)) MEF (M.Heikenwälder, Munich), MSC (P.Nelson, Munich (Zischek et al., 2009).

4.6. 3D cell culture

Polyurethane sponges were prepared as previously described (Tomei et al., 2009a). Briefly, alginate beads, with diameters of 50–500 μm, were prepared by extruding a solution of 2% sodium alginate (Fluka) in distilled water through a 25-gauge needle fitted with a syringe into a solution of 102 mM $CaCl_2$ in 0.9% NaCl (Sigma). After 1 h the beads were vacuum filtered and air-dried. Dried beads were packed in a

scaffold-casting device (chamber slides or 96-well plates) and a 25mg/ml solution of polyurethane (Pellethane 2363-80A; Dow Plastics) in *N*-methylpyrrolidon (Sigma) was poured onto the beads and allowed to penetrate into the spaces between the packed beads. After 90 min, the *N*-methylpyrrolidone solvent was removed from the polyurethane solution by solvent exchange with distilled water. The alginate beads were then dissolved with 0.5 M citric acid (Sigma) solution. The resulting polyurethane scaffold or sponge was rinsed in distilled water and autoclaved in PBS.

For 3D cultures in the Polyurethane-sponge, the collagen-solution was prepared as flowing: 1mg/ml type I collagen (Rat tail collagen, Cat.nbr.: 354249 BD Biosciences) was re-suspended in 10xPBS, 7.5% $NaHCO_3$ and complete RPMI medium. The pH was adjusted to 7.3-7.5. TRC cells (clone or line) were re-suspended at a concentration of 10^6 cells/ml in the collagen solution. Polyurethane sponges were placed in non-treated 24-wells (Nunc) and TRCs in the collagen solution were poured on top, until the macropores of the scaffold were completely filled. Collagen was allowed to polymerize at 37°C with 5% CO_2 for 2-4h and complete RPMI was added until the whole sponge-collagen culture was completely covered. All cultures were maintained in a humidified 37°C, 5% CO_2 incubator for the duration of the culture. To re-isolate TRCs from the 3D cultures, they were cut into small pieces using scissors and digested with 1mg/ml collagenase D (Roche) for 30-60min at 37°C.

4.7. Cytokine stimulation of TRC clones/lines

TRC cells were seeded in 6-wells (0.05 x 10^6 per well) or chamber slides (3000 cells per well). After overnight culture after overnight culture 10ng/ml IFNγ, 10ng/ml IL-1β, 10ng/ml TNFα, 10ng/ml LTα3, 25ng/ml IL-6, 5 or 50ng/ml IL-13, 0.2 or 10ng/ml IL-1α, 0.5 or 10ng/ml TGFβ, 1 or 20ng/ml PDGF-BB, (all from Peprotech), 0.5μg/ml LPS (Sigma), 2 or 20μg/ml Poly I:C (kind gift from J. Tschopp), 500 U/ml IFNα (PBL Interferon Source) or 1μg/ml of the agonistic antibody against LTβR (αLTβR; clone 4H8 WH2; provided by C.Ware) were added to stromal cells for indicated times (7h - 24h).

4.8. Generation of bone-marrow-derived dendritic cells (BMDCs)

Bone-marrow (BM) cells were obtained from femur and tibia of B6 mice by crushing bones with a mortar. After filtering through a 40 μm mesh, BM cells were cultured for 7 days in complete IMDM (Invitrogen) containing HEPES (10mM), penicillin (50IU/mL), streptomycin (50μg/mL), β-mercaptoethanol (50μM), 10% FCS, and 10% (vol/vol) GM-CSF–containing culture supernatant (COS line donated by F. Tacchini-Cottier, Lausanne) in untreated 100 mm plastic dishes (Falcon, Petri dish). Medium was changed on days 3 and 6 of culture. BMDCs were harvested on day 7 by adding PBS containing 2 mM EDTA and gentle pipetting. Cells were subsequently frozen in aliquots using standard procedures. For experiments BMDCs were thawed one day prior to use and cultivated overnight in complete IMDM.

4.9. T cell activation assay

Stromal cells: $1x10^4$ cells in complete RPMI were seeded in 24-wells and after overnight culture irradiated with 1000rad. Initially, experiments with non-irradiated or irradiated pLN2 were performed with no difference in the outcome (not shown) *Ex vivo* cells were isolated as described above, then non-adherent cells were gently washed away after overnight culture and complete RPMI was added. BMDCs: They were activated with 0.5µg/ml LPS (Sigma) for 6h at 37°C. 2h after LPS addition 1µM SIINFEKL peptide was added. Activated BMDCs were harvested by adding PBS containing 2mM EDTA and gentle pipetting. After washing two times, cells were counted using trypan blue to exclude dead cells and $1x10^4$ cells were added per 24-well. T cells: spleen and pLN were dissected from CO_2-killed B6 and OT-I transgenic mice. The organs were suspended by passing them across a 40µm mesh. After washing, cells were re-suspended in red blood cell lysis buffer (Tris-Ammonium chloride based) for 30 seconds at room temperature and washed again. CD8 cells were enriched by panning on Petri dishes coated with antibodies against B220 (3µg/ml; clone RA3-6B2), CD4 (2µg/ml; clone H129.19.6), CD11b (1µg/ml; clone M1/70) and CD11c (1µg/ml; clone N418). Cells were re-suspended in 5ml (10cm dish; surface $56cm^2$) or 10ml (15cm dish; surface $151cm^2$) in complete RPMI in a concentration of 1.5 – $2.5x10^6$ cells per cm^2 (=16.8 -28 x 10^6 cells/ml). Panning was done two times for 30 min at 4°C. The OT-I cells and 50% of the B6 WT cells were labelled with 2µM CFSE (Invitrogen) and counted again. Per 24-well 0.04 x 10^6 $CFSE^+$ OT-I cells together with 0.98 x 10^6 unlabelled B6 WT cells and 0.98 x 10^6 $CFSE^+$ B6 WT cells were added. The assay was performed in complete RPMI enriched with 1x MEM (Invitrogen), 3ng/ml recombinant murine IL-7 (Peprotech) and 10U/ml recombinant human IL-2 (Merck Serono). Cells were harvested by gently pipetting 2-4 days after start of co-culture. Cells were counted on an automated cell counter using trypan blue to exclude dead cells and analysed by flow cytometry. To better compare the decrease of T cell proliferation between experiments the attenuating effect by the stromal cells was defined as percentage of inhibition in divided OT-I T cell numbers relative to the 'no stroma' control: {1-(number of proliferated cells)$_{stroma}$ / (number of proliferated cells)$_{no\ stroma}$}*100). Transwell assay: Stromal cells were seeded in the lower chamber, while T cells and DCs were cultured in the upper chamber of a 0.4µm transwell chamber (HTS 24-well, Vitaris). For blocking experiments the following reagents and concentrations were used: 10µM indomethacin (Sigma), 1µM 1400W (= dihydrochloride; Sigma), 10µM 1-Methyl-L-tryptophan (1-MT; Sigma), 200µM (S)-(2-Boronoethyl)-L-cysteine (BEC, Calbiochem), 10µg/ml anti-PD-L1 (MIH5, eBioscience), 20µg/ml anti-IL-10 (kind gift from F. Tacchini-Cottier, Lausanne, Switzerland) and 30µg/ml anti-TGFβ (clone 1D11.16.8; BioXCell).

4.10. T cell activation by anti-CD3 and anti-28 beads

2500 stromal cells were seeded in 96-wells and after overnight culture irradiated with 1000rad. A total of 2.5 x 10^5 T cells mixed with 1.25 x 10^5 anti-CD3/28 beads (Dynabeads, Invitrogen) were added on top. After 2-3 days of co-culture cells were harvested by gentle pipetting. Live cells were counted on an automated cell counter and analysed by flow cytometry.

4.11. T cell activation by TRC-conditioned BMDCs

10000 pLN2 TRC lines were seeded per 24-well and after overnight culture LPS-activated and SIINFEKL-pulsed BMDCs (see T cell activation assay) were added in a ratio of 1:1. After overnight culture BMDCs were separated from stromal cells by magnetic cell sorting (MACS): Cells were stained with biotinylated anti-gp38- antibody (clone 8.1.1) and followed by magnetic-beads coupled streptavidin (Miltenyi) in MACS buffer (PBS containing 2% FCS and 2mM EDTA). Cells were separated using MS-columns (Miltenyi) according to the manufactures instructions. For the T cell activation assay 2500 TRC conditioned DCs were co-cultured with 0.01 x 10^6 CFSE labelled OT-I cells mixed with 0.48 x 10^6 unspecific WT T cells (of which 50% were CFSE labelled) per 96-well for 3 days (Ratios are the same as for the T cell activation assay described above).

4.12. T cell activation in chamber slides

Stromal cells were seeded a density of 3000 cells / well in 8-well chamber slides (Falcon). Co-culture experiments: After overnight culture 0.25 x 10^6 WT T cells and 0.125 x 10^6 anti-CD3/28 beads were added or 5000 CFSE-labelled OT-I T cells mixed with 0.245 x 10^6 WT T cells together with 5000 LPS-activated and SIINFEKL-pulsed BMDCs (as described above) were added.

4.13. *In vitro* cytotoxicity assay

Target cells: The spleen was dissected from CO_2-killed WT mice and meshed through a 40 μm-mesh. Red blood cells were removed by re-suspending the cells in red blood cell lysis buffer for 30 seconds at room temperature. Half of the cells were labelled with 0.16μM proliferation dye eFluor670 (eBioscience) (eFluor670^{low}) and the other half with 0.5μM proliferation dye eFluor670 (eFluor670^{high}). The eFluro670^{high} population was pulsed with 1 μM SIINFEKL peptide for 1h at 37°C. Per 96-well 5 x 10^3 eFluor670^{high} and 5 x 10^3 eFluor670^{low} cells were added. Effector cells: They were harvested from the T cell activation assay after 4 days of co-culture. Alternatively, they were isolated from homogenized spleen or pLN from VSV-infected mice. Effector cells were added to target cells in different ratios and incubated overnight. The ratio of target cells was analysed by flow cytometry, as were the input numbers of OT-I effector T cells allowing the calculation of the effective E/T ratio. Percentage specific lysis = {1-(specific survival)$_{sample}$/(specific survival)$_{control}$}*100 with specific survival = eFluor670^{high}/eFluor^{low}, (control: target cells only).

4.14. Nitrite detection

NO_2^- as read out for NO in cell culture supernatants was measured using the Griess assay. Briefly, 0.1% N-1-naphtylethylenediamine dihydrochloride (Sigma) was mixed with p-aminobenzensulfonamide (Sigma) in 5% phosphoric acid and 100μl of this mixture were incubated with 100μl cell culture supernatant. After 10min incubation at RT absorbance was measured at 550nm and background absorbance at 690nm was subtracted. The absorbance of complete RPMI was also subtracted. In each measurement a NO_2^- -standard series (100-0.1μM $NaNO_2$; Sigma) was included to assess the absolute

NO_2^- concentration in the supernatant. Only values above 0.5μM were considered to be above background. pLN2 cells were free of mycoplasma that can contribute to NO_2^- production.

4.15. Immunofluorescence microscopy

Lymph nodes dissected from CO_2-killed WT mice were fixed at 4°C in 4% (weight/vol) PFA and saturated for 3 h at 4°C in 30% (weight/vol) sucrose before being embedded in Tissue-Tek optimum cutting temperature compound (OCT, Sakura) followed by freezing in an ethanol dry ice bath. Cryostat sections (8μm thickness) collected on Superfrost/Plus glass slides (Fisher Scientific) were air-dried overnight. For cells cultured in chamber slides: chambers were removed according to the manufactures description. Then sections/cells were fixed for 10min in ice-cold acetone. After rehydration, sections were 'quenched' with 0.3% (vol/vol) H_2O_2, if tyramide amplification was used, then were blocked with 0.1% (weight/vol) BSA and 1–4% (vol/vol) normal mouse and donkey serum, followed by treatment with a homemade streptavidin-biotin blocking kit. Immunofluorescence staining was done with antibodies (table 4.2.) diluted in PBS containing 0.1% (weight/vol) BSA and 1% (vol/vol) normal mouse serum. For gp38, primary antibodies were visualized with secondary antibodies coupled to horseradish peroxidase, followed by treatment with the Tyramide Signal Amplification Kit #22 (Molecular Probes) according to the manufacturer's instructions, but with a borate buffer (0.1M boric acid (Applichem) in PBS, pH 8.5) for tyramide dilution. Images were acquired with a Zeiss Axioplan microscope and treated with ImageJ (http://rsbweb.nih.gov/ij/) and Photoshop software (Adobe).

Primary reagents				
Target	**Species**	**Clone or designation**	**Conjugate**	**Supplier**
iNOS	Rabbit	Polyclonal	purified	Millipore
gp38	Syrian hamster	8.1.1	purified	Hybridoma
CD31	Rat	GC-51	purified	Hybridoma
Alpha Smooth-muscle actin	Mouse	1A4	Cy3	Sigma
Collagen I	Goat		Purified	Southern Biotech
Desmin	Rabbit	Polyclonal	Purified	Progen
Fibronectin	Rabbit		Purified	Sigma
Laminin	Rabbit	Polyclonal	Purified	Progen
Secondary reagents				
Rat IgG	Donkey		APC	Jackson Immunoresearch
Rat IgG	Donkey		Cy3	Jackson Immunoresearch
Syrian Hamster IgG	Goat		Biotin or Cy3	Jackson

			Immunoresearch
Rabbit IgG	Donkey	Cy3	Jackson Immunoresearch
Rabbit IgG	Donkey	Alexa488	Molecular Probes
Rabbit IgG	Donkey	Alexa647	Molecular Probes
Goat IgG	Donkey	Alexa488	Molecular Probes
Streptavidin		Alexa488	Molecular Probes

Table 4.2: Primary and secondary reagents used for Immunofluorescence

4.16. Transcript analysis

RNA isolation (using Trizol, Invitrogen), reverse transcription and quantitative real-time PCR (using SYBR-Green and LightCycler, Roche Diagnostics) was performed as described previously (Link et al., 2007), including the primers for amplification of *Ccl19*, *Ccl21* and the two housekeeping genes *Hypoxanthine guanine phosphoribosyl transferase 1 (Hprt 1)* and *TATA-binding protein* (*Tbp)*. Additional primers used: *Inos*-F: gttctcagcccaacaatacaaga, *Inos*-R: gtggacgggtcgatgtcac. *Cox2*-F: tggtgcctggtctgatgatg, *Cox2*-R: gtggtaaccgctcaggtgttg. Efficiency-corrected expression of *Inos*, *Cox2*, *Ccl19* and *Ccl21* was normalized by dividing with the geometric mean of expression of the two housekeeping genes.

4.17. Statistical analysis

A F-test was performed to determine whether equal or unequal variance in the t-test should be used. For the F-test $p < 0.05$ was considered as unequal variance. Statistical significance was determined with a student's t-test

5. References

Aggarwal, S., and Pittenger, M. F. (2005). Human mesenchymal stem cells modulate allogeneic immune cell responses. Blood *105*, 1815–1822.

Aldinucci, A., Rizzetto, L., Pieri, L., Nosi, D., Romagnoli, P., Biagioli, T., Mazzanti, B., Saccardi, R., Beltrame, L., Massacesi, L., et al. (2010). Inhibition of immune synapse by altered dendritic cell actin distribution: a new pathway of mesenchymal stem cell immune regulation. J Immunol *185*, 5102–5110.

Allen, C. D. C., Okada, T., Tang, H. L., and Cyster, J. G. (2007). Imaging of germinal center selection events during affinity maturation. Science (New York, N.Y.) *315*, 528–531.

Allen, C. D., and Cyster, J. G. (2008). Follicular dendritic cell networks of primary follicles and germinal centers: phenotype and function. Semin Immunol *20*, 14–25.

Allen, S., Turner, S. J., Bourges, D., Gleeson, P. A., and van Driel, I. R. (2011). Shaping the T-cell repertoire in the periphery. Immunology and cell biology *89*, 60–69.

Amé-Thomas, P., Maby-El Hajjami, H., Monvoisin, C., Jean, R., Monnier, D., Caulet-Maugendre, S., Guillaudeux, T., Lamy, T., Fest, T., and Tarte, K. (2007). Human mesenchymal stem cells isolated from bone marrow and lymphoid organs support tumor B-cell growth: role of stromal cells in follicular lymphoma pathogenesis. Blood *109*, 693–702.

Anderson, G., Jenkinson, W. E., Jones, T., Parnell, S. M., Kinsella, F. a M., White, A. J., Pongrac'z, J. E., Rossi, S. W., and Jenkinson, E. J. (2006). Establishment and functioning of intrathymic microenvironments. Immunological reviews *209*, 10–27.

Anderson, G., Lane, P. J. L., and Jenkinson, E. J. (2007). Generating intrathymic microenvironments to establish T-cell tolerance. Nature reviews. Immunology *7*, 954–963.

von Andrian, U. H., and Mempel, T. R. (2003). Homing and cellular traffic in lymph nodes. Nat Rev Immunol *3*, 867–878.

Asperti-Boursin, F., Real, E., Bismuth, G., Trautmann, A., and Donnadieu, E. (2007). CCR7 ligands control basal T cell motility within lymph node slices in a phosphoinositide 3-kinase-independent manner. The Journal of experimental medicine *204*, 1167–1179.

Bajenoff, M., Egen, J. G., Koo, L. Y., Laugier, J. P., Brau, F., Glaichenhaus, N., and Germain, R. N. (2006). Stromal cell networks regulate lymphocyte entry, migration, and territoriality in lymph nodes. Immunity *25*, 989–1001.

Bajenoff, M., Egen, J. G., Qi, H., Huang, A. Y., Castellino, F., and Germain, R. N. (2007). Highways, byways and breadcrumbs: directing lymphocyte traffic in the lymph node. Trends Immunol *28*, 346–352.

Bajenoff, M., Glaichenhaus, N., and Germain, R. N. (2008). Fibroblastic Reticular Cells Guide T Lymphocyte Entry into and Migration within the Splenic T Cell Zone. The Journal of Immunology *181*, 3947–3954.

Barry, M., and Bleackley, R. C. (2002). Cytotoxic T lymphocytes: all roads lead to death. Nat Rev Immunol *2*, 401–409.

Batista, F. D., and Harwood, N. E. (2009). The who, how and where of antigen presentation to B cells. Nat Rev Immunol *9*, 15–27.

Belkaid, Y., and Rouse, B. T. (2005). Natural regulatory T cells in infectious disease. Nat Immunol *6*, 353–360.

Belz, G. T., and Kallies, A. (2010). Effector and memory CD8+ T cell differentiation: toward a molecular understanding of fate determination. Current opinion in immunology *22*, 279–285.

Bluestone, J. A., and Abbas, A. K. (2003). Natural versus adaptive regulatory T cells. Nat Rev Immunol *3*, 253–257.

Bogdan, C. (2001). Nitric oxide and the immune response. Nat Immunol *2*, 907–916.

Bogdan, C. (2011). Regulation of lymphocytes by nitric oxide. Methods Mol Biol *677*, 375–393.

Bogdan, C., Donhauser, N., Doring, R., Rollinghoff, M., Diefenbach, A., and Rittig, M. G. (2000). Fibroblasts as host cells in latent leishmaniosis. J Exp Med *191*, 2121–2130.

Bouffi, C., Bony, C., Jorgensen, C., and Noel, D. (2011). Skin fibroblasts are potent suppressors of inflammation in experimental arthritis. Ann Rheum Dis *70*, 1671–1676.

Bour-Jordan, H., Esensten, J. H., Martinez-Llordella, M., Penaranda, C., Stumpf, M., and Bluestone, J. a (2011). Intrinsic and extrinsic control of peripheral T-cell tolerance by costimulatory molecules of the CD28/B7 family. Immunological reviews *241*, 180–205.

Bousso, P. (2008). T-cell activation by dendritic cells in the lymph node: lessons from the movies. Nat Rev Immunol *8*, 675–684.

Britschgi, M. R., Favre, S., and Luther, S. a (2010). CCL21 is sufficient to mediate DC migration, maturation and function in the absence of CCL19. Eur J Immunol *40*, 1266–1271.

Campbell, I. K., O'Donnell, K., Lawlor, K. E., and Wicks, I. P. (2001). Severe inflammatory arthritis and lymphadenopathy in the absence of TNF. The Journal of clinical investigation *107*, 1519–1527.

Castellino, F., and Germain, R. N. (2006). Cooperation between CD4+ and CD8+ T cells: when, where, and how. Annu Rev Immunol *24*, 519–540.

Castro, A., Bono, M. R., Simon, V., Vargas, L., and Rosemblatt, M. (1997). Spleen-derived stromal cells. Adhesion molecules expression and lymphocyte adhesion to reticular cells. Eur J Cell Biol *74*, 321–328.

Caton, M. L., Smith-Raska, M. R., and Reizis, B. (2007). Notch-RBP-J signaling controls the homeostasis of CD8- dendritic cells in the spleen. The Journal of experimental medicine *204*, 1653–1664.

Chu, C. Q., Wittmer, S., and Dalton, D. K. (2000). Failure to suppress the expansion of the activated CD4 T cell population in interferon gamma-deficient mice leads to exacerbation of experimental autoimmune encephalomyelitis. The Journal of experimental medicine *192*, 123–128.

Chyou, S., Ekland, E. H., Carpenter, A. C., Tzeng, T. C., Tian, S., Michaud, M., Madri, J. A., and Lu, T. T. (2008). Fibroblast-type reticular stromal cells regulate the lymph node vasculature. J Immunol *181*, 3887–3896.

Clark, E. A., Grabstein, K. H., and Shu, G. L. (1992). Cultured human follicular dendritic cells. Growth characteristics and interactions with B lymphocytes. Journal of immunology (Baltimore, Md. : 1950) *148*, 3327–3335.

Coombes, J. L., and Robey, E. a (2010). Dynamic imaging of host-pathogen interactions in vivo. Nature reviews. Immunology *10*, 353–364.

Crotty, S. (2011). Follicular helper CD4 T cells (TFH). Annu Rev Immunol *29*, 621–663.

Cyster, J. G. (2010). B cell follicles and antigen encounters of the third kind. Nat Immunol *11*, 989–996.

Cyster, J. G. (2005). Chemokines, sphingosine-1-phosphate, and cell migration in secondary lymphoid organs. Annu Rev Immunol *23*, 127–159.

Dejardin, E., Droin, N. M., Delhase, M., Haas, E., Cao, Y., Makris, C., Li, Z.-W., Karin, M., Ware, C. F., and Green, D. R. (2002). The lymphotoxin-beta receptor induces different patterns of gene expression via two NF-kappaB pathways. Immunity *17*, 525–535.

Denton, A. E., Russ, B. E., Doherty, P. C., Rao, S., and Turner, S. J. (2011). Differentiation-dependent functional and epigenetic landscapes for cytokine genes in virus-specific CD8+ T cells. Proceedings of the National Academy of Sciences of the United States of America, 1–6.

Dominguez, P. M., and Ardavin, C. (2010). Differentiation and function of mouse monocyte-derived dendritic cells in steady state and inflammation. Immunol Rev *234*, 90–104.

Dustin, M. L., Allen, P. M., and Shaw, A. S. (2001). Environmental control of immunological synapse formation and duration. Trends Immunol *22*, 192–194.

Dustin, M. L., and de Fougerolles, a R. (2001). Reprogramming T cells: the role of extracellular matrix in coordination of T cell activation and migration. Curr Opin Immunol *13*, 286–290.

Dustin, M. L., and Long, E. O. (2010). Cytotoxic immunological synapses. Immunol Rev *235*, 24–34.

Fenyk-Melody, J. E., Garrison, a E., Brunnert, S. R., Weidner, J. R., Shen, F., Shelton, B. a, and Mudgett, J. S. (1998). Experimental autoimmune encephalomyelitis is exacerbated in mice lacking the NOS2 gene. J Immunol *160*, 2940–2946.

Feuerer, M., Eulenburg, K., Loddenkemper, C., Hamann, A., and Huehn, J. (2006). Self-limitation of Th1-mediated inflammation by IFN-gamma. Journal of immunology (Baltimore, Md. : 1950) *176*, 2857–2863.

Fife, B. T., and Bluestone, J. a (2008). Control of peripheral T-cell tolerance and autoimmunity via the CTLA-4 and PD-1 pathways. Immunological reviews *224*, 166–182.

Fischer-Lindahl, K. (1997). On naming H2 haplotypes: functional significance of MHC class Ib alleles. Immunogenetics *46*, 53–62.

Flanagan, K., Moroziewicz, D., Kwak, H., Horig, H., and Kaufman, H. L. (2004). The lymphoid chemokine CCL21 costimulates naive T cell expansion and Th1 polarization of non-regulatory CD4+ T cells. Cell Immunol *231*, 75–84.

Fletcher, A. L., Lukacs-Kornek, V., Reynoso, E. D., Pinner, S. E., Bellemare-Pelletier, A., Curry, M. S., Collier, A. R., Boyd, R. L., and Turley, S. J. (2010). Lymph node fibroblastic reticular cells directly present peripheral tissue antigen under steady-state and inflammatory conditions. J Exp Med *207*, 689–697.

Fletcher, A. L., Malhotra, D., Acton, S. E., Lukacs-Kornek, V., Bellemare-Pelletier, A., Curry, M., Armant, M., and Turley, S. J. (2011a). Reproducible Isolation of Lymph Node Stromal Cells Reveals Site-Dependent Differences in Fibroblastic Reticular Cells. Frontiers in Immunology *2*, 1–15.

Fletcher, A. L., Malhotra, D., and Turley, S. J. (2011b). Lymph node stroma broaden the peripheral tolerance paradigm. Trends Immunol *32*, 12–18.

Fooksman, D. R., Vardhana, S., Vasiliver-Shamis, G., Liese, J., Blair, D. A., Waite, J., Sacristan, C., Victora, G. D., Zanin-Zhorov, A., and Dustin, M. L. (2010). Functional anatomy of T cell activation and synapse formation. Annu Rev Immunol *28*, 79–105.

Friedl, P., and Gunzer, M. (2001). Interaction of T cells with APCs: the serial encounter model. Trends Immunol *22*, 187–191.

Friedman, R. S., Jacobelli, J., and Krummel, M. F. (2006). Surface-bound chemokines capture and prime T cells for synapse formation. Nat Immunol *7*, 1101–1108.

Frontera, V., Arcangeli, M.-L., Zimmerli, C., Bardin, F., Obrados, E., Audebert, S., Bajenoff, M., Borg, J.-P., and Aurrand-Lions, M. (2011). Cutting edge: JAM-C controls homeostatic chemokine secretion in lymph node fibroblastic reticular cells expressing thrombomodulin. Journal of immunology (Baltimore, Md. : 1950) *187*, 603–607.

Förster, R., Davalos-Misslitz, A. C., and Rot, A. (2008). CCR7 and its ligands: balancing immunity and tolerance. Nature reviews. Immunology *8*, 362–371.

Gallo, R. L., Murakami, M., Ohtake, T., and Zaiou, M. (2002). Biology and clinical relevance of naturally occurring antimicrobial peptides. Journal of Allergy and Clinical Immunology *110*, 823–831.

Gauzzi, M. C., Del Cornò, M., and Gessani, S. (2010). Dissecting TLR3 signalling in dendritic cells. Immunobiology *215*, 713–723.

Germain, R. N., Bajenoff, M., Castellino, F., Chieppa, M., Egen, J. G., Huang, A. Y., Ishii, M., Koo, L. Y., and Qi, H. (2008). Making friends in out-of-the-way places: how cells of the immune system get together and how they conduct their business as revealed by intravital imaging. Immunol Rev *221*, 163–181.

Giese, C., Demmler, C. D., Ammer, R., Hartmann, S., Lubitz, A., Miller, L., Muller, R., and Marx, U. (2006). A human lymph node in vitro--challenges and progress. Artif Organs *30*, 803–808.

Giese, C., Lubitz, A., Demmler, C. D., Reuschel, J., Bergner, K., and Marx, U. (2010). Immunological substance testing on human lymphatic micro-organoids in vitro. J Biotechnol *148*, 38–45.

Gollmer, K., Asperti-Boursin, F., Tanaka, Y., Okkenhaug, K., Vanhaesebroeck, B., Peterson, J. R., Fukui, Y., Donnadieu, E., and Stein, J. V. (2009). CCL21 mediates CD4+ T-cell costimulation via a DOCK2/Rac-dependent pathway. Blood *114*, 580–588.

Gretz, J. E., Anderson, A. O., and Shaw, S. (1997). Cords, channels, corridors and conduits: critical architectural elements facilitating cell interactions in the lymph node cortex. Immunol Rev *156*, 11–24.

Gretz, J. E., Kaldjian, E. P., Anderson, A. O., and Shaw, S. (1996). Sophisticated strategies for information encounter in the lymph node: the reticular network as a conduit of soluble information and a highway for cell traffic. J Immunol *157*, 495–499.

Gretz, J. E., Norbury, C. C., Anderson, A. O., Proudfoot, A. E., and Shaw, S. (2000). Lymph-borne chemokines and other low molecular weight molecules reach high endothelial venules via specialized conduits while a functional barrier limits access to the lymphocyte microenvironments in lymph node cortex. J Exp Med *192*, 1425–1440.

Griffith, L. G., and Swartz, M. A. (2006). Capturing complex 3D tissue physiology in vitro. Nat Rev Mol Cell Biol *7*, 211–224.

Grinnell, F. (2003). Fibroblast biology in three-dimensional collagen matrices. Trends in Cell Biology *13*, 264–269.

Gualde, N., and Harizi, H. (2004). Prostanoids and their receptors that modulate dendritic cell-mediated immunity. Immunology and Cell Biology *82*, 353–360.

Gunzer, M., Friedl, P., Niggemann, B., Brocker, E. B., Kampgen, E., and Zanker, K. S. (2000). Migration of dendritic cells within 3-D collagen lattices is dependent on tissue origin, state of maturation, and matrix structure and is maintained by proinflammatory cytokines. J Leukoc Biol *67*, 622–629.

Hammerschmidt, S. I., Ahrendt, M., Bode, U., Wahl, B., Kremmer, E., Forster, R., and Pabst, O. (2008). Stromal mesenteric lymph node cells are essential for the generation of gut-homing T cells in vivo. J Exp Med *205*, 2483–2490.

Haniffa, M. A., Collin, M. P., Buckley, C. D., and Dazzi, F. (2009). Mesenchymal stem cells: the fibroblasts' new clothes ? Haematologica *94(2)*, 258–263.

Haniffa, M. A., Wang, X. N., Holtick, U., Rae, M., Isaacs, J. D., Dickinson, A. M., Hilkens, C. M., and Collin, M. P. (2007). Adult human fibroblasts are potent immunoregulatory cells and functionally equivalent to mesenchymal stem cells. J Immunol *179*, 1595–1604.

Hanke, J. H., Gardner, J. P., Dow, R. L., Changelian, P. S., Brissette, W. H., Weringer, E. J., Pollok, B. a, and Connelly, P. a (1996). Discovery of a novel, potent, and Src family-selective tyrosine kinase inhibitor. Study of Lck- and FynT-dependent T cell activation. The Journal of biological chemistry *271*, 695–701.

Hara, T., Katakai, T., Lee, J.-H., Nambu, Y., Nakajima-Nagata, N., Gonda, H., Sugai, M., and Shimizu, A. (2006). A transmembrane chemokine, CXC chemokine ligand 16, expressed by lymph node fibroblastic reticular cells has the potential to regulate T cell migration and adhesion. International immunology *18*, 301–311.

Haring, J. S., Badovinac, V. P., and Harty, J. T. (2006). Inflaming the CD8+ T cell response. Immunity *25*, 19–29.

Harizi, H., and Gualde, N. (2006). Pivotal role of PGE2 and IL-10 in the cross-regulation of dendritic cell-derived inflammatory mediators. Cellular & molecular immunology *3*, 271–277.

Haycock, J. W. (2011). 3D cell culture: a review of current approaches and techniques. Methods Mol Biol *695*, 1–15.

He, C., Young, A. J., West, C. a, Su, M., Konerding, M. a, and Mentzer, S. J. (2002). Stimulation of regional lymphatic and blood flow by epicutaneous oxazolone. Journal of applied physiology (Bethesda, Md. : 1985) *93*, 966–973.

Henrickson, S. E., and von Andrian, U. H. (2007). Single-cell dynamics of T-cell priming. Current Opinion in Immunology *19*, 249–258.

Hornef, M. W., Wick, M. J., Rhen, M., and Normark, S. (2002). Bacterial strategies for overcoming host innate and adaptive immune responses. Nature immunology *3*, 1033–1040.

Hou, T. Z., Mustafa, M. Z., Flavell, S. J., Barrington, F., Jenkinson, E. J., Anderson, G., Lane, P. J. L., Withers, D. R., and Buckley, C. D. (2010). Splenic stromal cells mediate IL-7 independent adult lymphoid tissue inducer cell survival. European Journal of Immunology *40*, 359–365.

Hu, X., and Ivashkiv, L. B. (2009). Cross-regulation of signaling pathways by interferon-gamma: implications for immune responses and autoimmune diseases. Immunity *31*, 539–550.

Hugues, S., Fetler, L., Bonifaz, L., Helft, J., Amblard, F., and Amigorena, S. (2004). Distinct T cell dynamics in lymph nodes during the induction of tolerance and immunity. Nat Immunol *5*, 1235–1242.

Iannacone, M., Moseman, E. A., Tonti, E., Bosurgi, L., Junt, T., Henrickson, S. E., Whelan, S. P., Guidotti, L. G., and von Andrian, U. H. (2010). Subcapsular sinus macrophages prevent CNS invasion on peripheral infection with a neurotropic virus. Nature *465*, 1079–1083.

Jones, S., Horwood, N., Cope, A., and Dazzi, F. (2007). The antiproliferative effect of mesenchymal stem cells is a fundamental property shared by all stromal cells. J Immunol *179*, 2824–2831.

Junt, T., Moseman, E. A., Iannacone, M., Massberg, S., Lang, P. A., Boes, M., Fink, K., Henrickson, S. E., Shayakhmetov, D. M., Di Paolo, N. C., et al. (2007). Subcapsular sinus macrophages in lymph nodes clear lymph-borne viruses and present them to antiviral B cells. Nature *450*, 110–114.

Junt, T., Scandella, E., Förster, R., Krebs, P., Krautwald, S., Lipp, M., Hengartner, H., and Ludewig, B. (2004). Impact of CCR7 on priming and distribution of antiviral effector and memory CTL. Journal of immunology (Baltimore, Md. : 1950) *173*, 6684–6693.

Junt, T., Scandella, E., and Ludewig, B. (2008). Form follows function: lymphoid tissue microarchitecture in antimicrobial immune defence. Nat Rev Immunol *8*, 764–775.

Kaech, S. M., Wherry, E. J., and Ahmed, R. (2002). Effector and memory T-cell differentiation: implications for vaccine development. Nat Rev Immunol *2*, 251–262.

Kaldjian, E. P., Gretz, J. E., Anderson, a O., Shi, Y., and Shaw, S. (2001). Spatial and molecular organization of lymph node T cell cortex: a labyrinthine cavity bounded by an epithelium-like monolayer of fibroblastic reticular cells anchored to basement membrane-like extracellular matrix. International immunology *13*, 1243–1253.

Kallies, A., Xin, A., Belz, G. T., and Nutt, S. L. (2009). Blimp-1 transcription factor is required for the differentiation of effector CD8(+) T cells and memory responses. Immunity *31*, 283–295.

Kamijo, T., Zindy, F., Roussel, M. F., Quelle, D. E., Downing, J. R., Ashmun, R. A., Grosveld, G., and Sherr, C. J. (1997). Tumor Suppression at the Mouse INK4a Locus Mediated by the Alternative Reading Frame Product p19 ARF. Cell *91*, 649–659.

Kaminer-Israeli, Y., Shapiro, J., Cohen, S., and Monsonego, A. (2010). Stromal cell-induced immune regulation in a transplantable lymphoid-like cell constructs. Biomaterials *31*, 9273–9284.

Karrer, U., Althage, A., Odermatt, B., Roberts, C. W., Korsmeyer, S. J., Miyawaki, S., Hengartner, H., and Zinkernagel, R. M. (1997). On the key role of secondary lymphoid organs in antiviral immune responses studied in alymphoplastic (aly/aly) and spleenless (Hox11(-)/-) mutant mice. J Exp Med *185*, 2157–2170.

Kasic, T., Colombo, P., Soldani, C., Wang, C. M., Miranda, E., Roncalli, M., Bronte, V., and Viola, A. (2011). Modulation of human T-cell functions by reactive nitrogen species. European journal of immunology *41*, 1843–1849.

Kassiotis, G., and Kollias, G. (2001a). TNF and receptors in organ-specific autoimmune disease: multi-layered functioning mirrored in animal models. The Journal of clinical investigation *107*, 1507–1508.

Kassiotis, G., and Kollias, G. (2001b). Uncoupling the proinflammatory from the immunosuppressive properties of tumor necrosis factor (TNF) at the p55 TNF receptor level: implications for pathogenesis and therapy of autoimmune demyelination. The Journal of experimental medicine *193*, 427–434.

Katakai, T., Hara, T., Sugai, M., Gonda, H., and Shimizu, A. (2004). Lymph node fibroblastic reticular cells construct the stromal reticulum via contact with lymphocytes. J Exp Med *200*, 783–795.

Katakai, T., Suto, H., Sugai, M., Gonda, H., Togawa, A., Suematsu, S., Ebisuno, Y., Katagiri, K., Kinashi, T., and Shimizu, A. (2008). Organizer-like reticular stromal cell layer common to adult secondary lymphoid organs. J Immunol *181*, 6189–6200.

Kawai, T., and Akira, S. (2011). Toll-like Receptors and Their Crosstalk with Other Innate Receptors in Infection and Immunity. Immunity *34*, 637–650.

Keating, A. (2008). How Do Mesenchymal Stromal Cells Suppress T Cells? Cell Stem Cell *2*, 106–108.

Keating, A. (2006). Mesenchymal stromal cells. Current opinion in hematology *13*, 419–425.

Kelchtermans, H., Billiau, A., and Matthys, P. (2008). How interferon-gamma keeps autoimmune diseases in check. Trends in immunology *29*, 479–486.

Khan, O., Headley, M., Gerard, A., Wei, W., Liu, L., and Krummel, M. F. (2011). Regulation of T cell priming by lymphoid stroma. PloS one *6*, e26138.

Kim, H. S., Zhang, X., and Choi, Y. S. (1994). Activation and proliferation of follicular dendritic cell-like cells by activated T lymphocytes. Journal of immunology (Baltimore, Md. : 1950) *153*, 2951–2961.

Kim, S. K., Reed, D. S., Olson, S., Schnell, M. J., Rose, J. K., Morton, P. A., and Lefrancois, L. (1998). Generation of mucosal cytotoxic T cells against soluble protein by tissue-specific environmental and costimulatory signals. Proc Natl Acad Sci U S A *95*, 10814–10819.

Kleinman, H. K., Philp, D., and Hoffman, M. P. (2003). Role of the extracellular matrix in morphogenesis. Current Opinion in Biotechnology *14*, 526–532.

Kleinman, H. K., and Martin, G. R. (2005). Matrigel: basement membrane matrix with biological activity. Seminars in cancer biology *15*, 378–386.

Kobayashi, Y., and Watanabe, T. (2010). Synthesis of artificial lymphoid tissue with immunological function. Trends Immunol *31*, 422–428.

Kurata, K., Taniguchi, H., Fukunaga, T., Matsuda, J., and Higaki, H. (2007). Development of a Compact Microbubble Generator and Its Usefulness for Three-Dimensional Osteoblastic Cell Culture. Journal of Biomechanical Science and Engineering *2*, 166–177.

Kyewski, B., and Klein, L. (2006). A central role for central tolerance. Annu Rev Immunol *24*, 571–606.

Lachmann, H. J., Quartier, P., So, A., and Hawkins, P. N. (2011). The emerging role of interleukin-1β in autoinflammatory diseases. Arthritis and rheumatism *63*, 314–324.

Laemmermann, T., and Sixt, M. (2008). The microanatomy of T-cell responses. Immunol Rev *221*, 26–43.

Lavnikova, N., and Laskin, D. L. (1995). Unique patterns of regulation of nitric oxide production in fibroblasts. J Leukoc Biol *58*, 451–458.

Lee, J. W., Epardaud, M., Sun, J., Becker, J. E., Cheng, A. C., Yonekura, A. R., Heath, J. K., and Turley, S. J. (2007). Peripheral antigen display by lymph node stroma promotes T cell tolerance to intestinal self. Nat Immunol *8*, 181–190.

Lindquist, R. L., Shakhar, G., Dudziak, D., Wardemann, H., Eisenreich, T., Dustin, M. L., and Nussenzweig, M. C. (2004). Visualizing dendritic cell networks in vivo. Nat Immunol *5*, 1243–1250.

Link, A., Vogt, T. K., Favre, S., Britschgi, M. R., Acha-Orbea, H., Hinz, B., Cyster, J. G., and Luther, S. A. (2007). Fibroblastic reticular cells in lymph nodes regulate the homeostasis of naive T cells. Nat Immunol *8*, 1255–1265.

Liotta, F., Angeli, R., Cosmi, L., Filì, L., Manuelli, C., Frosali, F., Mazzinghi, B., Maggi, L., Pasini, A., Lisi, V., et al. (2008). Toll-like receptors 3 and 4 are expressed by human bone marrow-derived mesenchymal stem cells and can inhibit their T-cell modulatory activity by impairing Notch signaling. Stem Cells *26*, 279–289.

Liu, K., Iyoda, T., Saternus, M., Kimura, Y., Inaba, K., and Steinman, R. M. (2002). Immune tolerance after delivery of dying cells to dendritic cells in situ. J Exp Med *196*, 1091–1097.

Lukacs-Kornek, V., Malhotra, D., Fletcher, A. L., Acton, S. E., Elpek, K. G., Tayalia, P., Collier, A.-ris, and Turley, S. J. (2011). Regulated release of nitric oxide by nonhematopoietic stroma controls expansion of the activated T cell pool in lymph nodes. Nat Immunol *advance on*.

Luther, S. A., Tang, H. L., Hyman, P. L., Farr, A. G., and Cyster, J. G. (2000). Coexpression of the chemokines ELC and SLC by T zone stromal cells and deletion of the ELC gene in the plt/plt mouse. Proc Natl Acad Sci U S A *97*, 12694–12699.

Luther, S. A., Vogt, T. K., and Siegert, S. (2011). Guiding blind T cells and dendritic cells: A closer look at fibroblastic reticular cells found within lymph node T zones. Immunol Lett *138*, 9–11.

Von Luttichau, I., Notohamiprodjo, M., Wechselberger, A., Peters, C., Henger, A., Seliger, C., Djafarzadeh, R., Huss, R., and Nelson, P. J. (2005). Human adult CD34- progenitor cells functionally express the chemokine receptors CCR1, CCR4, CCR7, CXCR5, and CCR10 but not CXCR4. Stem Cells Dev *14*, 329–336.

Marsland, B. J., Battig, P., Bauer, M., Ruedl, C., Lassing, U., Beerli, R. R., Dietmeier, K., Ivanova, L., Pfister, T., Vogt, L., et al. (2005). CCL19 and CCL21 induce a potent proinflammatory differentiation program in licensed dendritic cells. Immunity *22*, 493–505.

Mempel, T. R., Henrickson, S. E., and von Andrian, U. H. (2004). T-cell priming by dendriticcells in lymph nodes occurs in three distinct phases. Nature *427*, 154–159.

Metzger, T. C., and Anderson, M. S. (2011). Control of central and peripheral tolerance by Aire. Immunological reviews *241*, 89–103.

Miller, M. J., Hejazi, A. S., Wei, S. H., Cahalan, M. D., and Parker, I. (2004a). T cell repertoire scanning is promoted by dynamic dendritic cell behavior and random T cell motility in the lymph node. Proc Natl Acad Sci U S A *101*, 998–1003.

Miller, M. J., Safrina, O., Parker, I., and Cahalan, M. D. (2004b). Imaging the single cell dynamics of CD4+ T cell activation by dendritic cells in lymph nodes. J Exp Med *200*, 847–856.

Miyasaka, M., and Tanaka, T. (2004). Lymphocyte trafficking across high endothelial venules: dogmas and enigmas. Nature reviews. Immunology *4*, 360–370.

Modi, S., Stanton, A. W. B., Mortimer, P. S., and Levick, J. R. (2007). Clinical Assessment of Human Lymph Flow Using Removal Rate Constants of Interstitial Macromolecules: A Critical Review of Lymphoscintigraphy. Lymphatic research and biology *5*, 183–202.

Mueller, S. N., Matloubian, M., Clemens, D. M., Sharpe, A. H., Freeman, G. J., Gangappa, S., Larsen, C. P., and Ahmed, R. (2007). Viral targeting of fibroblastic reticular cells contributes to immunosuppression and persistence during chronic infection. Proc Natl Acad Sci U S A *104*, 15430–15435.

Mueller, S. N., and Germain, R. N. (2009). Stromal cell contributions to the homeostasis and functionality of the immune system. Nat Rev Immunol *9*, 618–629.

Murphy, K. M., and Stockinger, B. (2010). Effector T cell plasticity: flexibility in the face of changing circumstances. Nat Immunol *11*, 674–680.

Nauta, A. J., and Fibbe, W. E. (2007). Immunomodulatory properties of mesenchymal stromal cells. Blood *110*, 3499–3506.

Ngo, V. N., Cornall, R. J., and Cyster, J. G. (2001). Splenic T zone development is B cell dependent. The Journal of experimental medicine *194*, 1649–1660.

Niedbala, W., Cai, B., and Liew, F. Y. (2006). Role of nitric oxide in the regulation of T cell functions. Ann Rheum Dis *65 Suppl 3*, iii37–iii40.

Nolte, M. A., Belien, J. A., Schadee-Eestermans, I., Jansen, W., Unger, W. W., van Rooijen, N., Kraal, G., and Mebius, R. E. (2003). A conduit system distributes chemokines and small blood-borne molecules through the splenic white pulp. J Exp Med *198*, 505–512.

Okamoto, N., Chihara, R., Shimizu, C., Nishimoto, S., and Watanabe, T. (2007). Artificial lymph nodes induce potent secondary immune responses in naive and immunodeficient mice. J Clin Invest *117*, 997–1007.

Onder, L., Scandella, E., Chai, Q., Firner, S., Mayer, C. T., Sparwasser, T., Thiel, V., Rülicke, T., and Ludewig, B. (2011). A novel bacterial artificial chromosome-transgenic Podoplanin – Cre mouse targets lymphoid organ stromal cells in vivo. Frontiers in Immunology *2*, 1–8.

Oshima, S., Nakamura, T., Namiki, S., Okada, E., Tsuchiya, K., Okamoto, R., Yamazaki, M., Yokota, T., Aida, M., Yamaguchi, Y., et al. (2004). Interferon regulatory factor 1 (IRF-1) and IRF-2 distinctively up-regulate gene expression and production of interleukin-7 in human intestinal epithelial cells. Molecular and cellular biology *24*, 6298–6310.

Palframan, R. T., Jung, S., Cheng, G., Weninger, W., Luo, Y., Dorf, M., Littman, D. R., Rollins, B. J., Zweerink, H., Rot, A., et al. (2001). Inflammatory chemokine transport and presentation in HEV: a remote control mechanism for monocyte recruitment to lymph nodes in inflamed tissues. J Exp Med *194*, 1361–1373.

Palmer, E. (2003). Negative selection--clearing out the bad apples from the T-cell repertoire. Nature reviews. Immunology *3*, 383–391.

Pampaloni, F., Reynaud, E. G., and Stelzer, E. H. (2007). The third dimension bridges the gap between cell culture and live tissue. Nat Rev Mol Cell Biol *8*, 839–845.

van de Pavert, S. a, and Mebius, R. E. (2010). New insights into the development of lymphoid tissues. Nature reviews. Immunology *10*, 664–674.

Pedersen, J. a, and Swartz, M. a (2005). Mechanobiology in the third dimension. Ann Biomed Eng *33*, 1469–1490.

Pellegrini, M., Calzascia, T., Toe, J. G., Preston, S. P., Lin, A. E., Elford, A. R., Shahinian, A., Lang, P. A., Lang, K. S., Morre, M., et al. (2011). IL-7 engages multiple mechanisms to overcome chronic viral infection and limit organ pathology. Cell *144*, 601–613.

Perona-Wright, G., Mohrs, K., and Mohrs, M. (2010). Sustained signaling by canonical helper T cell cytokines throughout the reactive lymph node. Nat Immunol *11*, 520–526.

Pham, T. H. M., Okada, T., Matloubian, M., Lo, C. G., and Cyster, J. G. (2008). S1P1 receptor signaling overrides retention mediated by G alpha i-coupled receptors to promote T cell egress. Immunity *28*, 122–133.

Phan, T. G., Gray, E. E., and Cyster, J. G. (2009). The microanatomy of B cell activation. Current opinion in immunology *21*, 258–265.

Phan, T. G., Grigorova, I., Okada, T., and Cyster, J. G. (2007). Subcapsular encounter and complement-dependent transport of immune complexes by lymph node B cells. Nat Immunol *8*, 992–1000.

Randolph, G. J., Ochando, J., and Partida-Sanchez, S. (2008). Migration of dendritic cell subsets and their precursors. Annu Rev Immunol *26*, 293–316.

Ren, G., Zhang, L., Zhao, X., Xu, G., Zhang, Y., Roberts, A. I., Zhao, R. C., and Shi, Y. (2008). Mesenchymal stem cell-mediated immunosuppression occurs via concerted action of chemokines and nitric oxide. Cell Stem Cell *2*, 141–150.

Rhee, S. (2009). Fibroblasts in three dimensional matrices: cell migration and matrix remodeling. Exp Mol Med *41*, 858–865.

Rocca, B., and FitzGerald, G. a (2002). Cyclooxygenases and prostaglandins: shaping up the immune response. International immunopharmacology *2*, 603–630.

Roozendaal, R., Mebius, R. E., and Kraal, G. (2008). The conduit system of the lymph node. Int Immunol *20*, 1483–1487.

Roozendaal, R., and Mebius, R. E. (2011). Stromal cell-immune cell interactions. Annu Rev Immunol *29*, 23–43.

Russell, J. H., and Ley, T. J. (2002). Lymphocyte-mediated cytotoxicity. Annu Rev Immunol *20*, 323–370.

Saini, M., Pearson, C., and Seddon, B. (2009). Regulation of T cell-dendritic cell interactions by IL-7 governs T-cell activation and homeostasis. Blood *113*, 5793–5800.

Sakaguchi, S., Yamaguchi, T., Nomura, T., and Ono, M. (2008). Regulatory T cells and immune tolerance. Cell *133*, 775–787.

Salmond, R. J., Filby, A., Qureshi, I., Caserta, S., and Zamoyska, R. (2009). T-cell receptor proximal signaling via the Src-family kinases, Lck and Fyn, influences T-cell activation, differentiation, and tolerance. Immunological reviews *228*, 9–22.

Sanchez-Sanchez, N., Riol-Blanco, L., and Rodriguez-Fernandez, J. L. (2006). The Multiple Personalities of the Chemokine Receptor CCR7 in Dendritic Cells. J Immunol *176*, 5153–5159.

Santerre, J. P., Woodhouse, K., Laroche, G., and Labow, R. S. (2005). Understanding the biodegradation of polyurethanes: from classical implants to tissue engineering materials. Biomaterials *26*, 7457–7470.

Sato, K., Ozaki, K., Mori, M., Muroi, K., and Ozawa, K. (2010). Mesenchymal stromal cells for graft-versus-host disease : basic aspects and clinical outcomes. Journal of clinical and experimental hematopathology : JCEH *50*, 79–89.

Sato, K., Ozaki, K., Oh, I., Meguro, A., Hatanaka, K., Nagai, T., Muroi, K., and Ozawa, K. (2007). Nitric oxide plays a critical role in suppression of T-cell proliferation by mesenchymal stem cells. Blood *109*, 228–234.

Scandella, E., Bolinger, B., Lattmann, E., Miller, S., Favre, S., Littman, D. R., Finke, D., Luther, S. A., Junt, T., and Ludewig, B. (2008). Restoration of lymphoid organ integrity through the interaction of lymphoid tissue-inducer cells with stroma of the T cell zone. Nat Immunol *9*, 667–675.

Schneider, K., Potter, K. G., and Ware, C. F. (2004). Lymphotoxin and LIGHT signaling pathways and target genes. Immunological reviews *202*, 49–66.

Serbina, N. V., Salazar-Mather, T. P., Biron, C. A., Kuziel, W. A., and Pamer, E. G. (2003). TNF/iNOS-producing dendritic cells mediate innate immune defense against bacterial infection. Immunity *19*, 59–70.

Shakhar, G., Lindquist, R. L., Skokos, D., Dudziak, D., Huang, J. H., Nussenzweig, M. C., and Dustin, M. L. (2005). Stable T cell-dendritic cell interactions precede the development of both tolerance and immunity in vivo. Nat Immunol *6*, 707–714.

Shalapour, S., Deiser, K., Sercan, O., Tuckermann, J., Minnich, K., Willimsky, G., Blankenstein, T., Hämmerling, G. J., Arnold, B., and Schüler, T. (2010). Commensal microflora and interferon-gamma promote steady-state interleukin-7 production in vivo. European journal of immunology *40*, 2391–2400.

Shapiro-Shelef, M., and Calame, K. (2005). Regulation of plasma-cell development. Nat Rev Immunol *5*, 230–242.

Shevach, E. M. (2006). From vanilla to 28 flavors: multiple varieties of T regulatory cells. Immunity *25*, 195–201.

Shi, F. D., Flodstrom, M., Kim, S. H., Pakala, S., Cleary, M., Ljunggren, H. G., and Sarvetnick, N. (2001). Control of the autoimmune response by type 2 nitric oxide synthase. J Immunol *167*, 3000–3006.

Siegert, S., Huang, H.-Y., Yang, C.-Y., Scarpellino, L., Carrie, L., Essex, S., Nelson, P. J., Heikenwalder, M., Acha-Orbea, H., Buckley, C. D., et al. (2011). Fibroblastic Reticular Cells From Lymph Nodes Attenuate T Cell Expansion by Producing Nitric Oxide. PLoS ONE *6*, e27618.

Sixt, M., Kanazawa, N., Selg, M., Samson, T., Roos, G., Reinhardt, D. P., Pabst, R., Lutz, M. B., and Sorokin, L. (2005). The conduit system transports soluble antigens from the afferent lymph to resident dendritic cells in the T cell area of the lymph node. Immunity *22*, 19–29.

Starr, T. K., Jameson, S. C., and Hogquist, K. a (2003). Positive and negative selection of T cells. Annual review of immunology *21*, 139–176.

Steinman, R. M., Hawiger, D., and Nussenzweig, M. C. (2003). Tolerogenic dendritic cells. Annu Rev Immunol *21*, 685–711.

Suematsu, S., and Watanabe, T. (2004). Generation of a synthetic lymphoid tissue-like organoid in mice. Nat Biotechnol *22*, 1539–1545.

Sumen, C., Mempel, T. R., Mazo, I. B., and von Andrian, U. H. (2004). Intravital microscopy: visualizing immunity in context. Immunity *21*, 315–329.

Svensson, M., Maroof, A., Ato, M., and Kaye, P. M. (2004). Stromal Cells Direct Local Differentiation of Regulatory Dendritic Cells. Immunity *21*, 805–816.

Svensson, M., and Kaye, P. M. (2006). Stromal-cell regulation of dendritic-cell differentiation and function. Trends Immunol *27*, 580–587.

Takeda, K., Kaisho, T., and Akira, S. (2003). Toll-like receptors. Annual review of immunology *21*, 335–376.

Tew, J. G., Wu, J., Fakher, M., Szakal, A. K., and Qin, D. (2001). Follicular dendritic cells: beyond the necessity of T-cell help. Trends Immunol *22*, 361–367.

Tomasek, J. J., Gabbiani, G., Hinz, B., Chaponnier, C., and Brown, R. a (2002). Myofibroblasts and mechano-regulation of connective tissue remodelling. Nature reviews. Molecular cell biology *3*, 349–363.

Tomei, A. A., Boschetti, F., Gervaso, F., and Swartz, M. A. (2009a). 3D collagen cultures under well-defined dynamic strain: A novel strain device with a porous elastomeric support. Biotechnology and Bioengineering *103*, 217–225.

Tomei, A. A., Siegert, S., Britschgi, M. R., Luther, S. A., and Swartz, M. A. (2009b). Fluid Flow Regulates Stromal Cell Organization and CCL21 Expression in a Tissue-Engineered Lymph Node Microenvironment. J Immunol *183*, 4273–4283.

Tsatsanis, C., Androulidaki, A., Venihaki, M., and Margioris, A. N. (2006). Signalling networks regulating cyclooxygenase-2. Int J Biochem Cell Biol *38*, 1654–1661.

Tsunoda, R., Nakayama, M., Onozaki, K., Heinen, E., Cormann, N., Kinet-Denoël, C., and Kojima, M. (1990). Isolation and long-term cultivation of human tonsil follicular dendritic cells. Virchows Archiv B Cell Pathology Including Molecular Pathology *59*, 95–105.

Turley, S. J., Fletcher, A. L., and Elpek, K. G. (2010). The stromal and haematopoietic antigen-presenting cells that reside in secondary lymphoid organs. Nat Rev Immunol *10*, 813–825.

Uccelli, A., Moretta, L., and Pistoia, V. (2008). Mesenchymal stem cells in health and disease. Nat Rev Immunol *8*, 726–736.

Vega, F., Coombes, K. R., Thomazy, V. A., Patel, K., Lang, W., and Jones, D. (2006). Tissue-specific function of lymph node fibroblastic reticulum cells. Pathobiology *73*, 71–81.

Vig, M., Srivastava, S., Kandpal, U., Sade, H., Lewis, V., Sarin, A., George, A., Bal, V., Durdik, J. M., and Rath, S. (2004). Inducible nitric oxide synthase in T cells regulates T cell death and immune memory. J Clin Invest *113*, 1734–1742.

Vignali, D. A., Collison, L. W., and Workman, C. J. (2008). How regulatory T cells work. Nat Rev Immunol *8*, 523–532.

Vinuesa, C. G., Linterman, M. A., Goodnow, C. C., and Randall, K. L. (2010). T cells and follicular dendritic cells in germinal center B-cell formation and selection. Immunol Rev *237*, 72–89.

Van Vliet, E., Melis, M., Foidart, J. M., and Van Ewijk, W. (1986). Reticular fibroblasts in peripheral lymphoid organs identified by a monoclonal antibody. Journal of Histochemistry & Cytochemistry *34*, 883–890.

Vondenhoff, M. F., Greuter, M., Goverse, G., Elewaut, D., Dewint, P., Ware, C. F., Hoorweg, K., Kraal, G., and Mebius, R. E. (2009). LTbetaR signaling induces cytokine expression and up-regulates lymphangiogenic factors in lymph node anlagen. Journal of immunology (Baltimore, Md. : 1950) *182*, 5439–5445.

Walker, L. S., and Abbas, A. K. (2002). The enemy within: keeping self-reactive T cells at bay in the periphery. Nat Rev Immunol *2*, 11–19.

Williams, M. A., and Bevan, M. J. (2007). Effector and memory CTL differentiation. Annu Rev Immunol *25*, 171–192.

Worbs, T., Bernhardt, G., and Forster, R. (2008). Factors governing the intranodal migration behavior of T lymphocytes. Immunol Rev *221*, 44–63.

Xiao, B. G., Ma, C. G., Xu, L. Y., Link, H., and Lu, C. Z. (2008). IL-12/IFN-gamma/NO axis plays critical role in development of Th1-mediated experimental autoimmune encephalomyelitis. Mol Immunol *45*, 1191–1196.

Zeng, M., Smith, A. J., Wietgrefe, S. W., Southern, P. J., Schacker, T. W., Reilly, C. S., Estes, J. D., Burton, G. F., Silvestri, G., Lifson, J. D., et al. (2011). Cumulative mechanisms of lymphoid tissue fibrosis and T cell depletion in HIV-1 and SIV infections. The Journal of Clinical Investigation *121*, 998–1008.

Zhang, M., Tang, H., Guo, Z., An, H., Zhu, X., Song, W., Guo, J., Huang, X., Chen, T., Wang, J., et al. (2004). Splenic stroma drives mature dendritic cells to differentiate into regulatory dendritic cells. Nat Immunol *5*, 1124–1133.

Zheng, B., Vogel, H., Donehower, L. A., and Bradley, A. (2002). Visual Genotyping of a Coat Color Tagged p53 Mutant Mouse Line. Cancer Biology & Therapy *1*, 424–426.

Zhu, J., Yamane, H., and Paul, W. E. (2010). Differentiation of effector CD4 T cell populations (*). Annu Rev Immunol *28*, 445–489.

Zhu, J., and Paul, W. E. (2008). CD4 T cells: fates, functions, and faults. Blood *112*, 1557–1569.

Zimmerli, C., Lee, B. P. L., Palmer, G., Gabay, C., Adams, R., Aurrand-Lions, M., and Imhof, B. a (2009). Adaptive immune response in JAM-C-deficient mice: normal initiation but reduced IgG memory. Journal of immunology (Baltimore, Md. : 1950) *182*, 4728–4736.

Zischek, C., Niess, H., Ischenko, I., Conrad, C., Huss, R., Jauch, K. W., Nelson, P. J., and Bruns, C. (2009). Targeting tumor stroma using engineered mesenchymal stem cells reduces the growth of pancreatic carcinoma. Ann Surg *250*, 747–753.